الخلاصة

ثل للهياكل الخرسانية المسلحة الثلاثية الأبعاد المعتمد على التحليل اللاخطي

في هذا البحث تم اقتراح طريقة تحليلية عامة لدراسة التصرف غير المرن للهياكل الخرسانية المسلحة المستوية أو الثلاثية الأبعاد (space frames). تتبع هذه الطريقة اسلوب الخطوة – خطوة مع التكرار (step by step incremental approach). تم إدخال عدة عوامل في الطريقة المقترحة و هي:1)اللاخطية في تصرف مادة المنشأ (material non-linearity). 2) اللاخطية الهندسية(geometric non-linearity) إضافة إلى إدخال تأثير التشوهات القصية (shear deformations).3) التأثير المتبادل للعزم – القوة المحورية. تم اشتقاق صيغ لحساب القوى في النهايات المثبتة (fixed-end forces) لحالة عضو إنشائي معرض لحمل موزع بانتظام , بالإضافة إلى الأخذ بنظر الاعتبار موقع القص = صفر كمقطع حرج إضافي في حالةعضاء المحملة بحمل منتظم. ثلاثة احتمالات للفشل تم أخذها بالاعتبار و هي: أ) الفشل بالسحق الموقعي (crushing failure) للخرسانة خلال مقطع معين. ب) آلية الانهيار. ج) الفشل بالأستقرارية.

تم صب نموذج واحد مصغر لهيكل خرساني مسلح ثلاثي الأبعاد و تم فحصه مختبريا إلى حد الفشل. قورنت النتائج مع التي تم الحصول عليها باستخدام طريقة التحليل المقترحة. من أهداف الفحص المختبري هو تأكيد صحة و فاعلية طريقة التحليل المقترحة ولدراسة سلوك المنشأ في الواقع.

و بالاعتماد على التحليل ي المقترح في هذا البحث. إن الطريقة المقترحة تستند علـــى البحث المباشر (**direct search method**) للحصول على افضل تصميم (اقل كلفة كلية). في عملية التصميم الأمثل اعتبرت أبعاد مقطع العضو الإنشائي و حديد التسليح (الرئيســـي و العرضي) في المقاطع الحرجة كمتغيرات للحصول على افضل كلفة كلية و التي تشمل كلفة كل من حديد التسليح, الخرسانة و كلفة القوالب.

ن اللإستنتاجات التي تم الحصول عليها ,إن نتائج طريقة التحليل في هذا البحث تتوافــق جيدا مع نتائج الفحص المختبري ونتائج البحوث السابقة مع فرق في قيمة حملفشل لا يزيد على (11.6%).

ABSTRACT

A general analytical method that studies the inelastic behavior of reinforced concrete (plane or space) frames is presented in this study. It follows a step – by – step incremental with iteration approach. Different parameters are included in the present method, they are: material non-linearity, effects of geometric non – linearity in addition to shear deformations, moment-axial force interaction thus presenting accurate expressions for stability functions. Fixed – end forces are derived for element under uniformly distributed load taking into account the position of zero shear as an additional critical section in the case of elements under uniformly distributed load. Three possible failure criteria can be used, they are: crushing failure for concrete at a specified section, plastic collapse mechanism and stability failure. One model of a reinforced concrete space frame was cast and tested experimentally up to failure. The results are compared with those obtained theoretically by the proposed method of analysis. One of the aims of the experimental study is to ensure the validity and the efficiency of the present method of analysis and to study the actual behavior of the structure.

A general optimal design algorithm for reinforced concrete (plane or space) frames is presented based on the proposed non – linear analysis. The algorithm is based on a direct search method to get the best design (minimum total cost). In the optimization process, the member dimensions and steel reinforcement (main and lateral reinforcement) at critical sections are taken as variables and the total cost which includes the cost of steel reinforcement, concrete and formwork, is taken to be as an objective function.

Among the conclusions obtained, the results of the present method of analysis show good agreement with the experimental results as well as with those of previous studies with a difference in failure load not more than (11.6 %).

ACKNOWLEDGEMENT

First of all, thanks for ***ALLAH*** who enabled me to achieve this work.

The author would like to express his sincere appreciation and deepest gratitude to Dr. **Nameer A. Alwash** and Dr. **Ammar Y. Ali** for their excellent guidance, endless support, valuable advice and encouragement throughout the preparation of this work..

Furthermore, thanks are devoted to my family for their care and encouragement during this work.

Finally, appreciation and thanks to my friends, especially **Mohammed Jawad, Husain Marred. Sadjad Amir, Jawad Talib** and to all other friends for their help and useful discussion.

(Appendix – A)
Derivation of Torsion Constant (J_m)

A cross – section of general shape is considered for a prismatic member subjected to pure torsion as shown below in Fig. (A – 1)

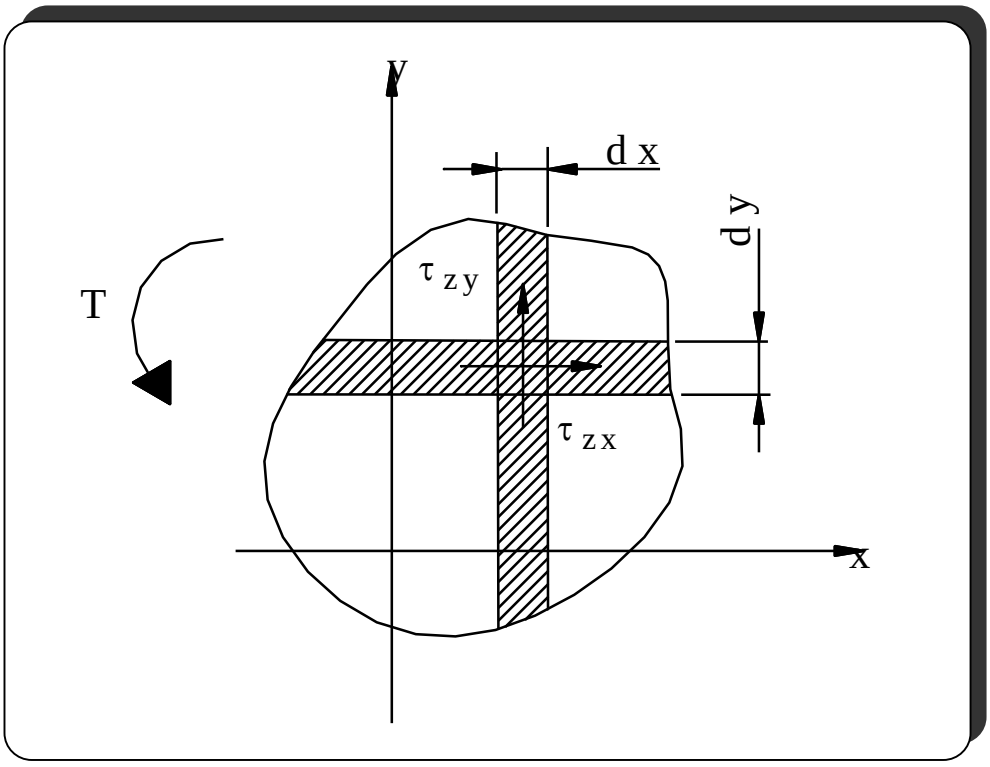

Fig. (A – 1): Shear Stresses in a Cross – Section of General Shape due to Pure Torsion.

The section constant (J_m) can be given by the following equation **[40]**

$$J_m = 2 \iint_{y\,x} \phi \, dx\, dy \qquad \text{---------- (A .1)}$$

where $\phi = \phi(x, y)$ is called Saint – Venant's stress function which has the property

$$\tau_{zx} = G\alpha \frac{\partial \phi}{\partial y} \quad , \quad \tau_{zy} = G\alpha \frac{\partial \phi}{\partial x}$$

where

G = Shear modulus of rigidity.

$\bar{\alpha} = \frac{\bar{\theta}}{L}$ constant rate of twist (free Warping).

Using the compatibility and 3D equilibrium, the following governing equation can be obtained

$$\frac{\partial^2 \phi}{\partial x^2} + \frac{\partial^2 \phi}{\partial y^2} = -2 \text{ or } \nabla^2 \phi = -2 \quad \text{---------- (A .2)}$$

To find the function $\phi(x, y)$ satisfying both equilibrium and compatibility, Prandtl's membrane analogy**[40]** can be utilized, in which, Eq. (A.2) is assumed to closely resemble the equilibrium equation describing the small deflection of a flat membrane subjected to an internal pressure P. The membrane analogy can be explained as follows.

A surface subjected to an internal pressure as shown in Fig. (A – 2) is considered. Here,

P = internal pressure per unit area.

T = constant tension per unit length.

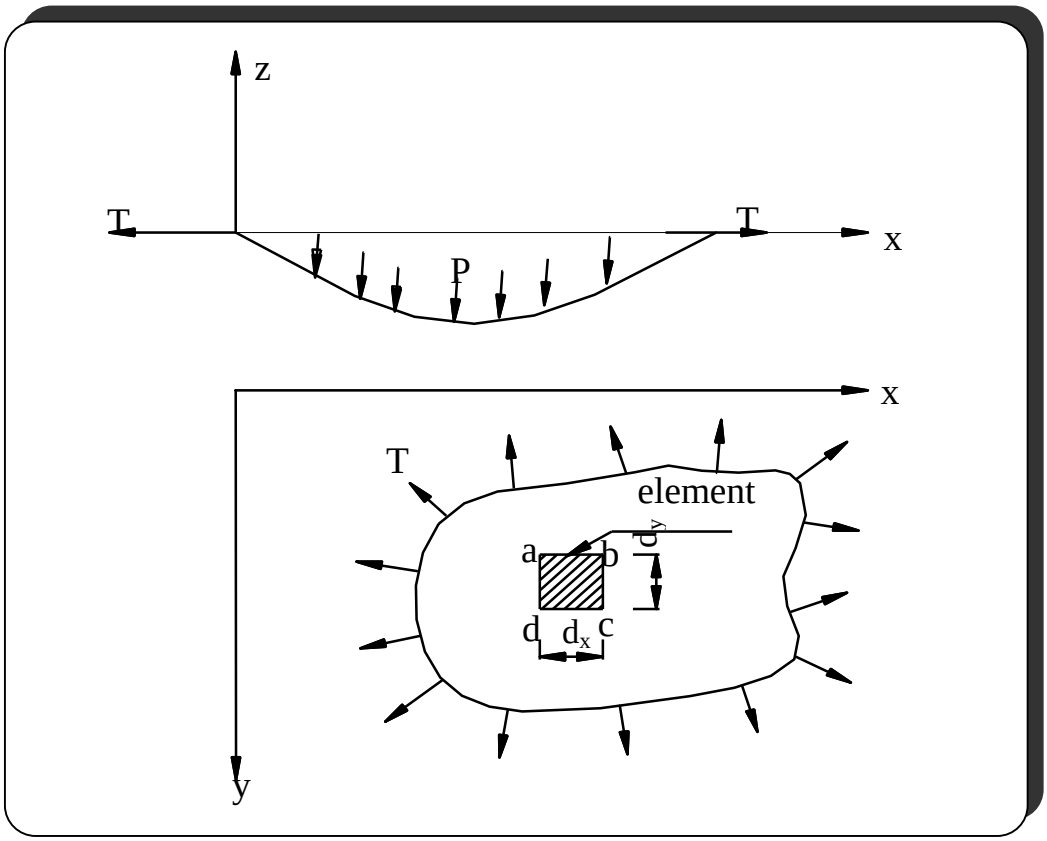

Fig. (A – 2): Membrane Analogy.

Utilizing the equilibrium of element (A) in z – direction, then

$$\left[T\left(\frac{\partial z}{\partial x}\right)_{ad} - T\left(\frac{\partial z}{\partial x}\right)_{bc}\right]dy + \left[T\left(\frac{\partial z}{\partial y}\right)_{ab} - T\left(\frac{\partial z}{\partial y}\right)_{dc}\right]dx - P\,dx\,dy = 0$$

---------- (A .3)

Knowing that

$$\lim_{dx \to 0} \frac{T\left(\partial z/\partial x\right)_x - T\left(\partial z/\partial x\right)_{x+dx}}{dx} = -T\frac{\partial^2 z}{\partial x^2} \quad \text{-------- (A .4)}$$

Similarly

$$\lim_{dy \to 0} \frac{T\left(\partial z/\partial y\right)_x - T\left(\partial z/\partial y\right)_{y+dy}}{dy} = -T\frac{\partial^2 z}{\partial y^2} \quad \text{---------- (A .5)}$$

Hence

$$\frac{\partial^2 z}{\partial x^2} + \frac{\partial^2 z}{\partial y^2} = -\frac{P}{T} \quad \text{---------- (A .6)}$$

Thus by comparison of equation (A.2) with equation (A .6) one can obtain ¤ from z as follows:

For a rectangular cross – section shown, it is assumed that

$$z = \sum_{n=1,3,5} \cos\frac{n\pi x}{2a}\, Y_n \quad \text{----------(A .7)}$$

$n = 1,2,3$ to get zero value for z at boundaries.

$$Y_n = f(y) \quad \text{----------(A .8)}$$

Also, using even expansion

$$\frac{P}{T} = \sum A_n \cos\frac{n\pi x}{2a} \quad \text{---------- (A .9)}$$

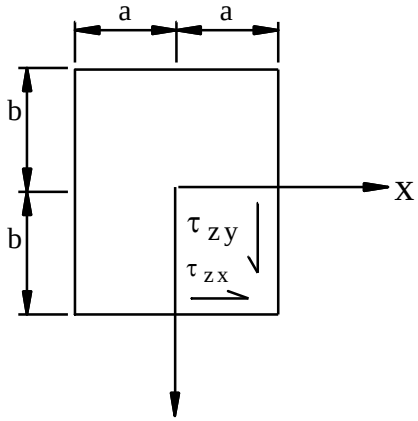

$$An = \frac{2}{a}\int_0^a \frac{P}{T}\cos\frac{n\pi x}{2a}\,dx = \frac{4}{n\pi}\frac{P}{T}\sin\frac{n\pi x}{2a}\Big|_0^a = \frac{4}{n\pi}\frac{P}{T}\sin\frac{n\pi}{2} \quad \text{---(A .10)}$$

$$\therefore \begin{cases} An = \dfrac{P}{T}(-1)^{\frac{n-1}{2}}\dfrac{4}{n\pi} & n = 1,3,5..... \\ = 0 & n = 0,2,4..... \end{cases} \quad \text{---------- (A .11)}$$

Substituting the value of $\left(P/T\right)$ in equation (A.6) and solving the differential equation , then

$$y = \bar{A}\sinh\left(\frac{n\pi}{2a}y\right) + \bar{B}\cosh\left(\frac{n\pi}{2a}y\right) + \frac{16Pa^2}{Tn^3\pi^3}(-1)^{\frac{n-1}{2}} \quad \text{----- (A .12)}$$

From the symmetry of the surface about x-axis $\therefore \bar{A} = 0$

At $y = \mp b \quad Yn = 0$

Thus

$$\bar{B} = -\frac{16Pa^2(-1)^{\frac{n-1}{2}}}{Tn^3\pi^3\cosh\left(\frac{n\pi b}{2a}\right)} \quad \text{---------- (A .13)}$$

$\therefore$

$$Z = \frac{P}{T}\frac{16a^2}{\pi^3}\sum_{n=1,3,5}^{\infty}\frac{1}{n^3}(-1)^{\frac{n-1}{2}}\left[1-\frac{\cosh(n\pi y/2a)}{\cosh(n\pi b/2a)}\right]\cos\frac{n\pi x}{2a}$$

---------- (A .14)

as mentioned before, from the comparison between equations (A.2) and (A .6), then

$$\phi(x,y) = 2z\frac{T}{P} \quad \text{---------- (A .15)}$$

Thus

$$\text{¤}(x, y) = \frac{32a^2}{\text{®}^3} \sum_{n=1,3,5} \left[\frac{1}{n^3}(-1)^{\frac{n-1}{2}} \left[1 - \frac{\cosh(n\text{®}\, y/2a)}{\cosh(n\text{®}\, b/2a)}\right] \cos\frac{n\text{®}\, x}{2a}\right]$$

----------(A .16)

Substituting for ¤ in equation (A.1), and after integrations, the section constant (J_m) have the following expression:

$$Jm = \frac{512a^3 b}{\text{®}^4} \sum_{n=1,3,5} \frac{1}{n^4}\left[1 - \frac{2a}{bn\text{®}} \tanh\left(\frac{n\text{®}\, b}{2a}\right)\right] \quad \text{----------(A .17)}$$

Replacing $2b$ by (H) and $2a$ by (B) so, for $n = 1$

$$Jm = \frac{HB^3}{3}\left[1 - \frac{192}{\text{®}^5}\frac{B}{H}\tanh\left(\frac{\text{®}\, H}{2B}\right)\right] \quad \text{----------(A .18)}$$

التَصْميـم الأمثل للمنشآت الخرْسانيّة المسلَّحة الثُلاثيّة الأبعاد المعتمد على التحْليل اللاخَطّي

رسالة مقدمة إلى
كلية الهندسة في جامعة بابل
كجزء من متطلبات نيل درجة الماجستير
في الهندسة المدنية

من قبل

مصعب عايد كصب الجنابي

بكالوريوس هندسة مدنية

جامعة بابل

إشراف

أ.م.الدكتور نمير عبد الأمير علوش

أ.م.الدكتور عمار ياسر علي

CERTIFICATE

We certify that the preparation of this thesis titled "**Optimal Design of Reinforced Concrete Space Structures Based on Nonlinear Analysis"** by (**Mus'ab Aied Qissab Al-Janabi)** was under our supervision at the University of Babylon in partial fulfillment of the requirements for the degree of Master of Science in Civil Engineering.

Signature :

Name: **Asst. Prof. Dr. Nameer A. Alwash**

(Supervisor)

Date: / / 2003

Signature :

Name: **Asst. Prof. Dr. Ammar.Y. Ali**

(Supervisor)

Date: / / 2003

CERTIFICATE

We certify as an examining committee that we have read this thesis titled "**Optimal Design of Reinforced Concrete Space Structures Based on Nonlinear Analysis**" , and examined the student (**Mus'ab Aied Qissab**) in its content and what related to it, and found it meets the standard of a thesis for the Degree of Master of Science in civil Engineering (Structures).

Signature :
Name: **Asst.Prof . Dr.Mustafa B. Dawood**
(Member)
Date: / / 2003

Signature :
Name: **Dr. Hayder Talib Nimnim**
(Member)
Date: / / 2003

Signature:
Name: **Prof. Dr. Husain M. Husain**
(Chairman)
Date: / / 2003

Signature :
Name: **Asst. Prof. Dr. Nameer A. Alwash**
(Supervisor)
Date: / / 2003

Signature :
Name: **Asst. Prof. Dr. Ammar.Y. Ali**
(Supervisor)
Date: / / 2003

Approval of the Civil Engineering Department

Signature:
Name: **Asst. Prof. Dr. Nameer A. Alwash**
Head of the Civil Engineering Department
Date: / / 2003

Approval of the Deanery of the College of Engineering

Signature:
Name: **Asst. Prof. Dr. Haroun A.K. Shahad**
Dean of the College of Engineering
Date: / / 2003

CHAPTER SEVEN

RESULTS, APPLICATIONS AND DISCUSSION

7.1 General:

In this chapter, the results of various ~~analysis~~ analyses and optimal design problems are presented based on~~,~~ the ~~new~~ present proposed non – linear analysis ~~that~~ which is formulated in chapters three and four, the optimal design approach ~~for~~for ~~reinforced~~reinforced concrete space frames which is formulated in chapter five ~~,~~ and the experimental model that is described in chapter six.

The results are presented in the following order:

1- Results of the tested space frame model. The results are compared with those obtained from the proposed non – linear analysis.

2- Other applications of the present non – linear analysis approach on reinforced concrete or steel frames that were analyzed theoretically by the proposed non – linear analysis or that were previously tested ~~in lab~~ or analyzed theoretically by others (in previous studies). They show the efficiency of the present method of analysis in solving various types of non – linear analysis problems of framed structures.

3- Results of the presented optimal design approach for reinforced concrete space frames. The approach is applied on several typical reinforced concrete frames.

Also in this chapter, the main parameters that may ~~effect~~ affect both the non – linear process and optimal design process and the accuracy of the results are discussed.

منسّق:خط اللغة العربية وغيرها: 10
منسّق:خط اللغة العربية وغيرها: 10
نقطة

7.2 Results of ~~The~~ the ~~Tested~~ tested Space Frame Model:

As stated earlier, one model of a reinforced concrete space frame was tested in a structural laboratory. The model was subjected to four concentrated loads at mid-~~-~~span of the members indicated in Fig. (6 – 1a). The details of steel and concrete properties with member dimensions are all ~~found~~ given in chapter six.

The model was also analyzed up to failure by the proposed method of analysis. The corresponding ~~considered~~ structure for the model is shown in Fig. (7 – 1).

Experimental and theoretical load – deflection curves are presented in figures (7 – 2) and (7 – 3) considering the lower chord deflection of nodes 8 and 11 respectively as shown in Fig. (7 – 1).

The load – deflection curves of ~~figures~~ Figures (7 – 2) and (7 – 3) show the effect of geometric non – linearity and section properties (gross ~~or~~, cracked and effective) on the behavior of the structure. From the prescribed figures, it is clear that the most representative curve is that when considering geometric non – linearity and adopting ~~effective~~ cracked section properties. However, the experimental load – deflection curves indicate lesser model stiffness than that predic~~a~~ted by the analysis which is based on ~~effective~~ cracked section properties especially after formation of several plastic hinges ~~formulation~~.

The ultimate load (P) of the model, as obtained from the proposed analytical solution is (P = 21.78 ~~KN~~kN) while the measured ultimate load is (P = 19.517 ~~KN~~kN) which is lesser by 11.~~5956~~%. Figure (7– 4) shows the pattern of cracking and plastic deformations ~~propagate~~ propagating into the joints of the model.

منسّق:خط اللغة العربية وغيرها: 10
منسّق:خط اللغة العربية وغيرها: 10
نقطة

The strains for different sections at the face of the joints are plotted versus loading as shown in Fig. (7–5). The strains are measured at reinforcement level (2 cm from the upper and lower extreme fibers).

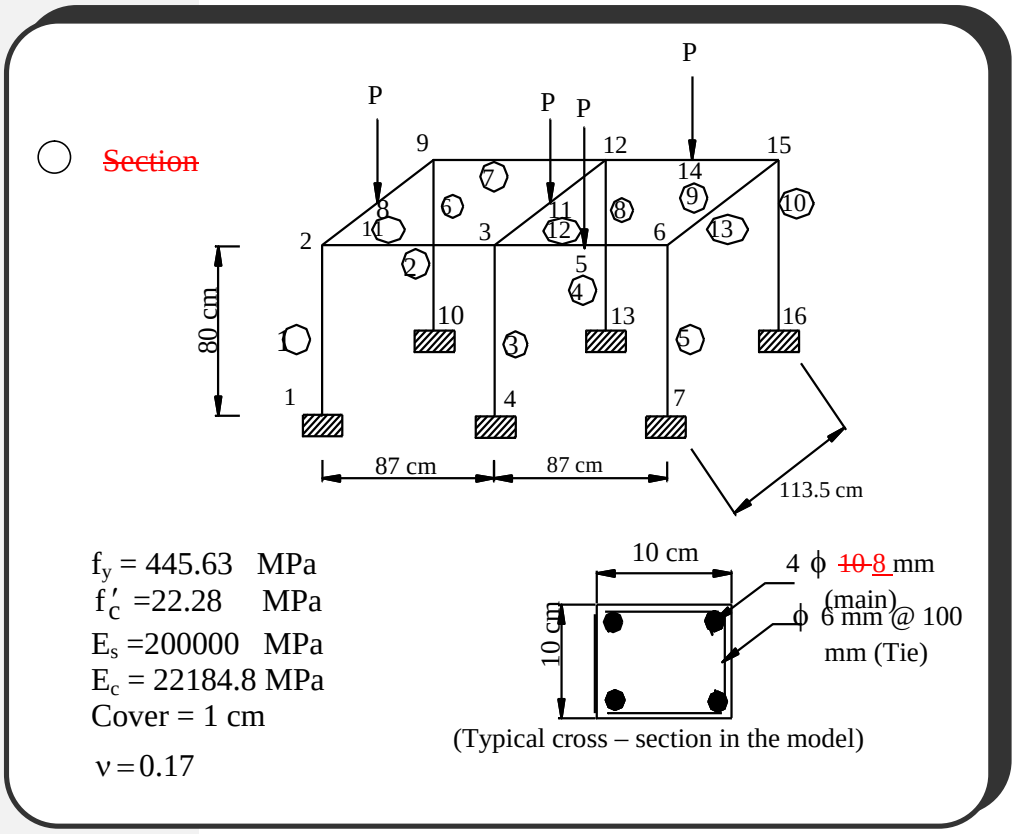

Fig. (7 – 1): Details of the ~~analyzed~~ Analyzed ~~structure~~ Structure

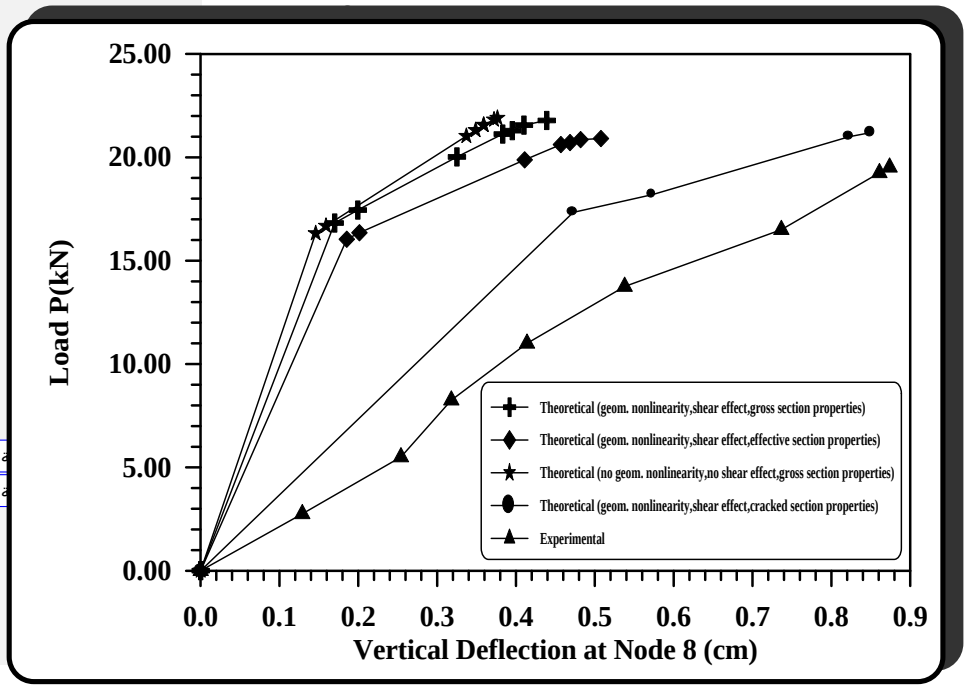

Fig. (7 – 2): Load – ~~deflection~~ Deflection ~~curves~~ Curves for the

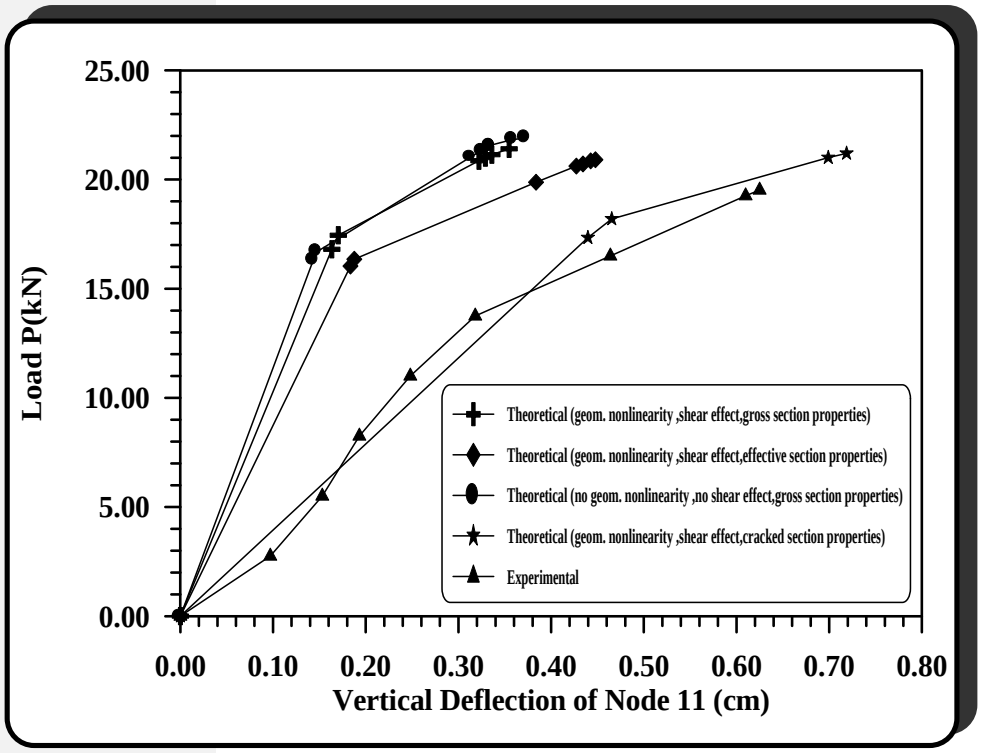

Fig. (7 – 3): Load – ~~deflection~~ Deflection ~~curves~~ Curves for the

منسّق:خط اللغة العربية وغيرها: 10
منسّق:خط اللغة العربية وغيرها: 10
نقطة

Fig. (7 – 4): Cracking ~~pattern~~ Pattern and ~~failure~~Failure.

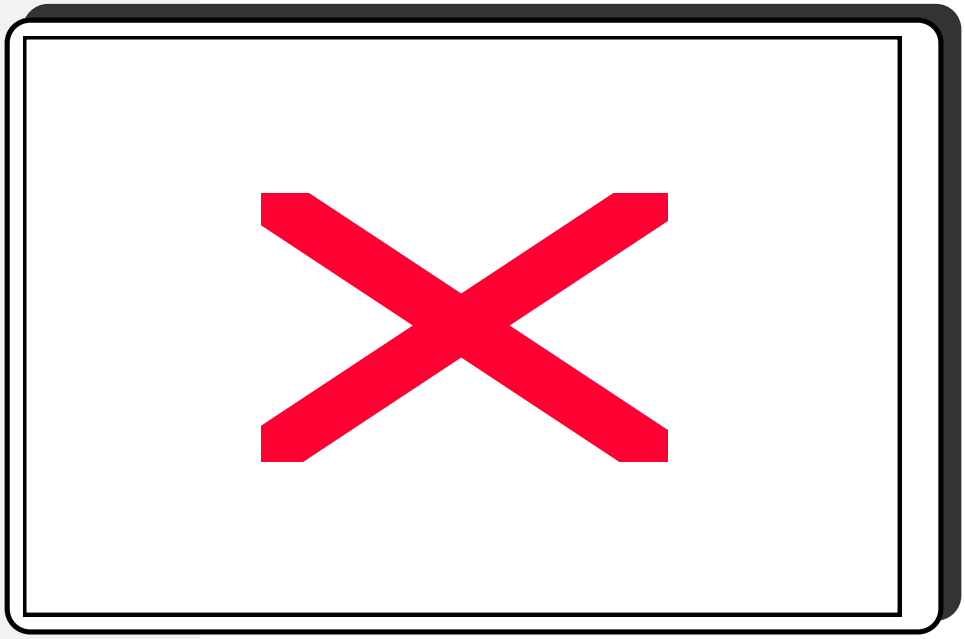

Fig. (7 – 2): Load – ~~deflection~~ Deflection ~~curves~~ Curves for the

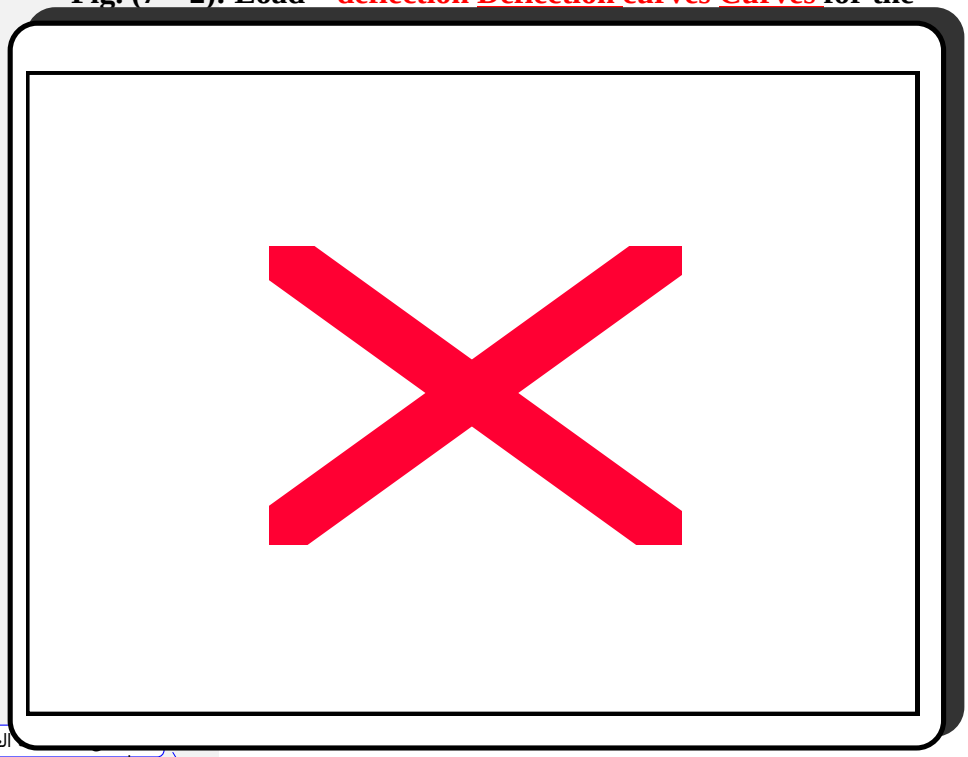

Fig. (7 – 3): Load – ~~deflection~~ Deflection ~~curves~~ Curves for the

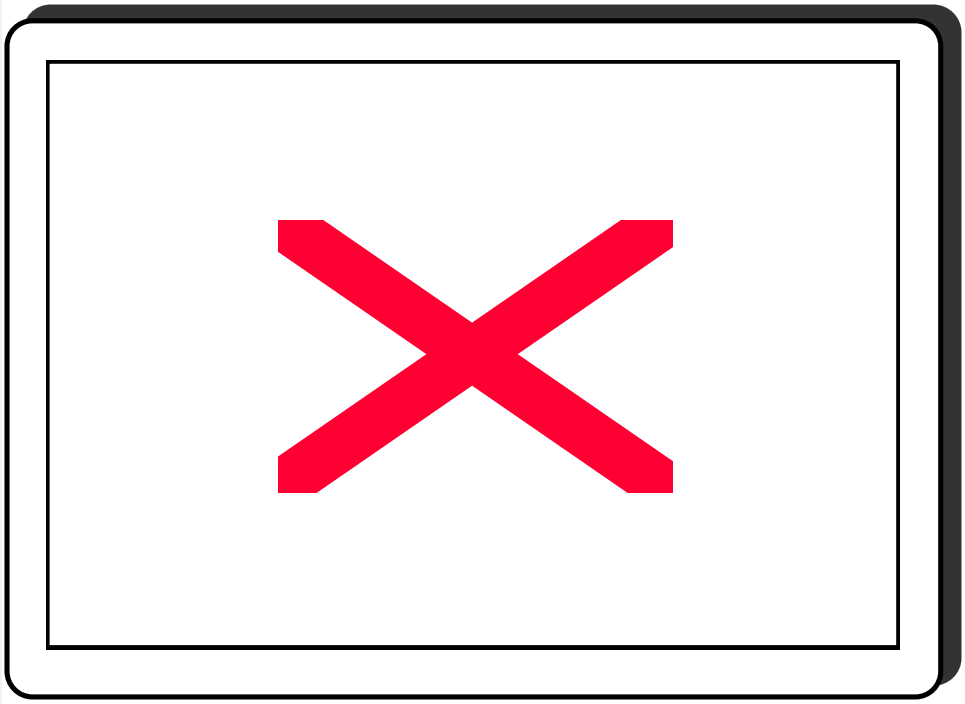

It may be noted that the strain ≥ 0.002 in such levels (in steel or concrete) indicates the formation of a plastic hinge. The comparison between the plastic hinges distribution as obtained theoretically with those observed experimentally is given in Fig. (7 – 6), ~~which~~They are generally seen to be in good agreement with those observed experimentally.

The moments and axial forces at collapse~~,~~ as obtained from analysis are given in ~~table~~ Table (7 – 1).

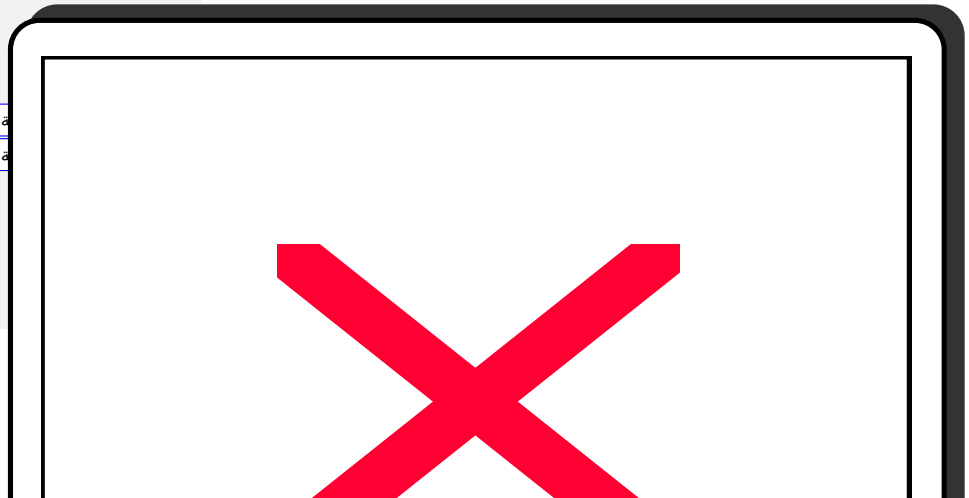

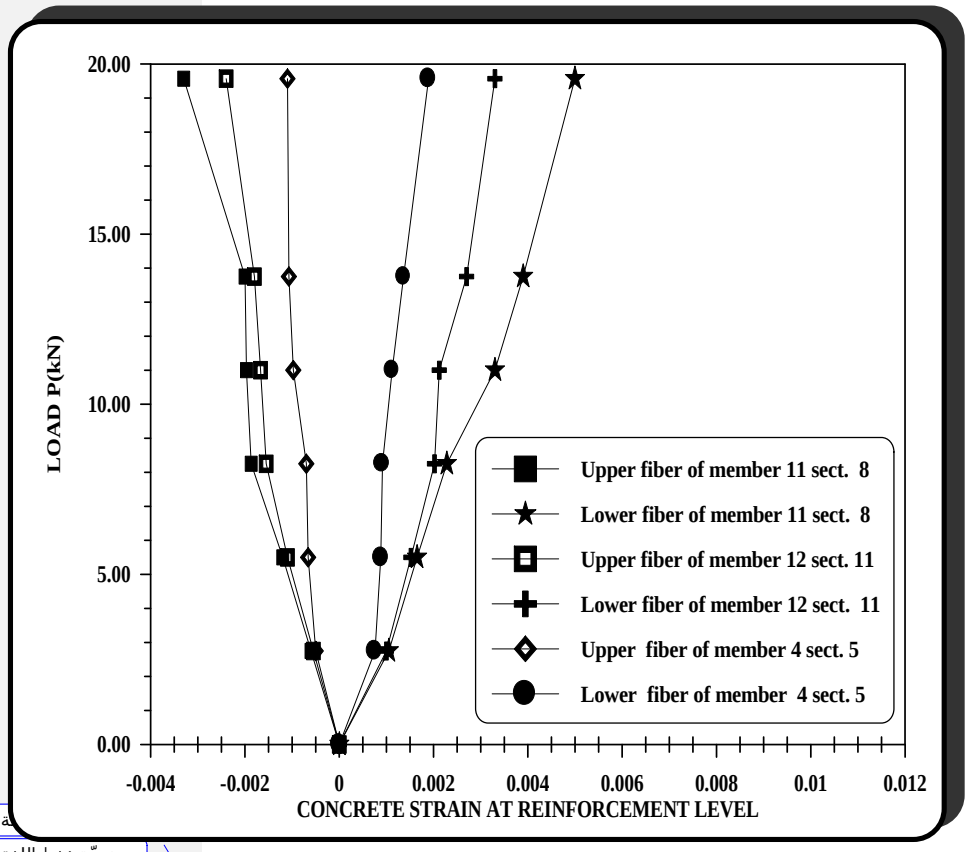

Fig. (7 – 5): Load – ~~strain~~ Strain ~~curves~~ Curves ~~for~~ for the

منسّق:خط اللغة العربية وغيرها: 10
منسّق:خط اللغة العربية وغيرها: 10

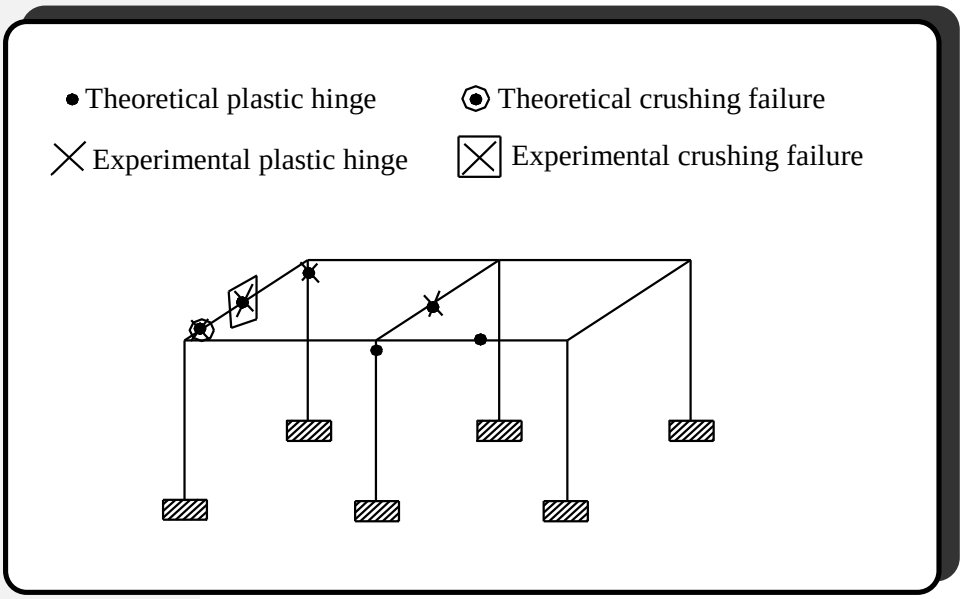

Fig. (7 – 6): Location of ~~plastic~~ Plastic ~~hinges~~ Hinges for the

Table (7 – 1): Moments and Axial Forces at Collapse for the Model

Member No.	Section No.	Axial force (~~KN~~kN)	M_y (~~KN~~kN.m)	M_z (~~KN~~kN.m)
1	1	9.39	0.90	-0.07
	2		2.97	0.13
2	2	-0.16	0.07	-0.13
	3		0.11	-0.96
3	3	23.46	-2.67	-1.05
	4		-0.93	-0.43
4	3	1.70	-0.10	2.03
	5		0.00	-3.04
	6		-0.08	-1.24

منسّق:خط اللغة العربية وغيرها: 10
منسّق:خط اللغة العربية وغيرها: 10
نقطة

5	6	9.97	-0.43	1.22
	7		-0.23	0.26

Table (7 – 1): Continued.~~Table (7 – 1): Moments and axial forces at collapse for the model~~

Member No.	Section No.	Axial force (~~KN~~kN)	M_y (~~KN~~kN.m)	M_z (~~KN~~kN.m)
6	9	9.71	2.53	0.75
	10		0.73	0.17
7	9	-0.001	0.07	-0.09
	12		0.12	-0.82
8	12	23.32	2.59	-0.008
	13		1.14	-0.14
9	12	2.46	-0.12	2.09
	14		-0.015	-2.98
	15		-0.09	-1.29
10	15	9.76	0.02	1.31
	16		-0.08	0.50
11	2	4.61	0.00	3.08
	8		0.00	-3.08
	9		-0.05	-3.14
12	3	4.89	0.006	3.06
	11		0.00	-3.08
	12		0.01	-3.08
13	6	0 .60	0.078	-0.095
	15		0.085	0.21

~~**Table (7 – 1): Continue.**~~

منسّق: خط اللغة العربية وغيرها: 10
منسّق: خط اللغة العربية وغيرها: 10
نقطة

7.3 Other Applications:

7.3.1 Frame (A1):

The portal frame (A1)~~,~~ shown in Fig. (7 – 7)~~,~~ was analyzed by **Mekha [~~25~~24]** following a mathematical programming method namely "**Imposed Rotation Method**", and by **Alwash [~~16~~15]** following non – linear incremental stiffness method of analysis. **Mekha** and **Alwash** considered both ~~model~~ modes of failure (local crushing failure and collapse mechanism failure) and included the possibility of local unloading. Also, **Mekha** considered ~~a~~ prismatic members and neglecting the geometric non – linearity while **Alwash** considered ~~a~~ prismatic members but considering geometric non – linearity. The frame is analyzed by the present proposed non – linear method of analysis by considering the geometric non – linearity and neglecting the possibility of local unloading. Since **Mekha** and **Alwash** adopted gross section properties during the analysis stages, the gross section properties are also adopted in the present analysis in order to verify the efficiency of the present method with the previous methods.

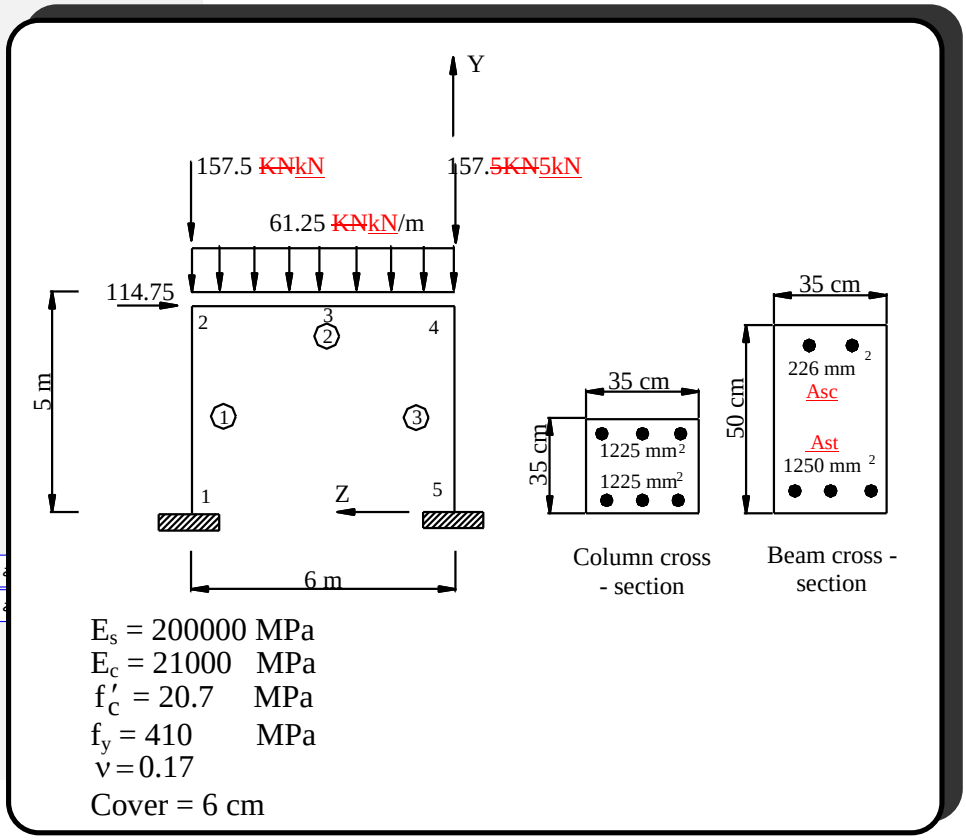

Fig. (7 – 7): Details of ~~frame~~ Frame (A1).

~~Section~~ Node

◯ Member No.

To examine the validity of the computer program, the frame in (Y – Z) plane is analyzed as a space frame since it ~~have~~ has the response of a space frame in (Y – Z) plane.

In each of the proposed method of analysis (I), non – linear method of analysis presented by **Alwash** (II) and Imposed Rotation Method (III), the type of failure is local crushing in element No.3 at node No.4 as shown in Fig. (7 – 8a). Also, the location of plastic hinges at collapse stage as indicated by the three methods, are shown in Fig. (7 – 8a). In the present method (I), the failure load factor is (0.~~864~~861), while in method (II) it is equal to (0.862) which is ~~smaller~~ greater by (0.~~23~~ 12 %) than method (I), and in method (III) it is equal to (0.915) which is greater by (~~55.90~~ 90 %) than method (I). The moment and axial force distribution at ($\lambda = 0.$~~864~~861) is given in Fig. (7 – 8b) for the three analysis approaches. The location of zero shear section in beam is being at distance (0.378 * 6 m) from the left column as indicated by the three methods.

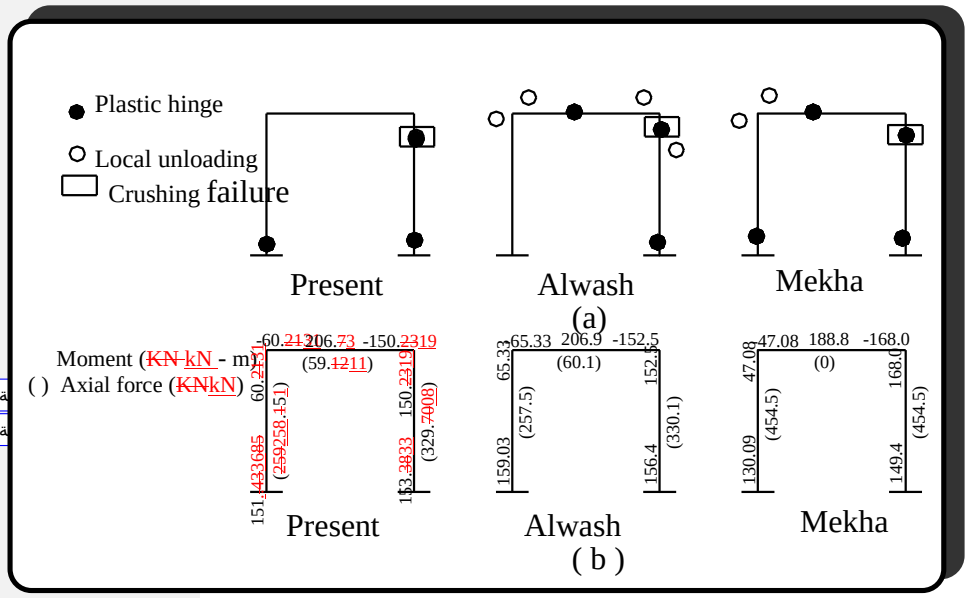

Fig. (7 – 8): (a) Location of ~~plastic~~ Plastic ~~hinges~~ Hinges for ~~frame~~ Frame (A1)

(b) Moments and ~~axial~~ Axial ~~forces~~ Forces ~~distribution~~ Distribution(at collapse) for ~~frame~~ Frame (A1).

It can be seen from the previous results of frame (A1) that, the values given by methods (II) and (III) are generally in good agreement with the values obtained from the proposed method. However, there are some differences which can be attributed to:

1- Local stress unloading which is neglected in method (I) while it was considered in methods (II) and (III).

2- Shear deformations and geometric non – linearity which are included in present method (I) while they were neglected in method (III).Also, bowing effect was neglected in methods (II) and (III) while it is considered in the present study.

منسقة: تعدادات نقطية ورقمية

3- The moment – axial interaction, which is considered in both beams and columns in the present method (I), was neglected for beams in method (III). In addition, the axial force that was considered for columns in method (III) was computed initially in approximate manner for load factor (^{a} = 1). In the present analysis, the axial forces are updated at each stage of analysis and after each plastic hinge formation (in either beams or columns).

7.3.2 Frame (A2):

The multistory multibay plane frame (A2) shown in Fig.(7 – 9) was analyzed by **Alwash [~~16~~15]** following a non – linear elastic – plastic analysis and by **Hashim [~~29~~27]** adopting plastic zone model with an incremental approach. Frame (A2) is analyzed by the present method of analysis by considering gross – section properties, as in the other two

منسّق: خط اللغة العربية وغيرها: 10

منسّق: خط اللغة العربية وغيرها: 10

نقطة

methods of analysis, in computing the flexural and axial stiffness of the members in order to show the effect of other parameters.

The present analysis (I) predicts a crushing failure in element No.1 at node No.1 at load factor ($\lambda = 3.126$) after 12 plastic hinges formation. The non – linear method of analysis (II) as proposed by **Alwash**, also, predicts crushing failure, but in element No.3 at load factor ($\lambda = 3.0886$) after 14 plastic hinges formation.

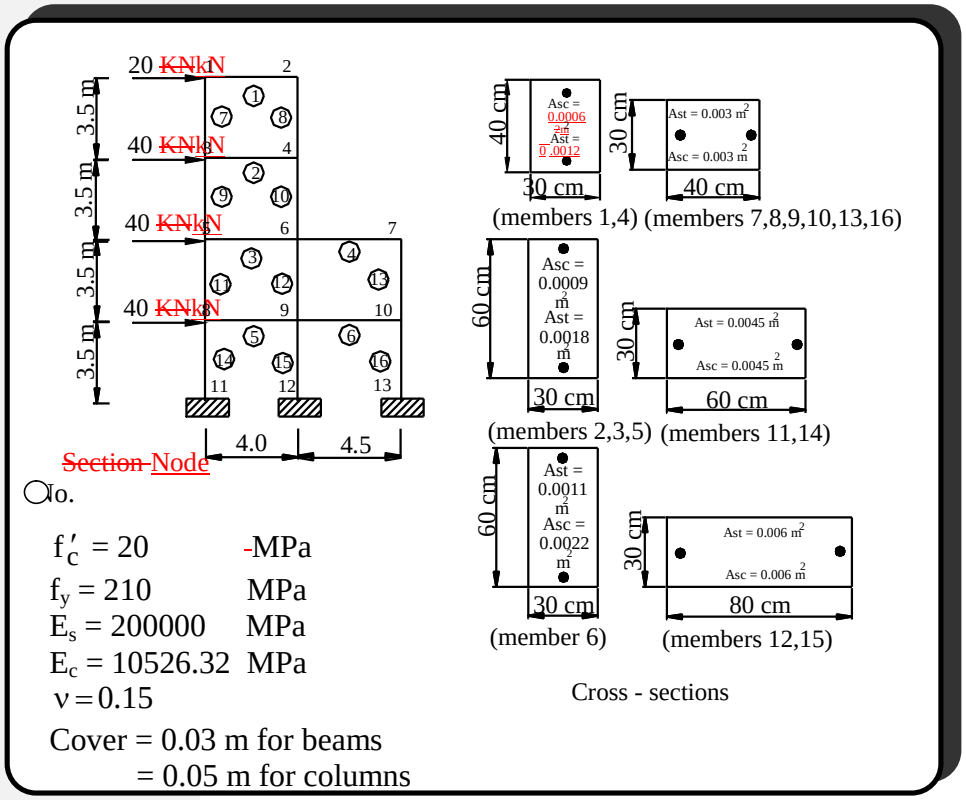

Fig. (7 – 9): Details of ~~frame~~ Frame (A2).

The incremental approach of **Hashim** (III) predicts a crushing failure in element No.4 at load factor ($\lambda = 3.1019$) after 13 plastic zones formation. Fig. (7 – 10a) shows the plastic hinges (zones in method (III)) distribution obtained from the three analysis approaches. Fig. (7 – 10b) gives the moment distribution at collapse for the three methods. Fig. (7 – 10b) shows some differences in moment values which can resulted from:

منسّق: خط اللغة العربية وغيرها: 10
منسّق: خط اللغة العربية وغيرها: 10
نقطة

1- Local stress unloading, which is neglected in the present method while it was considered in methods (II) and (III).

2- The geometric non – linearity, which is considered accurately in the present method while it was considered in method (III) in a simplified manner. ~~in~~ In addition, methods (II) and (III) neglected the bowing effect while it was considered well in the present method.

3- In the present method (I), the shear deformation~~s~~ is considered through the derivation of ~~a~~ more ~~exact~~ accurate expressions for the stability functions while it was neglected in method (III).

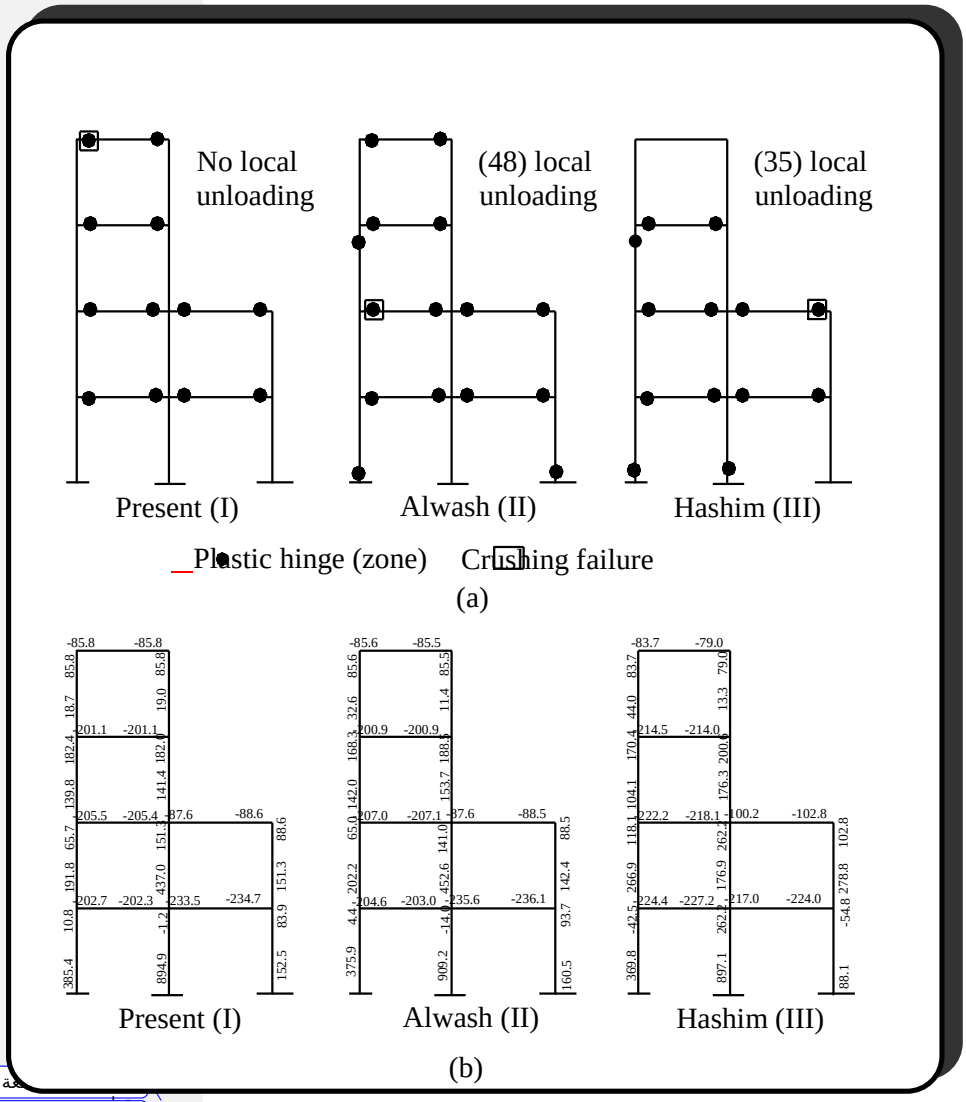

Fig. (7 – 10): (a) Location of ~~plastic~~ Plastic ~~hinges~~ Hinges for ~~frame~~ Frame (A2).

(b) Moment ~~distribution~~ Distribution at ~~collapse~~

The load – deflection curves are presented in Fig. (7 – 11) showing ~~a~~ very good agreement ~~between~~ for the three analysis approaches. However, considering the geometric non – linearity in addition to shear deformation produces a failure load factor ($\lambda = 3.126$), while neglecting the effect of geometric non – linearity produces a final load factor ($\lambda = 3.146$) which is greater by (0.64 %) than the full effect. The effect of shear deformations and bowing are not significant (i.e. no important difference in final load factor).

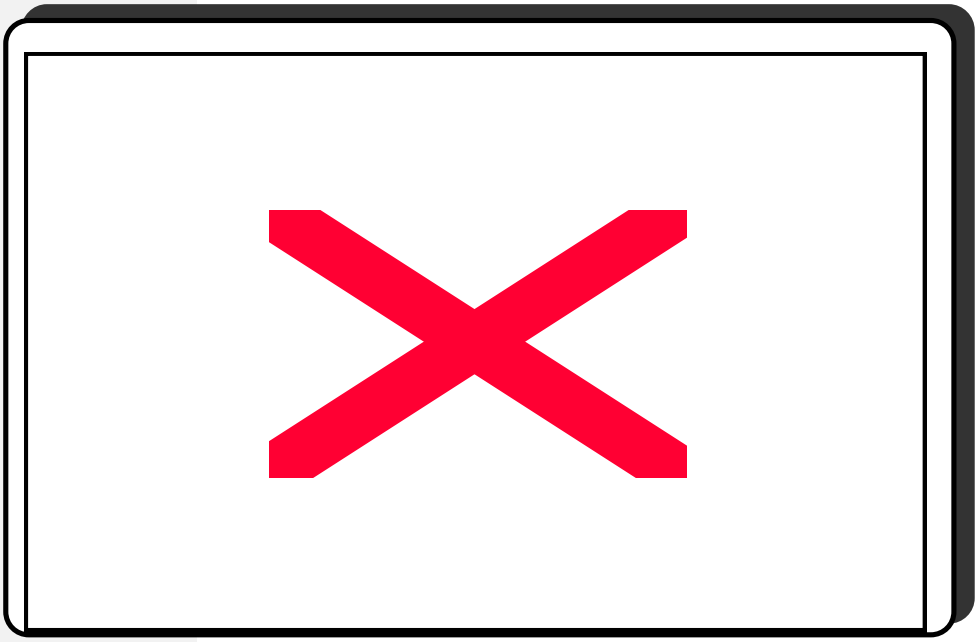

Fig. (7 – 11): Load – ~~deflection~~ Deflection ~~curves~~ Curves for ~~frame~~ Frame (A2)

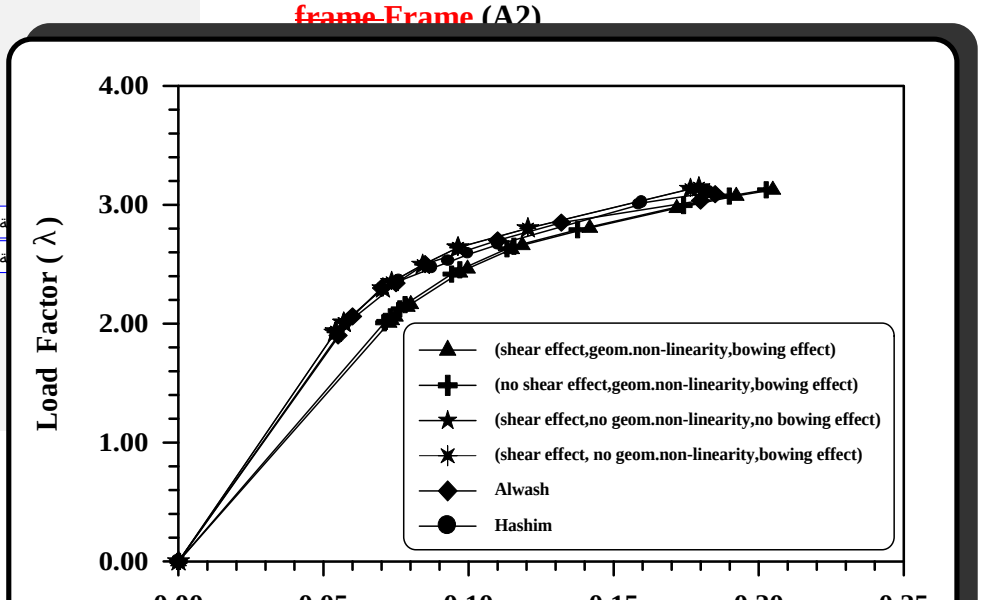

7.3.3 Frame (A3):

The rectangular frame (A3) shown in Fig. (7 – 12)~~,~~ was tested by **Furlong** and **Ferguson [6]** and ~~analysis~~ analyzed by **Gunnin et al [6]**. This frame is analyzed by the proposed method. An additional critical section "Joint" was placed at mid – height of the columns in order to account for magnification of bending moments in the columns due to axial load.

Fig. (7 – 13) shows the load – deflection curves at the mid – height of the left column as obtained from the proposed and other studies, and also ,it shows the effect of geometric non – linearity. It can be seen from Fig.(7 –13) that the effect of geometric non – linearity is rather significant. In other words, considering the effect of geometric non – linearity produces a failure load P (1+ α) = ~~259~~267.~~52~~ 51 ~~KN~~kN, while neglecting the effect of geometric non – linearity produces a failure load P (1+ α) = ~~269~~309.89~~.84~~ ~~K~~kN~~N~~ which is greater by (~~3.98~~15.84 %).

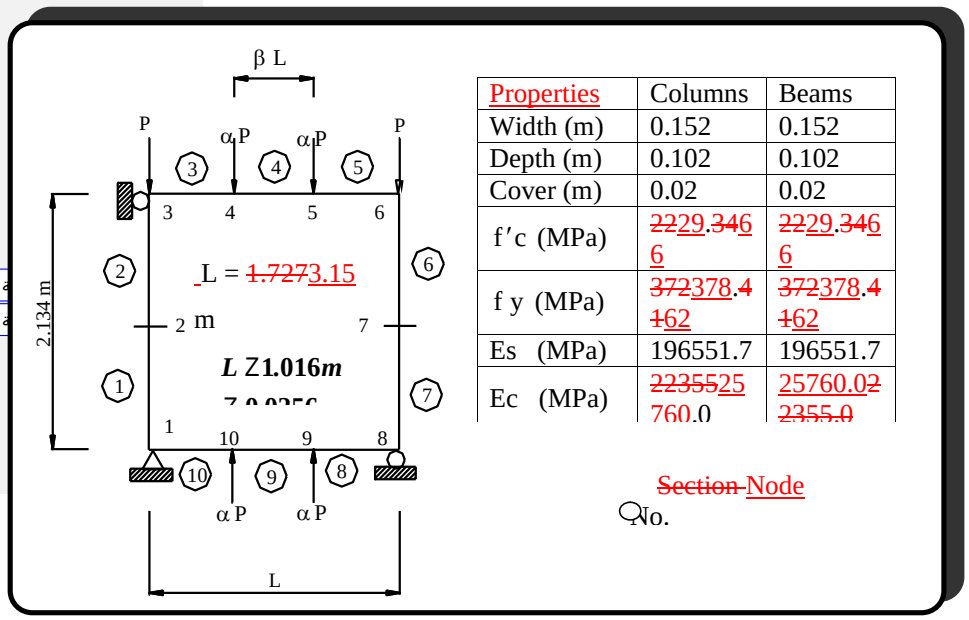

Properties	Columns	Beams
Width (m)	0.152	0.152
Depth (m)	0.102	0.102
Cover (m)	0.02	0.02
f′c (MPa)	~~22~~29.~~34~~66	~~22~~29.~~34~~66
f y (MPa)	~~372~~378.~~4~~ ~~1~~62	~~372~~378.~~4~~ ~~1~~62
Es (MPa)	196551.7	196551.7
Ec (MPa)	~~22355~~25760.0	25760.02 ~~2355.0~~

~~Section~~ Node No.

Fig. (7 – 12): ~~details~~ Details of ~~frame~~ Frame

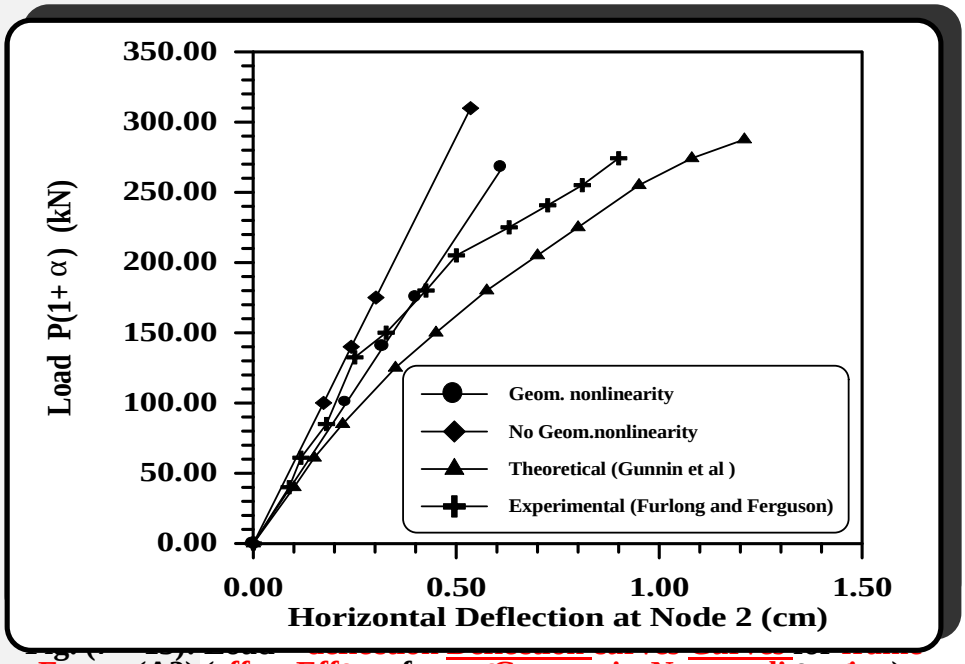

Fig. (7 – 13): Load – ~~deflection~~ Deflection ~~curves~~ Curves for ~~frame~~ Frame (A3) (~~effect~~ Effect of ~~geom~~Geometric. ~~Non~~non-linearity.).

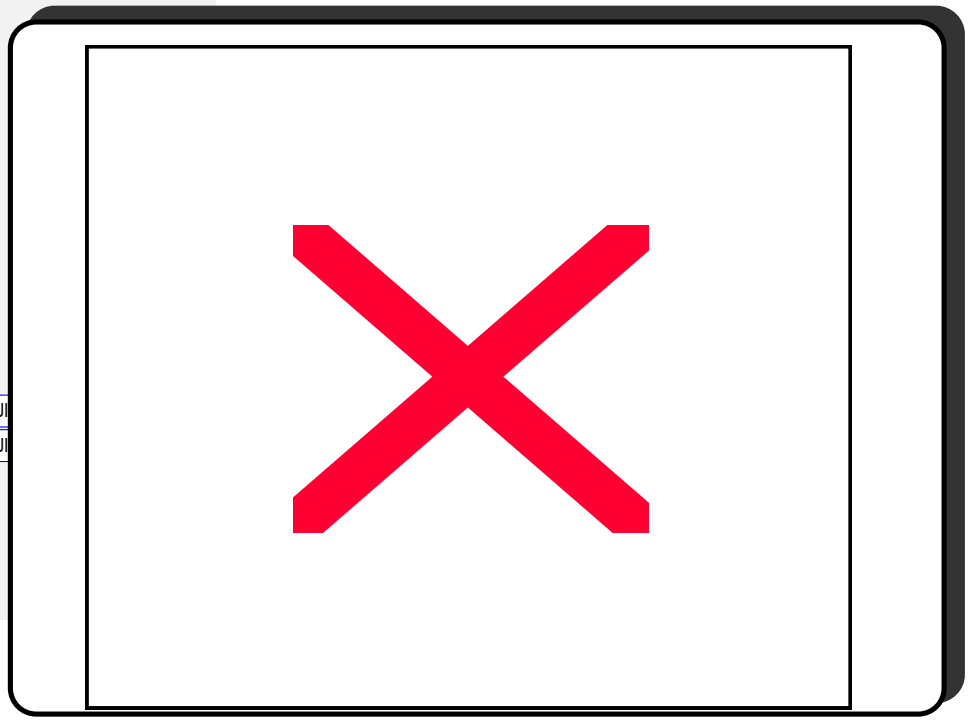

Fig. (7 – 14): Load – ~~deflection~~ Deflection ~~curves~~ Curves for ~~frame~~ Frame (A3) (~~effect~~ Effect of ~~selection~~ Selection of ~~section~~ Section

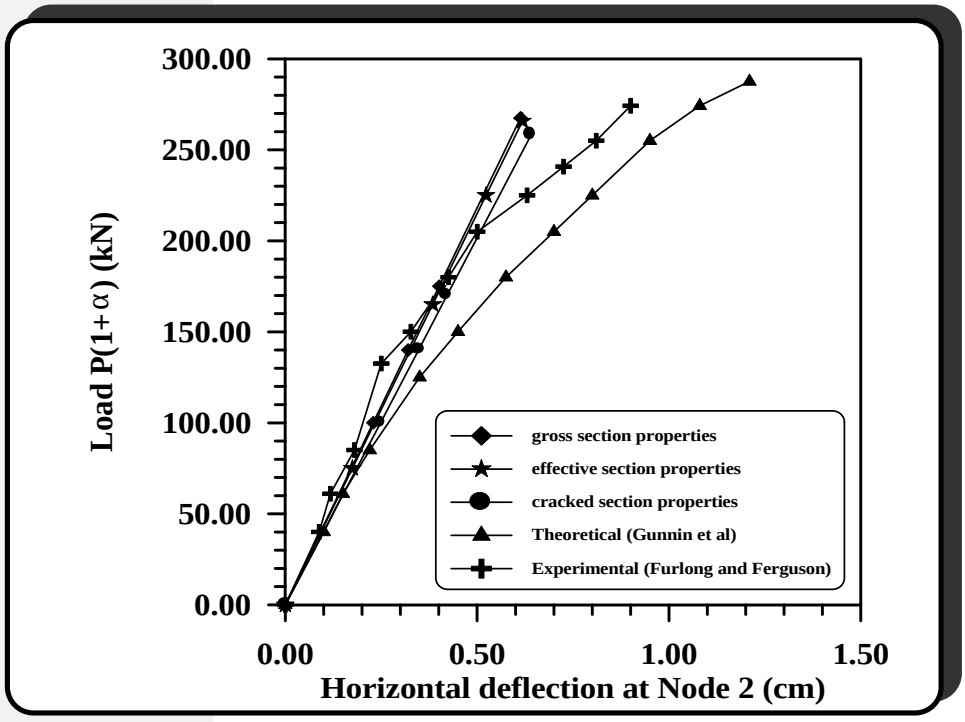

Fig. (7 – 14): Load – ~~deflection~~ Deflection ~~curves~~ Curves for ~~frame~~ Frame (A3) (~~effect~~ Effect of ~~selection~~ Selection of ~~section~~ Section

In Fig. (7 – 14), the effect of the selected section properties on the resulting behavior is considered. It may be ~~stated~~ noted that the cracked section properties, gross section properties and effective section properties ~~is~~ are ~~conservative~~ close to each other since the axial compressive forces in the columns limit the development of tensile cracking at the mid height of the columns. ~~and better than the effective section properties in obtaining the flexure and axial stiffness of members~~

منسّق:خط اللغة العربية وغيرها: 10
منسّق:خط اللغة العربية وغيرها: 10
نقطة

~~as shown in Fig. (7 – 14). Considering the effective section properties give a failure load~~

~~P(1+ α)=237.056 KN, while adopting cracking section properties produce a failure load P(1+ α)=229.31 KN which lesser by (3.26 %).~~

Frame (A3) fails, in the present analysis, by crushing ~~failure~~ at node No.7 after one plastic hinge formation at the mid height of the right column at column load (P (1+ α) = ~~229.31~~265.732 ~~KN~~kN) (considering effective section properties), while the experimental failure column load is (P (1+ α) =~~233.5~~274.18 ~~KN~~kN)~~.~~ (by **Furlong** and **Ferguson**) and theoretically at column load (P (1+ α) = ~~199.7~~287.53 ~~KN~~kN) (by **Gunnin et al**).It can be seen from Figures (7-13) and (7-14) that the proposed method of analysis is in good agreement with the experimental results.

7.3.4 Frame (A4) (horizontal steel bent):

The two member horizontal bent shown in Fig. (7 – 15)~~.~~ ~~Was~~ was analyzed previously by **Al ~~asady~~ Asady [~~17~~16]** and by **Kassimali [~~17~~16]**. In both analyses, **Kassimali's** joint orientation matrix was used. The structure is analyzed by the proposed method following an incremental elastic analysis. The load – deflection curve is plotted as shown in Fig. (7 – 16) and rather good agreement between the present study and other works is obtained. The maximum deflection at point (c) obtained from the proposed method is larger than that obtained from other works by (10.41 %).

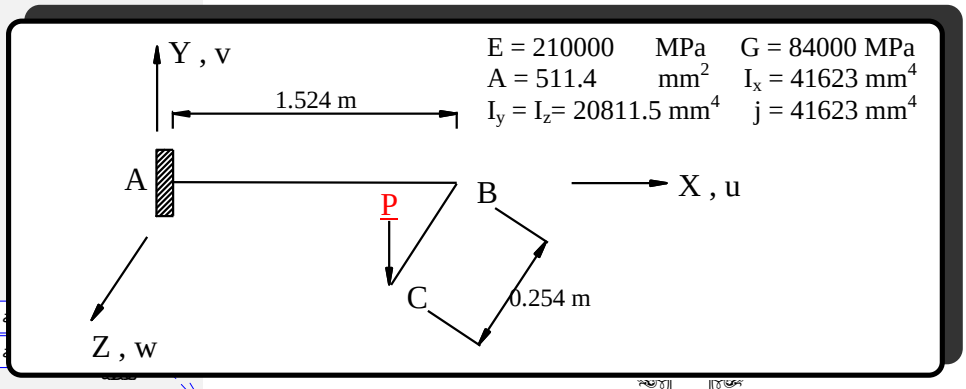

Fig. (7 – 15): Geometry of ~~frame~~ Frame (A4).

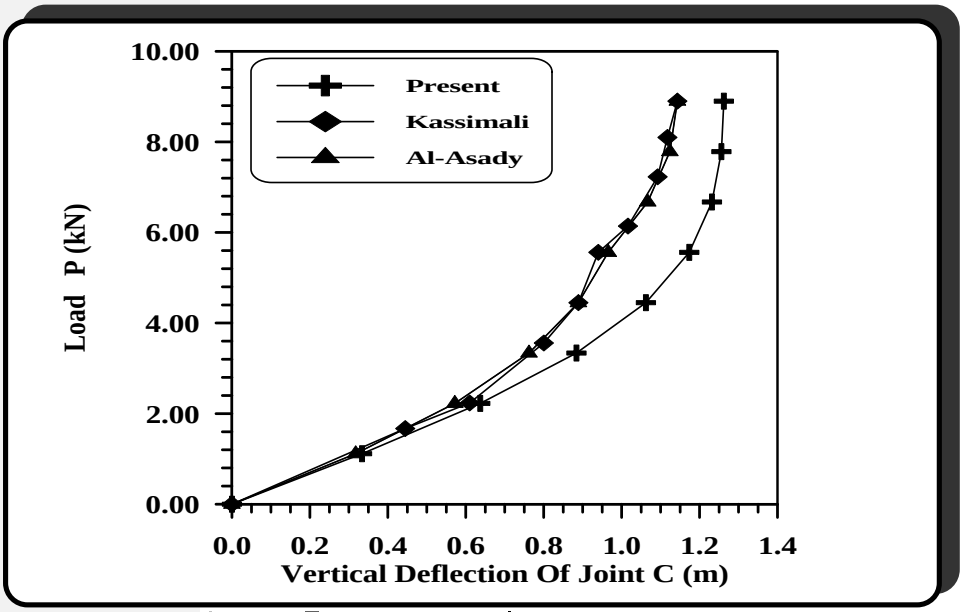

Fig. (7 – 16): Load – ~~deflection~~ Deflection ~~curves~~ Curves for ~~frame~~ 7.3.5 Frame (A5).

— The one – bay, one story space frame shown in Fig. (7 – 1~~7~~6)~~,~~ is analyzed by the proposed method. Initially the frame is analyzed by including the full effect (i.e. geometric non – linearity, shear and bowing deformations). The frame fails by crushing ~~failure~~ at element No.7 at node No.6 at a load factor (λ ~~=~~ 2.116). In order to study the effect of shear deformations, the frame is then analyzed by neglecting only the shear deformations. The frame fails at a load factor (λ = 2.115) by crushing ~~failure~~ at element No.7 at node No.6. There is no significant ~~deference~~ difference in load factor but the vertical deflection at node No.9 is less~~er~~ than the full effect by (2.78 %), while the transverse displacement of node No.6 is reduced by (1.48 %). Also, to ~~verify~~ assess the effect of geometric non – linearity, the frame is analyzed as in the initial case but the geometric non – linearity is neglected. The frame, in

منسّق:خط اللغة العربية وغيرها: 10
منسّق:خط اللغة العربية وغيرها: 10
نقطة

general, is found to be rather stiffer and it failed by crushing ~~failure~~ at element No.10 at node No.4 at a load factor equal to (1.997), i.e. the load factor decreased by (5.62 %) while the vertical deflection at node No.9 is increased by (42.81 %). Similarly, ~~-~~ the transverse displacement of node No.6 is increased by (5.18 %). ~~At last~~Finally, to study the effect of bowing deformations on the frame behavior, the frame is analyzed as in the third case (i.e. neglecting the geometric non – linearity but including the bowing effect). The effect of bowing is found to be insignificant since there is no ~~deference~~difference in frame deflections. Figures (7 – 1~~8~~7) and (7 – 1~~9~~8) represent the load – deflection curves at nodes (9 and 6) respectively for all the analysis cases as mentioned before.

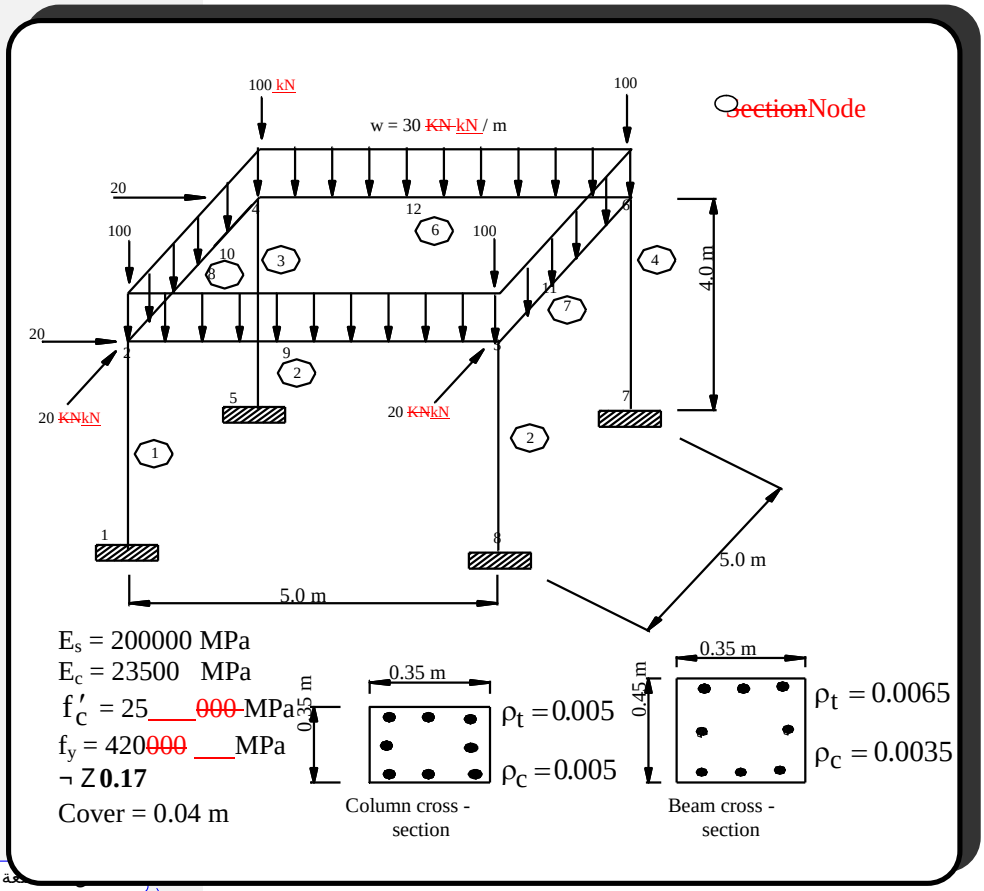

Fig. (7 – 1~~7~~6): Details of ~~frame~~ Frame (A5).

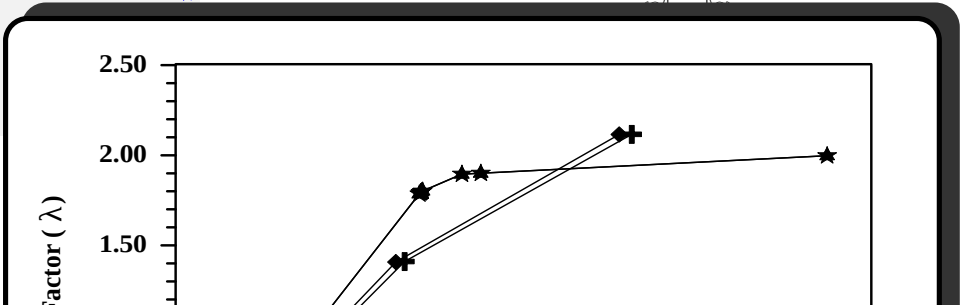

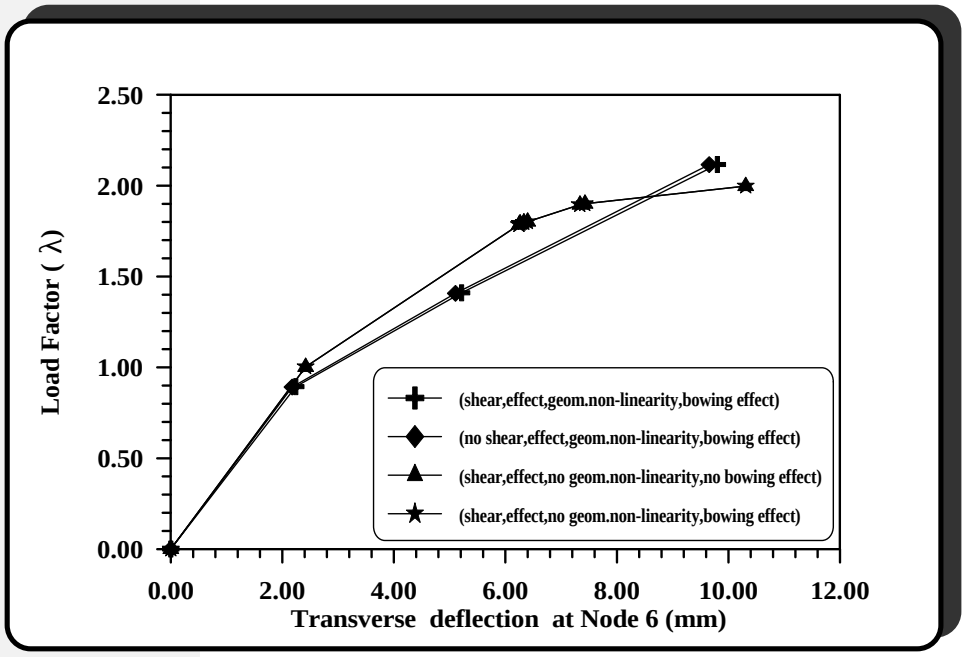

Fig. (7 – ~~18~~19): Load – ~~deflection~~ Deflection ~~curves~~ Curves for

The locations of plastic hinges and axial forces and moments distribution at collapse are shown in Fig. (7 – 20~~19~~) and ~~table~~ Table (7 – 2) respectively.

منسّق:خط اللغة العربية وغيرها: 10
منسّق:خط اللغة العربية وغيرها: 10
نقطة

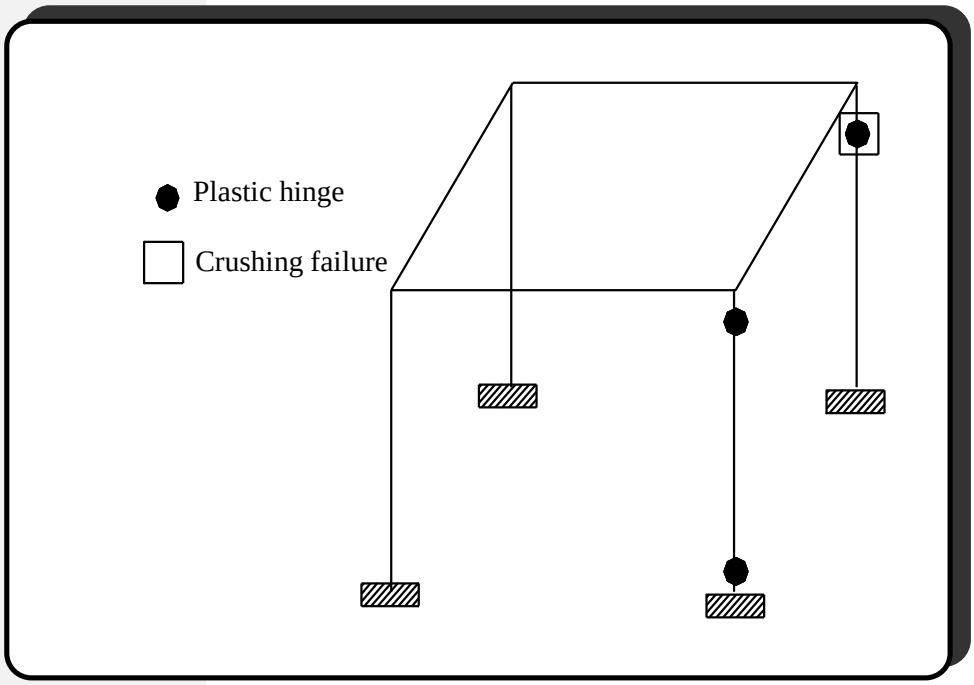

Fig. (7 – ~~19~~20): Location of ~~plastic~~ Plastic ~~hinges~~ Hinges for ~~frame~~ Frame

Table (7 – 2): Axial ~~force~~ Forces and ~~bending~~ Bending ~~moments~~ Moments at ~~collapse~~ Collapse ~~stage~~ Stage for ~~frame~~ Frame

Member No.	Section No.	Axial force (KN)	M_y (KN.m)	M_z (KN.m)
1	1	499.53	-16.32	51.57
	2		41.48	-23.70
2	3	534.36	-25.00	87.84
	8		40.48	106.48
3	4	541.85	-25.23	-66.93
	5		13.38	-74.29
4	6	540.64	49.51	49.51
	7		42.68	-26.38
5	2	41.76	-12.73	23.00
	9		1.21	148.24
	3		-12.73	-82.12
6	4	35.85	-12.79	30.85

منسّق:خط اللغة العربية وغيرها: 10
منسّق:خط اللغة العربية وغيرها: 10
نقطة

	12		-1.18	-155.97
	6		-12.83	-55.23
7	3	34.73	11.08	32.39
	11		1.03	-150.71
	6		11.12	-65.26
8	2	54.48	11.06	34.08
	10		1.02	-123.75
	4		11.14	-122.43

7.3.6 Frame (A6):

The one bay, two-story space frame shown in Fig. (7 – ~~20~~21)~~,~~ is analyzed by using the proposed approach. First the frame is analyzed by considering ~~each of~~ geometric non – linearity, shear and bowing deformations. The frame fails by crushing at element No.3 at node No.4 at load factor ($\lambda = 2.343$).

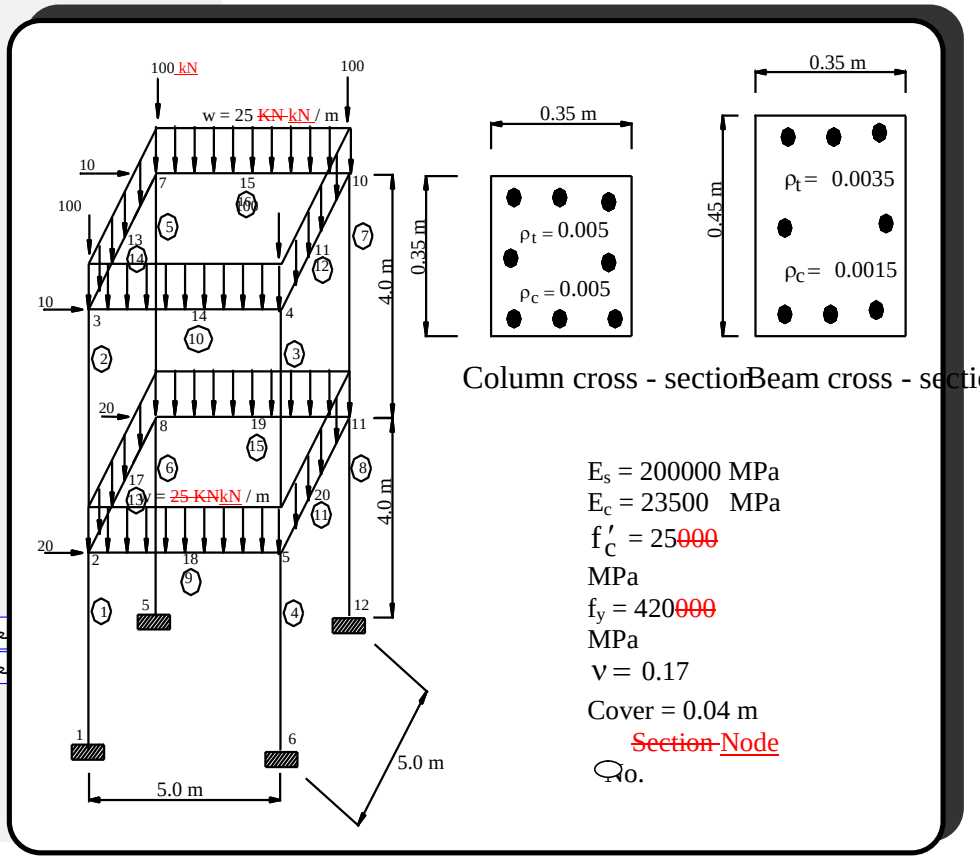

Fig. (7 – 2~~1~~0): Details of ~~frame~~ Frame (A6).

The analysis is repeated to study the effect of shear deformations. It is found that including the shear deformations- increases the final horizontal deflection of node No.4 by (1.88 %). To verify the effect of geometric non – linearity on the behavior of the frame, the frame is analyzed by including all effects except the geometric non – linearity. It is concluded that including the geometric non – linearity increases the deflection of node No.4 by (6.94 %). Also, it is found that including the bowing effect on the axial stiffness is insignificant. The load – deflection curves for the frame for the prescribed cases is shown in Fig. (7 – ~~21~~22). The locations of plastic hinges are shown in Fig. (7 – ~~22~~23), while the axial forces and bending moments at collapse stage are given in ~~table~~ Table (7 – 3).

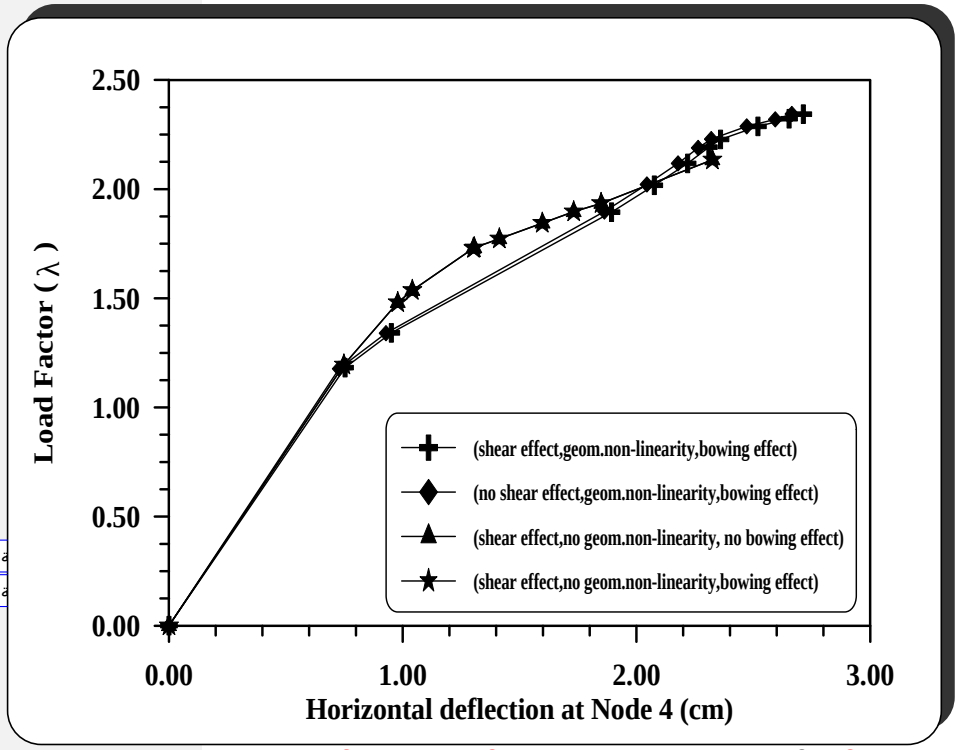

Fig. (7 – ~~21~~22) Load-~~deflection~~ Deflection ~~curves~~ Curves for ~~frame~~ Frame (A6)

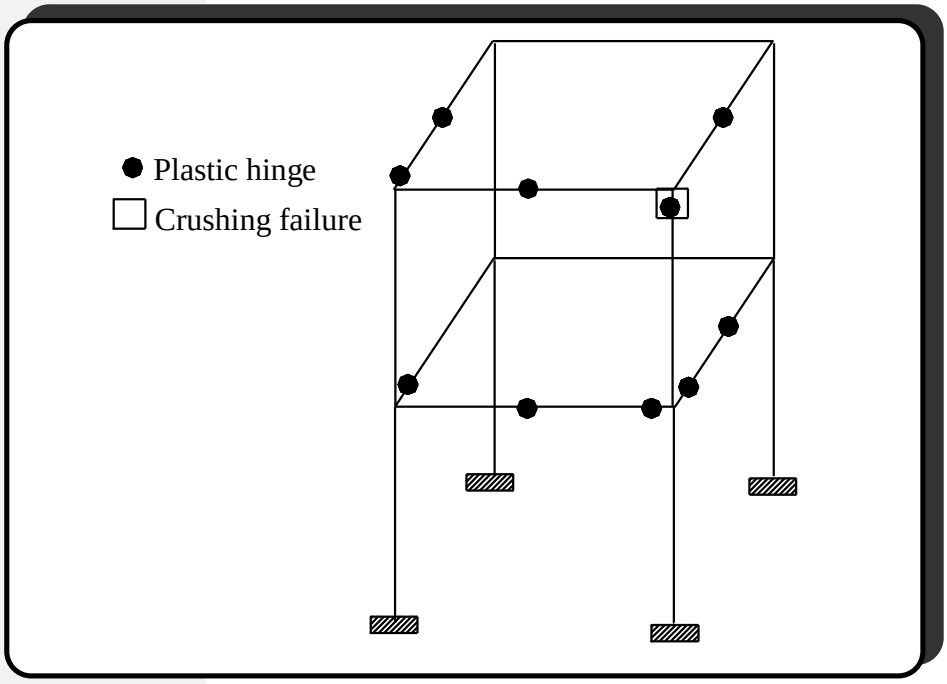

Fig. (7 – 2~~32~~): Locations of ~~plastic~~ Plastic ~~hinges~~ Hinges for ~~frame~~ Frame

Table (7 – 3~~):~~: Axial ~~force~~ Forces and ~~bending~~ Bending ~~moments~~ Moments at ~~collapse~~ Collapse ~~stage~~ Stage for ~~frame~~ Frame

Member No.	Section No.	Axial force (~~KN~~kN)	M_y (~~KN~~kN.m)	M_z (~~KN~~kN.m)
1	1	806.72	30.47	79.72
	2		24.63	20.52
2	2	522.47	90.68	-29.82
	3		136.63	-29.79
3	4	525.87	-44.46	62.75
	5		-70.15	45.90

منسّق:خط اللغة العربية وغيرها: 10
منسّق:خط اللغة العربية وغيرها: 10
نقطة

4	5	836.62	-9.28	59.93
	6		-7.23	99.15
5	7	505.32	-18.03	-3.07
	8		9.97	-15.87
6	8	737.45	18.89	-18.28
	9		24.79	-25.84
7	10	555.32	-43.00	-10.76
	11		7.15	-19.91
8	11	899.76	-8.09	-11.68
	12		-.213	-20.39
9	2	9.96	-5.36	18.68
	18		0.00	-120.62
	5		0.00	-91.89
10	3	33.22	18.52	34.67
	14		0.45	-129.26
	4		20.58	-75.84
11	5	-23.92	0.00	83.35
	20		0.00	-95.02
	11		6.18	-89.61

Table (7 – 3): Continued.

Member No.	**Section No.**	**Axial force (~~KN~~kN)**	**M_y (~~KN~~kN.m)**	**M_z (~~KN~~kN.m)**
12	4	34.27	-22.66	76.52
	16		0.00	-91.13
	10		-22.55	-124.75
13	2	-41.88	0.00	111.40
	17		-0.84	-94.03

منسّق:خط اللغة العربية وغيرها: 10
منسّق:خط اللغة العربية وغيرها: 10
نقطة

	8		6.47	-63.87
14	3	47.53	0.00	104.56
	13		0.00	-92.19
	7		-19.56	-88.60
15	8	-4.26	-8.22	-30.12
	19		-2.12	-105.35
	11		-7.52	-224.10
16	7	48.98	19.35	31.79
	15		0.47	-108.57
	10		21.73	-123.91

7.3.7 Frame (A7):

Using the proposed method of analysis, the two – bay, ~~One~~ one story space frame shown in Fig. (7 – 2~~43~~) is analyzed. First, the frame is analyzed by including the effect ~~of each~~ of geometric non – linearity and shear deformations. The frame fails by crushing ~~failure~~ at element No.2 at node No.3 at load factor (λ = 2.767). The locations of plastic hinges and crushing failure are shown in Fig. (7 – 2~~5~~4). To study the effect of shear deformations on the behavior of the frame, the frame is analyzed first by considering shear deformations and neglecting the geometric non – linearity. Then the frame is analyzed by neglecting ~~each of~~ geometric non –linearity and shear defo-

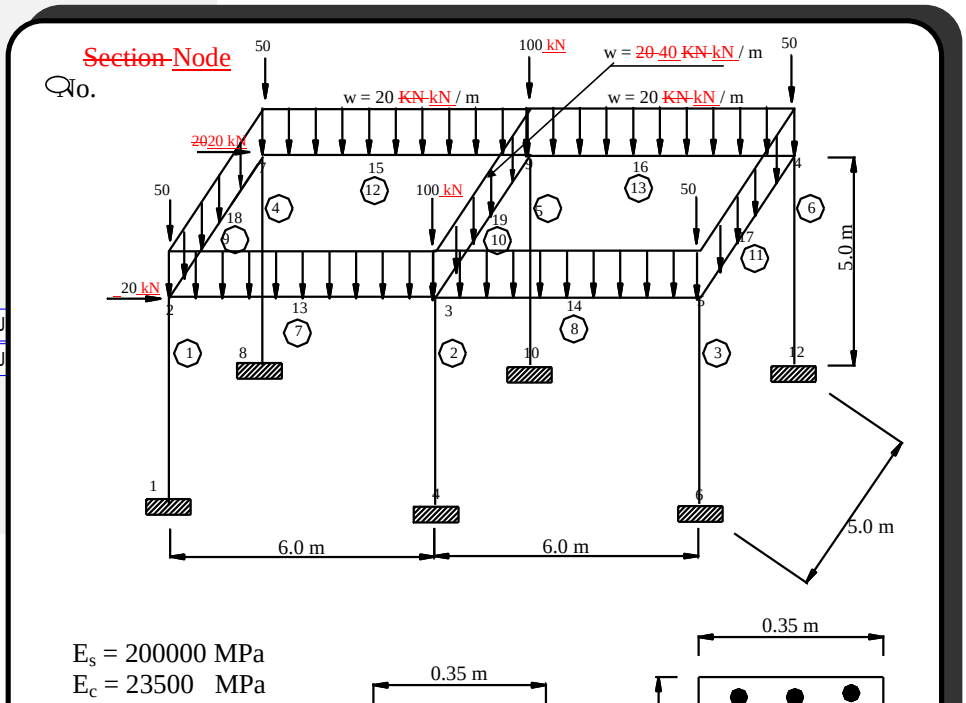

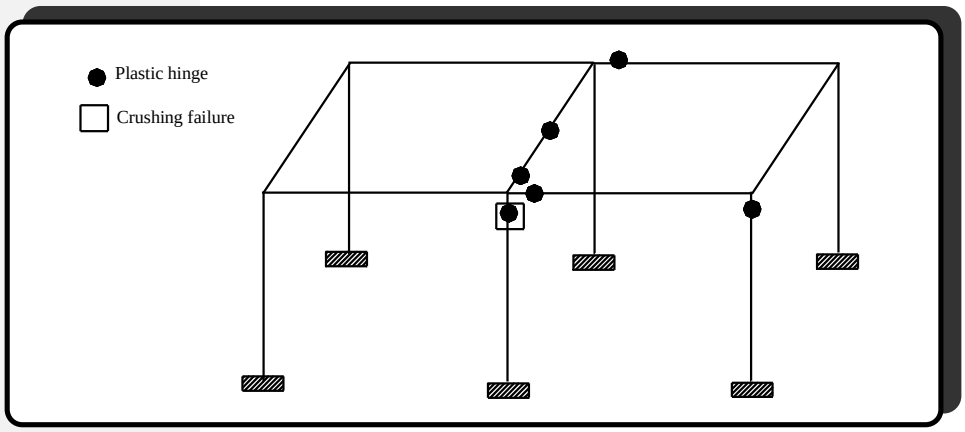

Fig. (7 – ~~24~~25): Locations of ~~plastic~~ Plastic ~~hinges~~ Hinges

~~linearity and shear defor~~mations. It is found that including the effect of shear deformations increase<u>s</u> the final vertical deflection of node No.19 by (6.29%).Also, it is found that including the effect of geometric non<u>-</u>linearity increase<u>s</u> the deflection of node No.19 by (29.87%). To ~~verify~~ <u>assess</u> the effect of bowing deformation~~s~~ on axial stiffness, the analysis is repeated and it is found that its effect is negligible. In other words,

منسّق:خط اللغة العربية وغيرها: 10
منسّق:خط اللغة العربية وغيرها: 10
نقطة

including the bowing effect increases the final deflection of node No.19 by (0.087 %). The load – deflection curves for all the analysis cases are shown in Fig. (7 – 2526).

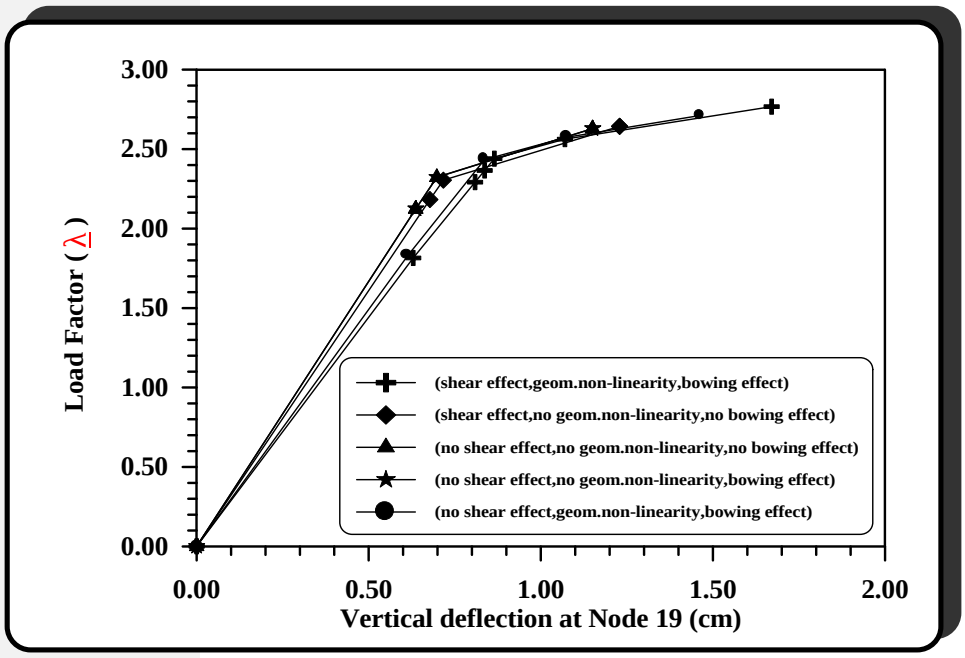

Fig. (7 – 2526) Load-deflection Deflection curves Curves for frame Frame (A7)

7.4 Results of Optimal Design Problems:

To show the ability and the validity of the optimization problem formulation, four examples of reinforced concrete structures are selected as follows:

1- Example (O1): two – bay, portal frame.

2- Example (O2): one – bay, one – story space frame.

3- Example (O3): one – bay, two – story space frame.

4- Example (O4): two – bay, one – story space frame.

Figure (7–2527) shows the geometry of each frame. In all examples, the following general data is used:

منسّق:خط اللغة العربية وغيرها: 10
منسّق:خط اللغة العربية وغيرها: 10
نقطة

E_s = 200000 N / mm^2 , f_y = 420 N / mm^2

E_c = 23500 N / mm^2 , f'_c = 25 N / mm^2

W_c = 24 ~~KN~~ kN / m^3 , W_s = 78.5 ~~KN~~ kN / m^3

C_s = 200 units / ton , C_c= 10 units / m^3

C_f = 1 unit / m^2

The initial dimensions and reinforcements are given in ~~table~~ Table (7 – 4).

Table (7 – 4): Initial Dimensions and Reinforcements for the Design Examples

Example No.	$b_{initial}$ (mm)	$h_{initial}$ (mm)	$\rho = A_{sT} / bh$
O1	300	600	0.0114
O2	300	600	0.0114
O3	300	600	0.0114
O4	350	650	0.0114

منسّق:خط اللغة العربية وغيرها: 10
منسّق:خط اللغة العربية وغيرها: 10
نقطة

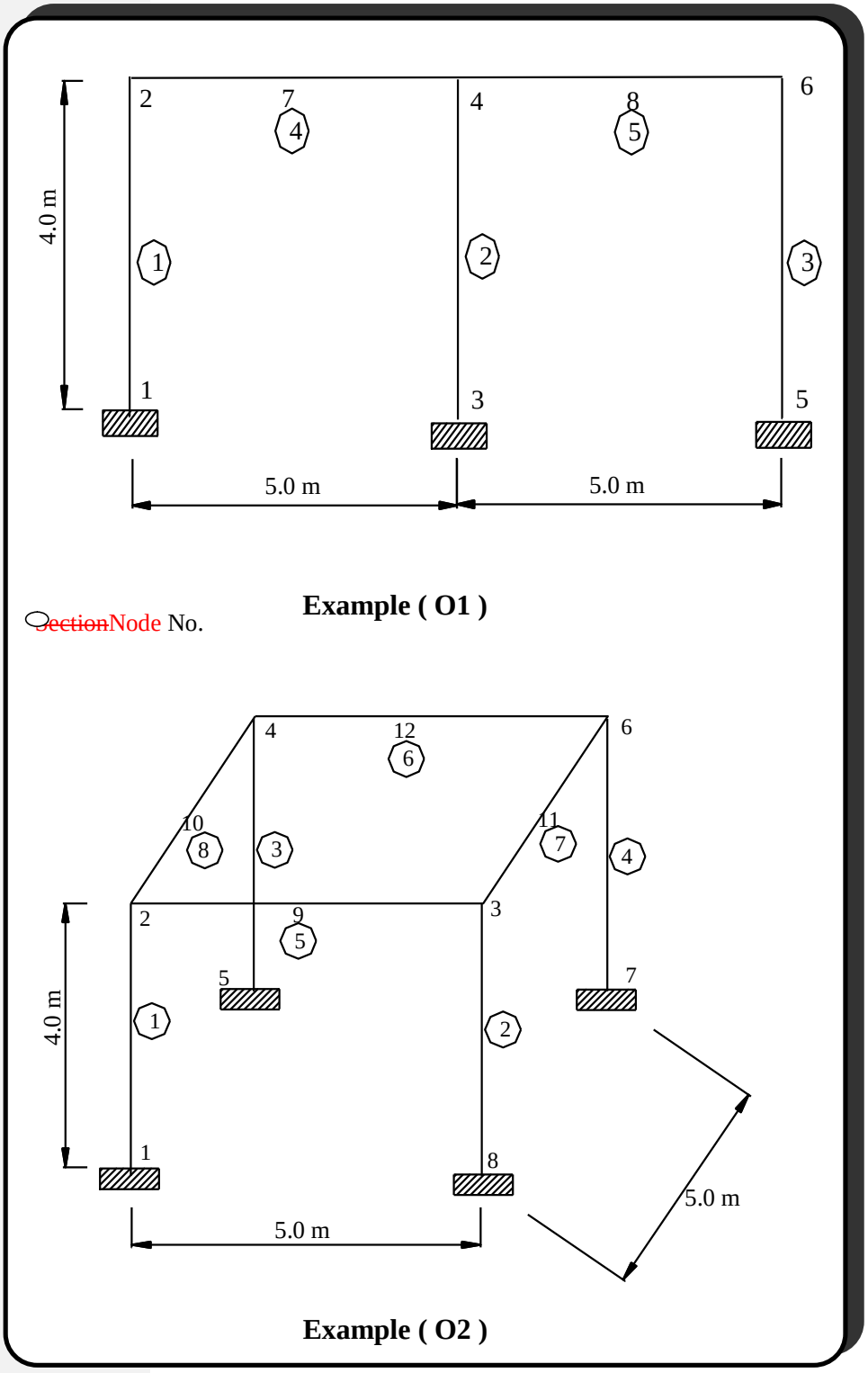

Fig. (7 – ~~26~~27): Structural

منسّق:خط اللغة العربية وغيرها: 10
منسّق:خط اللغة العربية وغيرها: 10
نقطة

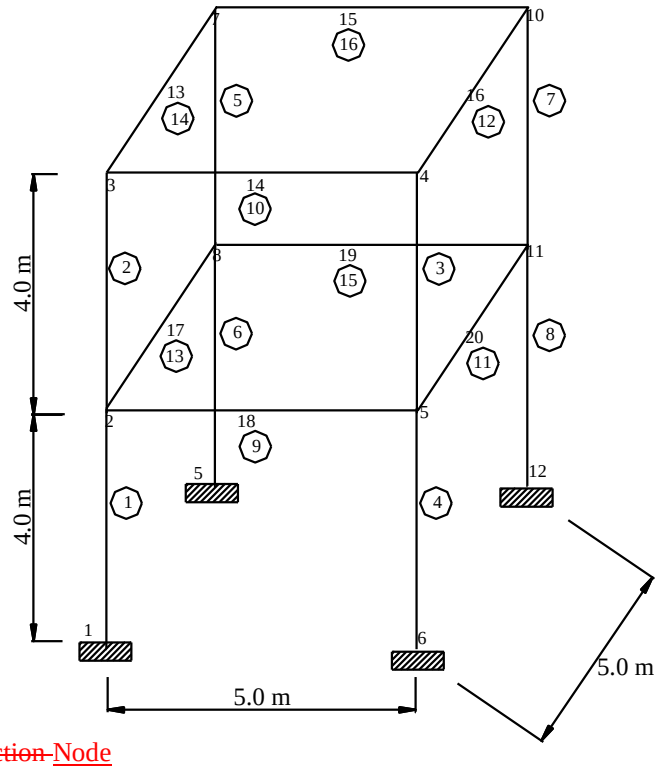

~~Section~~ Node No.

Example (O3)

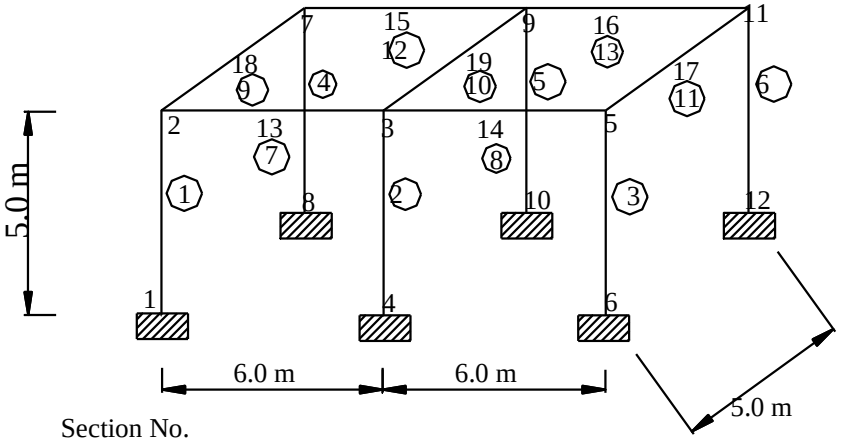

Section No.
Member

Example (O4)

منسّق:خط اللغة العربية وغيرها: 10
منسّق:خط اللغة العربية وغيرها: 10
نقطة

Fig. (7 – ~~26~~27): Continued

In the absence of earthquake load, the sources of loads are dead load, live load and wind load. Typical arrangements of live loads are considered from intuition to high-light maximum effects. Wind is considered to act in any direction. Figure (7–~~27~~28) shows the load applications. The load combinations used are:

$$U = 0.75(1.4D.L. + 1.7L.L. + 1.7W.L.)$$
$$U = 1.4D.L. + 1.7L.L.$$

At the end of the optimization process, the structure under optimization is analyzed under service loading to check the deflection requirements.

The results are presented in ~~figures~~ Figures (7 – ~~28~~29) - (7 – ~~31~~32) and ~~tables~~ Tables (7 – 5) – (7 – 9). Figures (7 – ~~28~~29) – (7 – ~~31~~32) show the variation of total cost with the number of optimization cycles for examples (-O1, O2, O3 and O4-). It can be seen from these figures that~~,~~ inelastic analysis gives more economical cost than the elastic analysis. This is to be excepted because the inelastic analysis utilizes the ability of the frame to re – distribute moments. The saving in cost resulting from adopting the inelastic ~~,~~analysis, however, is seen to be in the range between (1.50% - 6.04%) only. This can be explained by the fact that the side constraints referring to minimum dimensions and minimum steel ratios often limit the possibility of obtaining greater saving.

Table (7– 5) gives the number of cycles required for the optimal solution, initial cost and optimal cost for both types of analysis (elastic and inelastic). Tables (7–6) – (7 – 9) give the optimal design parameters for the structural examples.

منسّق:خط اللغة العربية وغيرها: 10
منسّق:خط اللغة العربية وغيرها: 10
نقطة

Tables (7–6) to (7–9) show that the optimal design of width of most members is governed by the side limit (250 mm). Also, it can be noted that the optimum steel percentage for main reinforcement is close to (1.0 %) for most members in all structural examples. From ~~table~~ Table (7 – 10), the deflection constraints ~~is~~ are obviously ineffective since the computed deflection under live load is smaller than the allowable value (~~L / 240~~ ***L* / 240**) **[38]**.

In all design examples considered in the present work, the effect of torsion can be neglected since it is less than the lower limit specified by the ACI-Code. Also, from the presented results of the optimization problems, it can be seen that the (**Direct Search Method**) is quite stable and the optimal solution is reached only after several cycles.

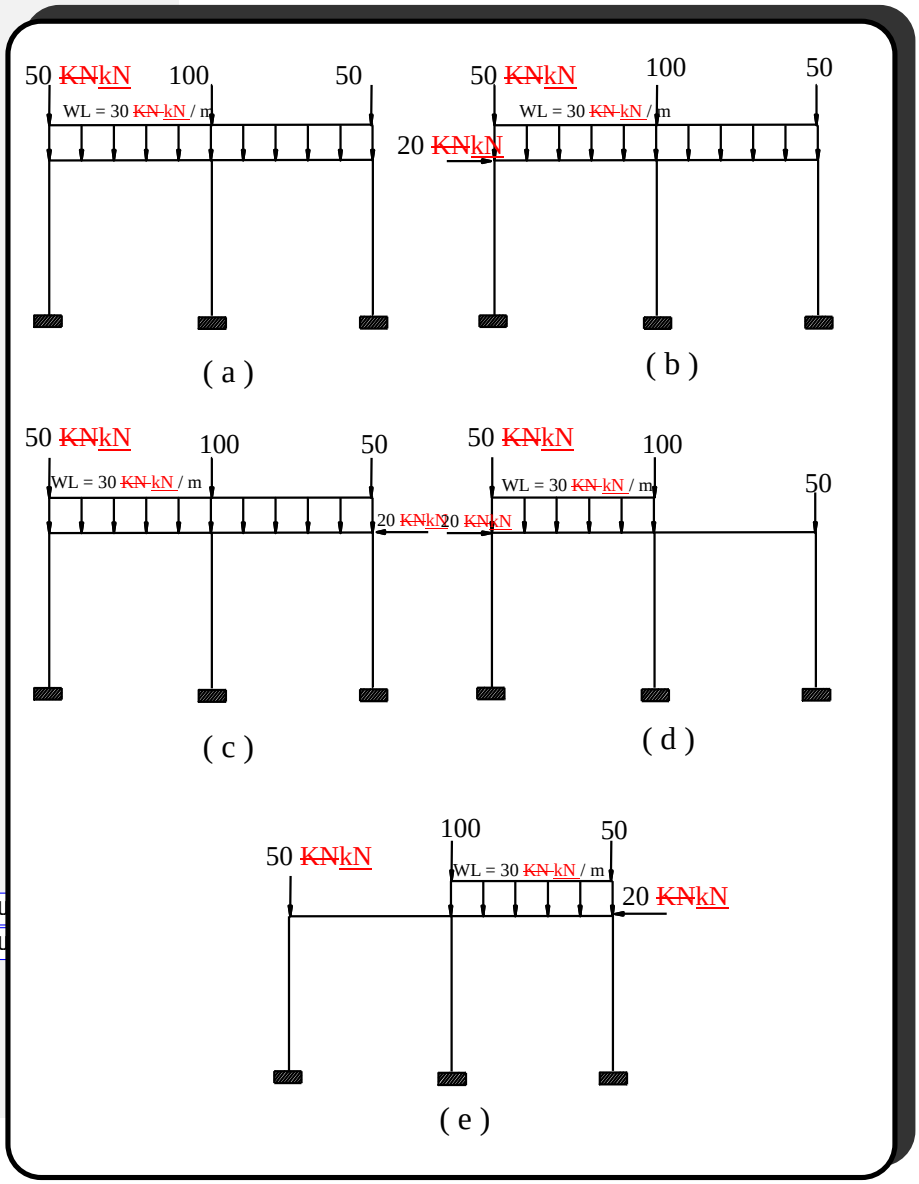

Fig. (7 – ~~27a~~28a): Loading Cases for Example (O1).

لغة العربية وغيرها: 10

لغة العربية وغيرها: 10

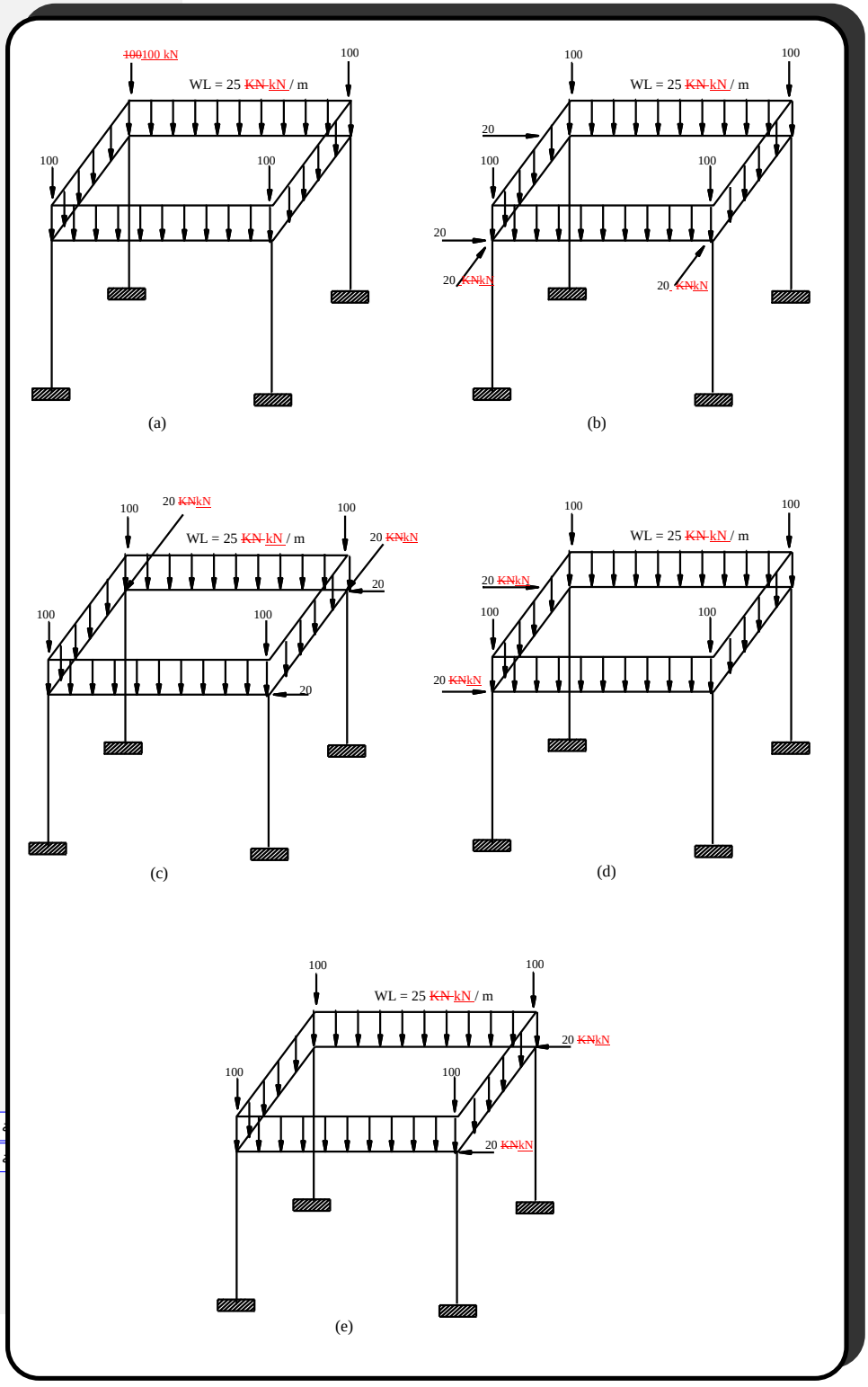

Fig. (7 – 2<u>8</u>~~7~~b): Loading Cases for Example (O2).

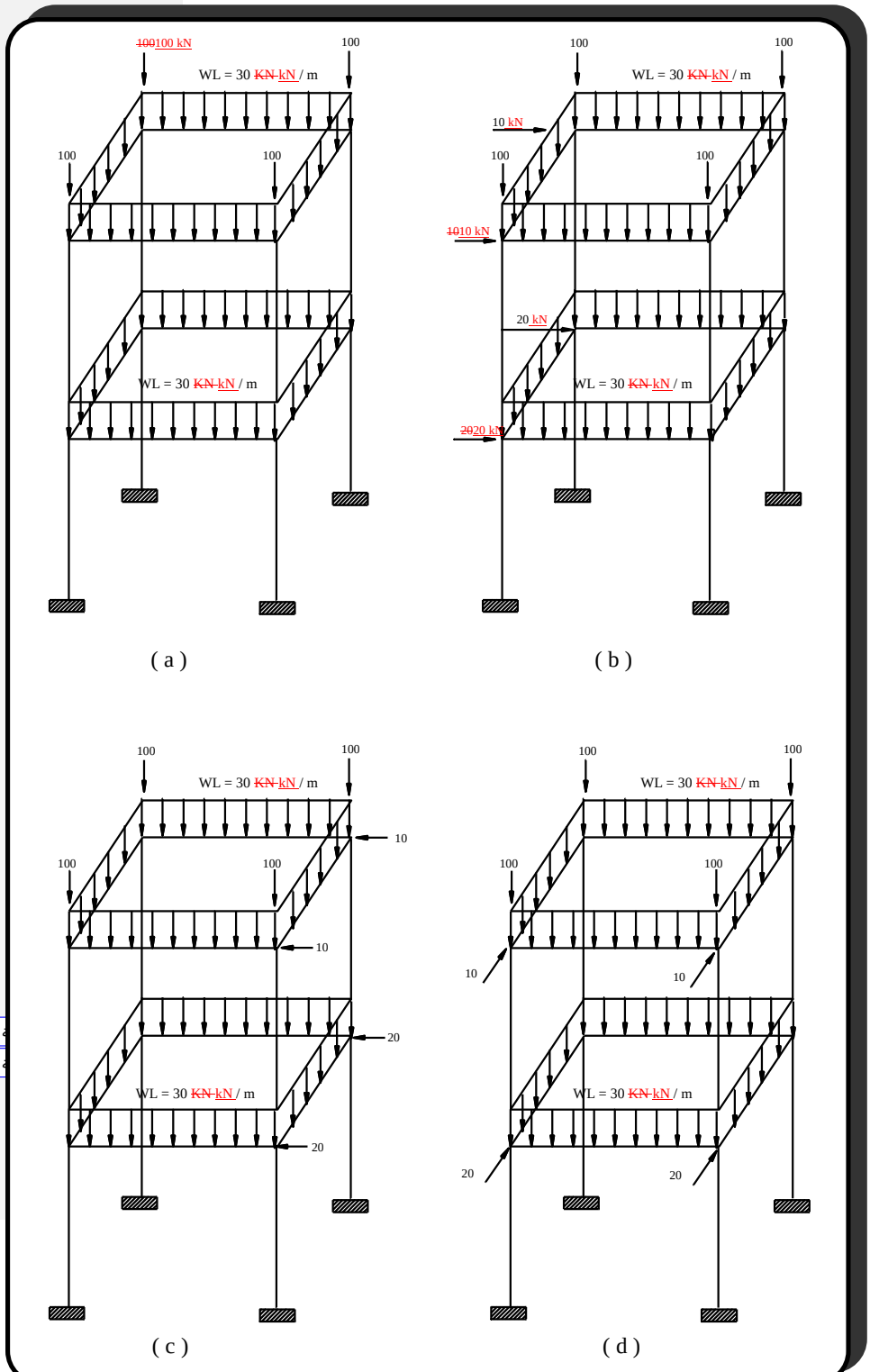

ة العربية وغيرها: 10

ة العربية وغيرها: 10

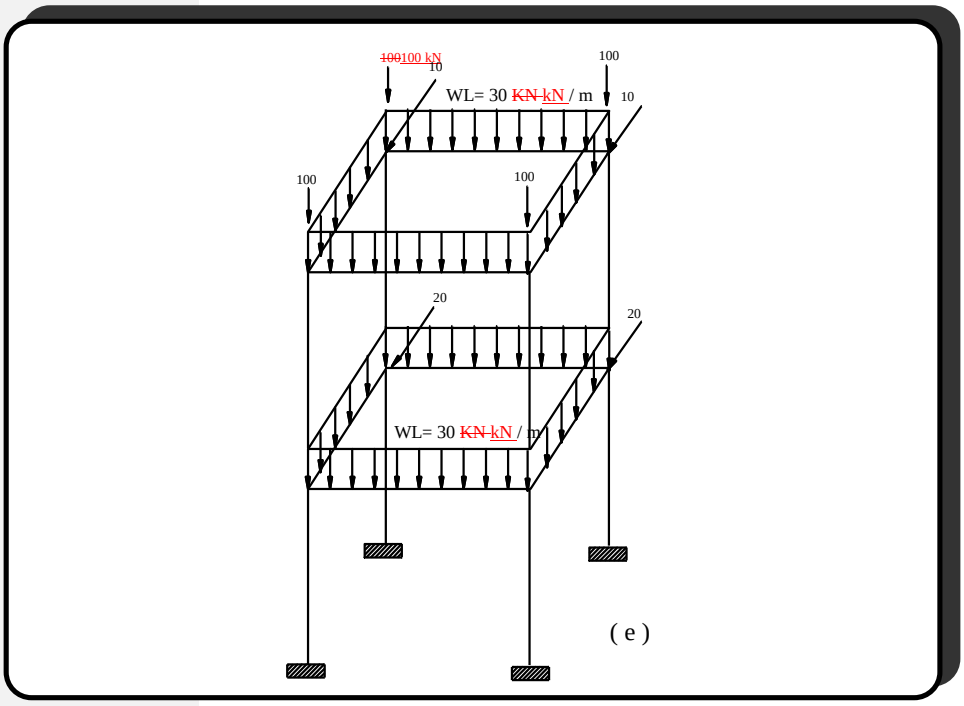

Fig. (7 – ~~27c~~28c): Continued.

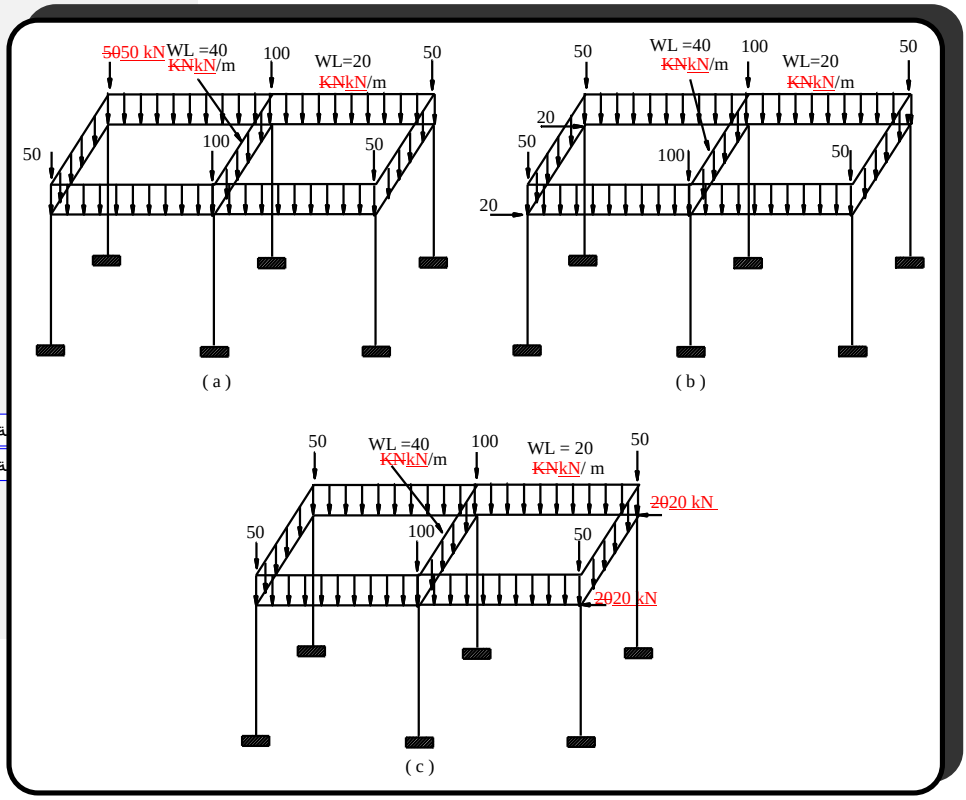

ة العربية وغيرها: 10
ة العربية وغيرها: 10

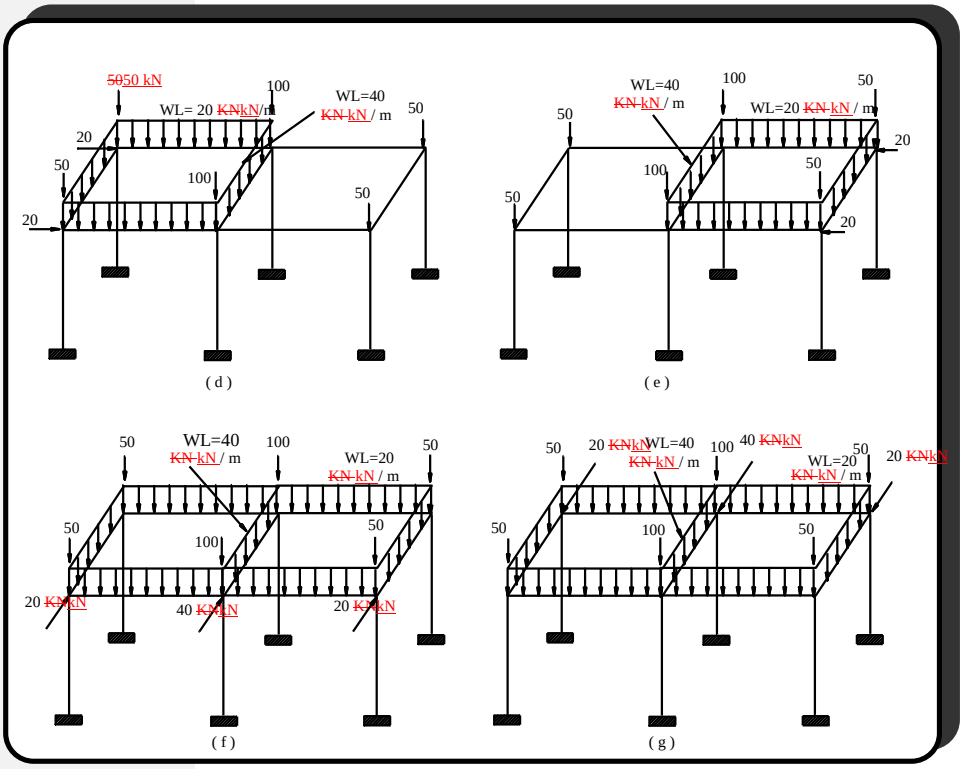

Fig. (7 – ~~27d~~28d): Continued.

Note: (All the applied loads are considered as live loads in addition to wind load, while the self-weight is considered ~~the~~ as the dead load).

منسّق:خط اللغة العربية وغيرها: 10
منسّق:خط اللغة العربية وغيرها: 10
نقطة

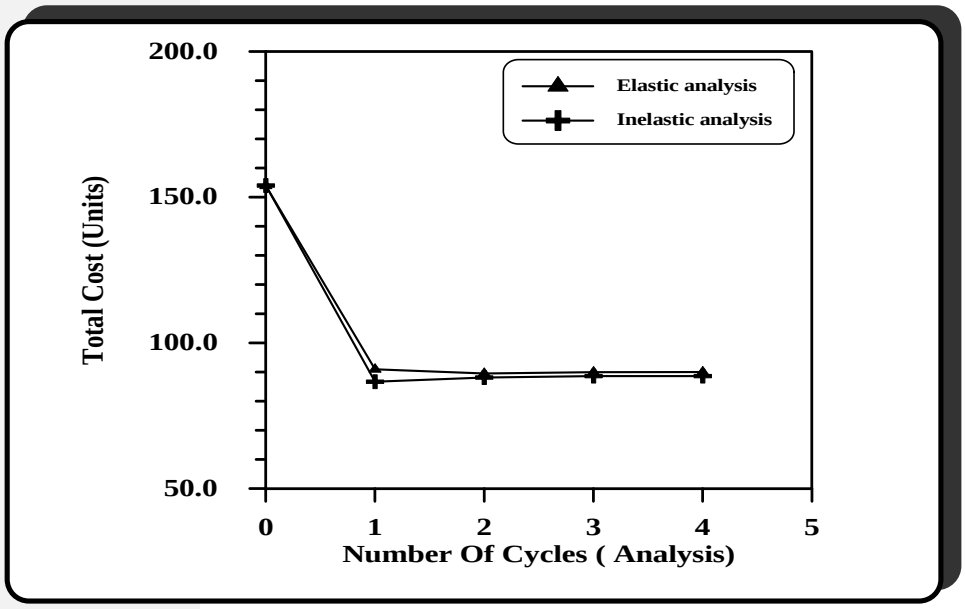

Fig. (7 – ~~28~~29): Variation of ~~total~~ Total ~~coast~~ Cost with No. of ~~analysis~~ Analysis (~~optimization~~ Optimization ~~cycles~~ Cycles for

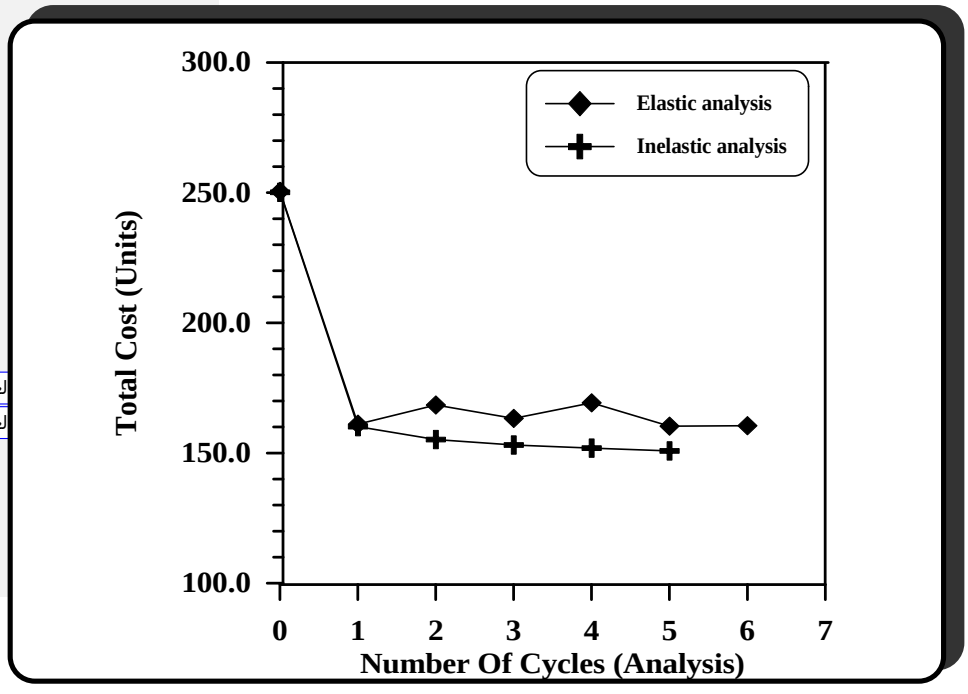

Fig. (7 – ~~29~~30): Variation of ~~total~~ Total ~~coast~~ Cost with No. of ~~analysis~~ Analysis (~~optimization~~ Optimization ~~cycles~~ Cycles for

العربية وغيرها: 10
العربية وغيرها: 10

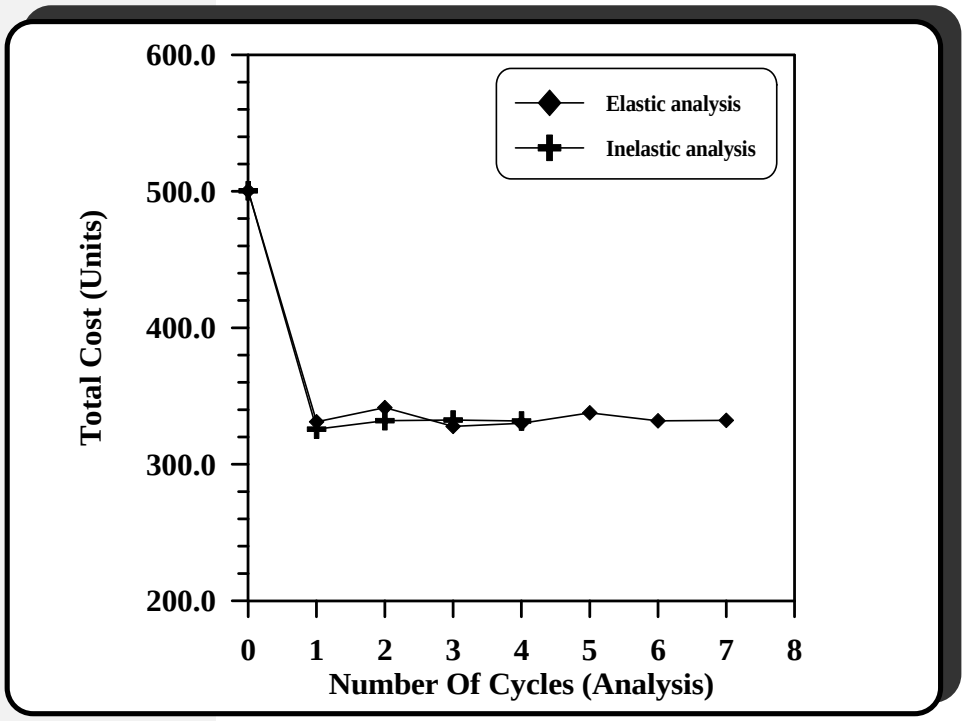

Fig. (7 – ~~30~~31): Variation of ~~total~~ Total ~~coast~~ Cost with No. of ~~analysis~~ Analysis (~~optimization~~ Optimization ~~cycles~~ Cycles for

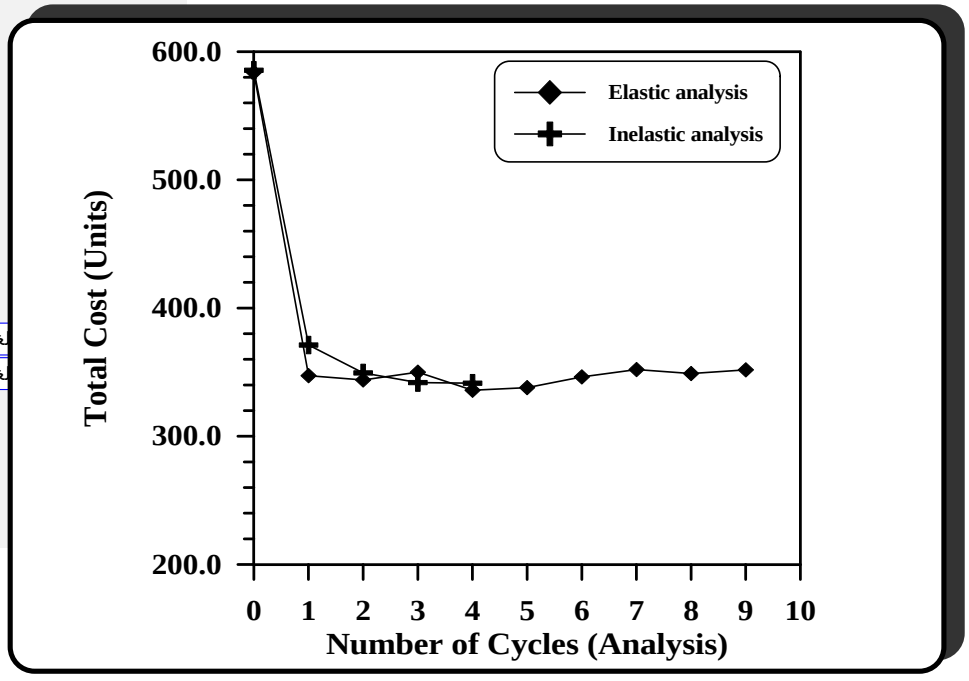

Fig. (7 – 3132): Variation of ~~total~~ Total ~~coast~~ Cost with No. of

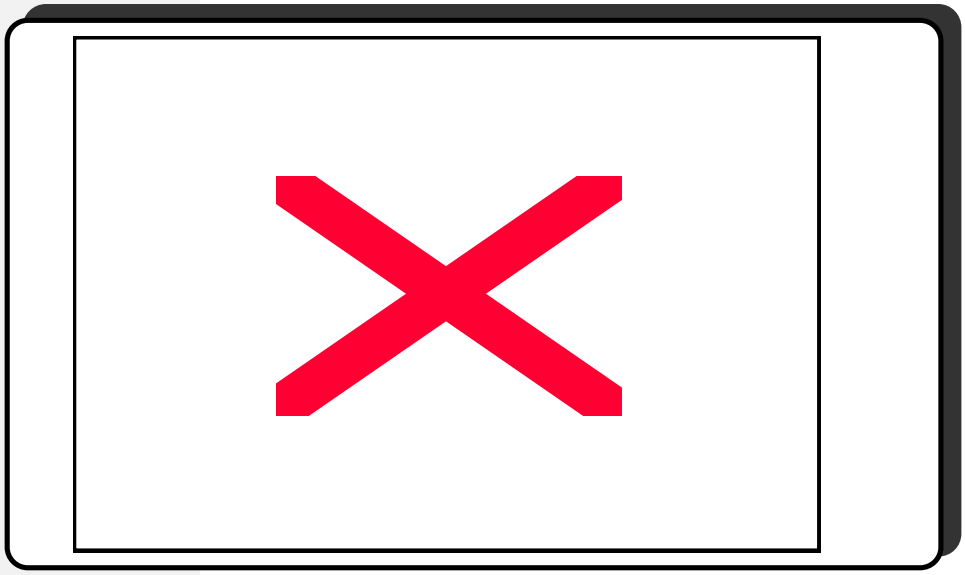

Fig. (7 – ~~28~~29): Variation of ~~total~~ Total ~~coast~~ Cost with No. of ~~analysis~~ Analysis (~~optimization~~ Optimization ~~cycles~~ Cycles for

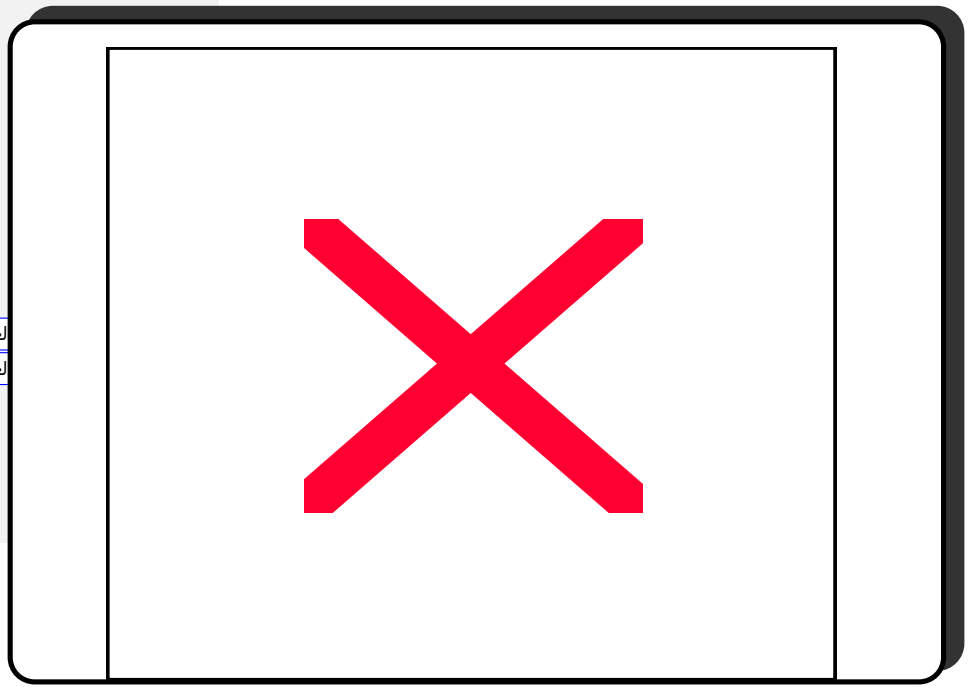

العربية وغيرها: 10

العربية وغيرها: 10

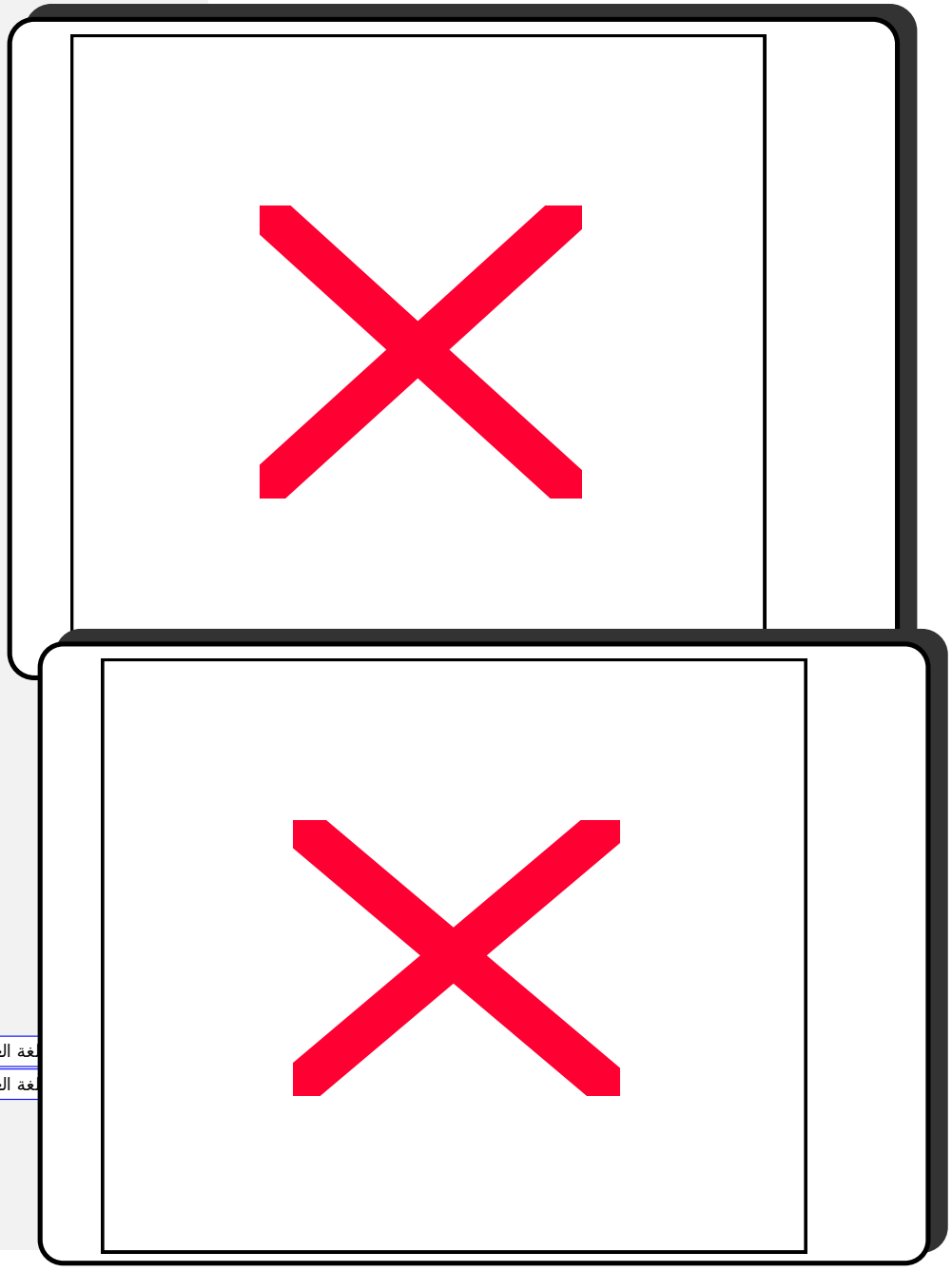

Fig. (7 – ~~31~~32): Variation of ~~total~~ Total ~~coast~~ Cost with No. of ~~analysis~~ Analysis (~~optimization~~ Optimization ~~cycles~~ Cycles for

Table (7 – 5): Optimum Design Solutions.

Example No.	Type of Analysis	No. of Analysis	Initial Cost (units)	Optimum Cost (units)
O1	Elastic	4	153.89	89.94
	Inelastic	4	153.96	88.59
O2	Elastic	6	250.49	160.46
	Inelastic	5	250.13	150.76
O3	Elastic	7	500.29	332.17
	Inelastic	4	500.29	331.68
O4	Elastic	9	583.64	351.73
	Inelastic	4	585.43	341.37

Table (7 – 6): Optimum Values of Design Parameters for Example (O1) (Elastic Analysis).

Member No.	Member Dimensions		Main reinforcement		Tie spacing (mm)	A_{sT} / bh %
	Width (mm)	Depth (mm)	$A_s(mm^2)$	$A_s'(mm^2)$		
1	250	255	526	226	107	1.18
2	250	260	426	226	110	1.00
3	250	260	526	226	110	1.15

منسّق:خط اللغة العربية وغيرها: 10
منسّق:خط اللغة العربية وغيرها: 10
نقطة

4	250	516	1226	226	200	1.12
5	250	517	1226	226	200	1.12

Table (7 – 7): Optimum Values of Design Parameters for Example (O2) (Elastic Analysis).

Member No.	**Member Dimensions**		**Main reinforcement**				**Tie spacing (mm)**	**A_l (mm^2)**	**ρ A_{sT} / bh %**
	Width (mm)	**Depth (mm)**	**A_s (mm^2)**	**D_b (mm)**	**S_b (mm)**	**S_h (mm)**			
1	309	509	1752	14.93	71.35	206.93	234	0	1.11
2	250	389	1052	11.57	52.87	148.61	174	0	1.08
3	250	391	1052	11.57	52.87	149.51	175	0	1.07
4	250	436	1152	12.11	52.69	172.04	193	0	1.05
	Width (mm)	**Depth (mm)**	**$A_s(mm^2)$**		**$A_s'(mm^2)$**		**Tie spacing (mm)**	**A_l (mm^2)**	**ρ A_{sT} / bh %**
5	250	392	926		226		176	0	1.17
6	250	420	926		226		190	0	1.09
7	250	448	926		226		200	0	1.03
8	250	396	926		226		178	0	1.16

منسّق:خط اللغة العربية وغيرها: 10
منسّق:خط اللغة العربية وغيرها: 10
نقطة

Table (7 – 8): Optimum Values of Design Parameters for Example (O3) (Inelastic Analysis).

Member No.	Member Dimensions		Main reinforcement				Tie spacing (mm)	A_l (mm^2)	ρ A_{sT} / bh %
	Width (mm)	Depth (mm)	A_s (mm^2)	D_b (mm)	S_b (mm)	S_h (mm)			
1	250	368	1052	11.57	52.87	138.12	163	0	1.14
2	265	564	1552	14.05	56.85	234.97	224	0	1.04
3	251	451	1252	12.62	52.92	178.98	202	0	1.10
4	250	368	1052	11.57	52.87	138.11	163	0	1.14
5	250	533	1352	13.12	52.36	219.84	209	0	1.01
6	250	268	1052	11.57	52.87	88.02	113	0	1.57
7	250	519	1352	13.12	52.36	212.94	209	0	1.04
8	250	299	1052	11.57	52.87	103.61	129	0	1.40
	Width (mm)	Depth (mm)	$A_s(mm^2)$		$A_s'(mm^2)$		Tie spacing (mm)	A_l (mm^2)	ρ A_{sT} / bh %

منسّق:خط اللغة العربية وغيرها: 10
منسّق:خط اللغة العربية وغيرها: 10
نقطة

9	250	415	226	926	187	0	1.11
10	250	550	626	826	200	0	1.05
11	250	490	326	926	200	0	1.02
12	250	497	926	326	200	0	1.00
13	250	406	226	826	182	0	1.03
14	250	455	926	226	200	0	1.01
15	250	444	226	926	200	0	1.03
16	250	427	926	226	193	0	1.08

Table (7 – 9): Optimum Values of Design Parameters for Example (O4) (Inelastic Analysis).

Member No.	Member Dimensions		Main reinforcement				Tie spacing (mm)	A_l (mm^2)	ρ A_{sT} / bh %
	Width (mm)	Depth (mm)	A_s (mm^2)	D_b (mm)	S_b (mm)	S_h (mm)			
1	264	561	1594	14.24	56.45	233.48	227	0	1.07
2	288	588	1794	15.11	64.36	246.54	241	0	1.06
3	250	340	1093	11.79	52.86	124.00	149	0	1.28
4	250	373	1093	11.79	52.86	140.50	166	0	1.17
5	250	481	1293	12.83	52.52	194.28	205	0	1.07
6	250	338	1093	11.79	52.86	122.80	148	0	1.29
	Width (mm)	Depth (mm)	$A_s(mm^2)$		$A_s'(mm^2)$		Tie spacing (mm)	A_l (mm^2)	ρ A_{sT} / bh %
7	250	508	1097		297		200	0	1.09
8	250	509	1097		297		200	0	1.09
9	250	405	797		297		182	0	1.08
10	250	528	1197		297		200	0	1.13

منسّق:خط اللغة العربية وغيرها: 10
منسّق:خط اللغة العربية وغيرها: 10
نقطة

Table (7 – 9): Optimum values of design parameters for example (04) (inelastic analysis).

11	250	420	797	297	189	0	1.04
12	250	537	1097	297	200	0	1.04
s13	250	528	1097	297	200	0	1.06

Table (7 – 10): Maximum and Allowable Deflections for Examples (O1, O2, O3 and O4) (Elastic Analysis).

Example No.	Maximum Deflection (cm)	Allowable Deflection (cm)
O1	0.63	2.083
O2	1.26	2.083
O3	1.24	2.083
O4	1.07	2.083

منسّق:خط اللغة العربية وغيرها: 10
منسّق:خط اللغة العربية وغيرها: 10
نقطة

منسّق:خط اللغة العربية وغيرها: 10

منسّق:خط اللغة العربية وغيرها: 10
نقطة

CHAPTER
Eight

CONCLUSIONS AND RECOMMENDATIONS

8.1 Conclusions:

From the results and discussions of these results given in Chapter Seven, the following conclusions can be drawn:

1- The proposed non-linear analysis technique is suitable with a sufficient accuracy for a variety of problems of reinforced concrete frames since it includes many different parameters . The maximum difference in the failure load between the present theoretical analysis and the experimental results is found to be not more than (11.6 %)

2- The proposed algorithm is capable to predict the three types of failure (i.e. local crushing failure, plastic collapse mechanism and stability failure) and detecting the one which occurs prior to others. However, in all structures analyzed by the proposed method, the type of failure is local crushing failure.

3- Through comparing the results obtained from the proposed method of analysis with the experimental results, it is found that the suggested cracked section properties is more suitable than the effective section properties and gross section properties in finding the flexural and axial stiffnesses of members of reinforced concrete frames.

4- The interaction among bending, shear and axial forces must be considered in analyzing the reinforced concrete structures. Such problem is considered well in the present analysis.

5- The optimal design of reinforced concrete frames based on inelastic analysis is more economical than that based on elastic analysis. The additional saving in the cost obtained in the present study based on inelastic analysis is in the range of (1.5-6.04%) in comparison with that based on elastic analysis.

6- In all considered examples, the width of most members is governed by the minimum width dictated by practical considerations.

7- The optimum steel percentage for most members has been found to be close to (1%) as recommended by the ACI-Code. This agrees with the selected objective function in which the steel cost is the major portion in the total cost.

8- The effect of deflection constraints is insignificant for examples considered in the present study.

8.2 Recommendations for Future Work:

1- Extending the proposed method of analysis to the analysis of space frames under cyclic loads.

2- Extending the proposed method of analysis to analyze space frames having non-prismatic members.

3- Studying the optimal design of reinforced concrete space frames subjected to dynamic and earthquake loading.

4- Extension of the optimization problem using the multi-level approach to involve an optimal design of slabs and foundations in addition to space frames.

CHAPTER FIVE

FORMULATION OF OPTIMAL DESIGN PROBLEM

5.1 General:

In this chapter, the complete formulation of the optimal design problem of reinforced concrete space frames, made of prismatic members of rectangular cross – section, is presented.

The design is based on ACI 318 – 95 Code **[38]** provisions. The total cost, involving cost of steel reinforcement (main and lateral), concrete and formwork, is considered to be the objective function. Several design constraints, which include strength constraints and side constraints are related to functional, architectural and constructional requirements and they are taken into account in the formulation of the optimization problem. Finally, the optimization method used in this work is explained with the aid of flow charts.

5.2 Design Variables:

The frames, considered here, consist of two types of members;(1) horizontal (i.e. lying in horizontal plane) or inclined (in space) members, which are subjected to self-weight (distributed) loads in addition to the applied loads, and (2) vertical members ignoring their self – weight. However, all members are designed as axially loaded members subjected to axial force plus bending moments. Story heights, columns, spacing, steel and concrete properties as well as concrete cover of reinforcement are predefined as data. Each member is considered to be defined when its

dimensions and area of longitudinal and tie steel reinforcement are known. The member will be designed for two critical sections at the extremities of its elastic length portion unless a zero shear point exists between them and a third critical section at such point would be considered. The usual practical construction employing prismatic members and non – equal main reinforcement at opposite faces is assumed. Also, the main reinforcement is considered to be constant along each member in addition to the fixed spacing ties along the member length. For each uniaxially loaded member of a frame, the vector of independent design variables ($X = \{ X_i \}$ ($i = 1, 2, \text{--------}, n$)) may be chosen as : ($X_1 = h$), ($X_2 = b$), ($X_3 = A_s$) and ($X_4 = A_s'$) where A_s *and* A_s' are the reinforcement at lower and upper faces of the section, respectively. For biaxially loaded members, ($X_1 = h$), ($X_2 = b$), ($X_3 = A_{sT}$ =total reinforcement), (X_4 = the number of steel bars along h) and (X_5 = number of steel bars along b). Here, it is assumed that the reinforcing bars in the same direction have the same spacing. The dependent variables are assumed to be: the member strength, tie spacing (s_v), spacing of main reinforcing bars and their diameter (d_b).

5.3 Objective Function:

The non – linear cost objective function (Z) involving the cost of : steel reinforcement, concrete and formwork is used in the optimization problem of this study.

$$Z = \sum_{i=1}^{n} Z_i \qquad \text{---------- (5 – 1)}$$

where

n = number of members

Z_i = cost of member (i)

Z_i is found as follows

Cost of steel

$$C_s \left[A_{sTi} + A_{li} \right] L_i + 2 \left(b_i + h_i \right) 2 c_o + d_{sv} \left[A_{sv} N_{svi} W_s \right]$$

---------- (5 – 2)

Cost of concrete = $C_c b_i h_i L_i$ ---------- (5 – 3)

Cost of formwork (horizontal or inclined members)

$$= C_f \left(b_i + 2 h_i \right) L_i \quad \text{----(5 – 4a)}$$

Cost of formwork (vertical members) = $2 C_f \left(b_i + h_i \right) L_i$ -----(5 – 4b)

where

C_s = unit price of steel reinforcement involving material and labour cost.

A_{sTi} = total area of main reinforcement of member (i) = maximum required area along those of critical sections in member (i).

A_{li} = area of longitudinal torsional reinforcement of member (i).

L_i = c / c length of member (i).

h_i = depth of member (i).

b_i = width of member (i).

c_o = concrete cover = 40 mm.

d_{sv} = bar diameter of shear reinforcement.

A_{sv} = cross – sectional area of shear reinforcement bar.

N_{svi} = number of ties in member (i) = (l_i / s_{vi}).

l_i = clear length of member (i).

s_{vi} = spacing of ties based on maximum shear force plus the maximum torsional moment along member (i).

W_s = unit weight of steel.

C_c = unit price of concrete involving material and labour cost.

C_f = unit price of formwork.

5.4 Constraints:

The objective function is minimized subject to a set of constraints. Some of these constraints can be explicitly defined in terms of the design variables (i.e., side constraints), while others are implicitly related to design variables (i.e., flexure, shear, --------- etc).

5.4.1 Flexure

5.4.1.1 Members with Uniaxial Loads:

Constraints for the member with uniaxial loads may be expressed as follows

$$g_1 = P_f - P_r \le 0 \quad \text{---------- (5 – 5)}$$

$$g_2 = M_f - M_r \le 0 \quad \text{---------- (5 – 6)}$$

$$g_3 = (x_3 + x_4)/(x_1 x_2) - 0.04 \le 0 \quad \text{---------- (5 – 7)}$$

$$g_4 = 0.01 - (x_3 + x_4)/(x_1 x_2) \le 0 \quad \text{---------- (5 – 8)}$$

$$g_5 = max(d_b, 25) - (s - d_b) \le 0 \quad \text{---------- (5 – 9)}$$

$$g_6 = (s - d_b) - 300 \le 0 \quad \text{---------- (5 – 10)}$$

$$g_7 = 11.3 - d_b \le 0 \quad \text{---------- (5 – 11)}$$

$$g_8 = d_b - 56.4 \le 0 \quad \text{---------- (5 – 12)}$$

$$g_9 = x_2 - x_1 \le 0 \quad \text{---------- (5 – 13)}$$

$$g_{10} = x_1 - 1000 \le 0 \quad \text{---------- (5 – 14)}$$

$$g_{11} = 250 - x_2 \le 0 \quad \text{---------- (5 – 15)}$$

Also, additional practical limitations are used:

$$g_{12} = 226 - x_3 \le 0 \quad \text{---------- (5 – 16)}$$

$$g_{13} = 226 - x_4 \le 0 \quad \text{---------- (5 – 17)}$$

$$g_{14} = \frac{1.4}{f_y} b d - x_3 \le 0 \quad \text{---------- (5 – 18)}$$

where

P_f, M_f = force state at the section, resulting from the combination of factored loads according to ACI – Code, which are found from the analysis (elastic or inelastic), and P_r, M_r = axial and bending resistance capacity of the section which are found through equilibrium equations as follows:

For axial compressive force:

$$P_r = 0.85 f'_c \beta_1 c_b b + A'_s f'_s - 0.85 f'_c A_s f_s \quad \text{-------- (5 –19a)}$$

For axial tensile force:

$$P_r = A_s 0.85 f'_c + f_s A'_s f_y - 0.85 f'_c \beta_1 c_b \quad \text{--------- (5 –19b)}$$

$$M_r = P_r e = P_r \left[M_f / P_f \right] \quad \text{---------- (5 – 20)}$$

where

c = the neutral axis depth (which its determination is completely explained in chapter four).

$$f'_s = \frac{c - d_1}{c} E_s \varepsilon_{cu} \le f_y$$

$$f_s = \frac{d - c}{c} E_s \varepsilon_{cu} \le f_y$$

g_1 and g_2 are the constraints imposed on the member to be able to resist the applied loads. g_3 and g_4 are the constraints for the reinforcement ratio. ACI – Code limits the longitudinal reinforcement in axially loaded members to between 1 and 8 percent of the gross area. However, practically the maximum reinforcement ratio is taken equal to 4 percent of the gross area. Constraints g_5 and g_6 are for spacing of the reinforcing bars (s = spacing of the reinforcing bars). ACI – Code requires the clear distance between the parallel bars in a layer should not be less than the maximum of (d_b, or 25 mm). Moreover, for an axially loaded member,

the clear distance between adjacent longitudinal bars shall not be greater than 300 mm. Constraints g_7 and g_8 are on the diameter of bars (d_b). The reinforcing bars should be between No.10 (11.3 mm) and No.55 (56.4mm). g_9 ,g_{10} and g_{11} are the side constraints. Constraints g_{12}, g_{13} and g_{14} are the practical limitations on the longitudinal tension and compression reinforcement.

5.4.1.2 Members with Biaxial Loads:

Constraints for the member with biaxial loads may be expressed as follows

$$g_1 = P_f - P_r \geq 0 \quad \text{---------- (5 – 21)}$$

$$g_2 = M_{fz} - M_{rz} \geq 0 \quad \text{---------- (5 – 22)}$$

$$g_3 = M_{fy} - M_{ry} \geq 0 \quad \text{---------- (5 – 23)}$$

$$g_4 = x_3/(x_1 x_2) - 0.04 \geq 0 \quad \text{---------- (5 – 24)}$$

$$g_5 = 0.01 - x_3/(x_1 x_2) \geq 0 \quad \text{---------- (5 – 25)}$$

$$g_6 = max(d_b, 25) - (s_h - d_b) \geq 0 \quad \text{---------- (5 – 26)}$$

$$g_7 = max(d_b, 25) - (s_b - d_b) \geq 0 \quad \text{---------- (5 – 27)}$$

$$g_8 = (s_h - d_b) - 300 \geq 0 \quad \text{---------- (5 – 28)}$$

$$g_9 = (s_b - d_b) - 300 \geq 0 \quad \text{----------(5 – 29)}$$

$$g_{10} = 11.3 - d_b \geq 0 \quad \text{---------- (5 – 30)}$$

$$g_{11} = d_b - 56.4 \geq 0 \quad \text{---------- (5 – 31)}$$

$$g_{12} = x_1 - 1000 \geq 0 \quad \text{---------- (5 – 32)}$$

$$g_{13} = x_2 - 1000 \geq 0 \quad \text{---------- (5 – 33)}$$

$$g_{14} = 250 - x_1 \geq 0 \quad \text{---------- (5 – 34)}$$

$$g_{15} = 250 - x_2 \geq 0 \quad \text{---------- (5 – 35)}$$

where

P_f, M_{fz} and M_{fy} = axial force and bending moments about principal axes, which are found from the analysis (elastic or inelastic) of the structure under the load combination according to ACI – Code. P_r, M_{rz} and M_{ry} = axial and moment resistance provided by the section which are found through the equilibrium equations as follows

For axial compressive force:

$$P_r = 0.85 f'_c A_c + \sum_{i=1}^{n} f_{si} A_{si} \quad \text{---------- (5 –36)}$$

$$M_{rz} = \sum_{i=1}^{n} f_{si} A_{si} Y_i + 0.85 f'_c Q_{cx} + P_r \frac{h}{2} \quad \text{---------- (5 – 37)}$$

$$M_{ry} = \sum_{i=1}^{n} f_{si} A_{si} X_i + 0.85 f'_c Q_{cy} + P_r \frac{b}{2} \quad \text{---------- (5 – 38)}$$

or $M_{rz} = P_r e_z \;,\; M_{ry} = P_r e_y$ ---------- (5 – 39)

For axial tensile force:

$$P_r = \sum_{i=1}^{n} f_{si} A_{si} + 0.85 f'_c A_c \quad \text{---------- (5 – 40)}$$

$$M_{rz} = 0.85 f'_c Q_{cx} + \sum_{i=1}^{n} f_{si} A_{si} Y_i + P_r \frac{h}{2} \quad \text{---------- (5 – 41)}$$

$$M_{ry} = 0.85 f'_c Q_{cy} + \sum_{i=1}^{n} f_{si} A_{si} X_i + P_r \frac{b}{2} \quad \text{---------- (5 – 42)}$$

or $M_{rz} = P_r e_z \;,\; M_{ry} = P_r e_y$ ---------- (5 – 43)

The unknowns in equations (5 – 36) through (5 – 38) and equations (5 – 40) through (5 – 42) are previously defined in chapter four for both axial compressive force and axial tensile force.

g_1, g_2 and g_3 are the constraints imposed on the member in order to be able to resist the applied loads. g_4 and g_5 are the constraints for the reinforcement ratio as in the case of uniaxial loads. Constraints g_6 through g_9 are for spacing of reinforcement. s_h, s_b = spacing of main reinforcing bars along h and b, respectively. Constraints g_{10} and g_{11} are on the diameter of reinforcing bars. Constraints g_{12} through g_{15} are the side constraints.

In all previous equations

¤ Z *0.9 for tension* H *flexure or pure flexure*

¤ Z *0.7 for compression* H *flexure*

5.4.2 Shear:

Each member is designed by assuming biaxial shear state (i.e. V_{uy} *and* V_{uz}) taking the maximum shearing forces (V_{uy} *and* V_{uz}) at a distance (d, b J b_1) from faces of support, respectively, as follows

V_{uy} Z ¤ V_{ny} Z ¤ [V_{s1} H V_y F ----------(5–44)

V_{uz} Z ¤ V_{nz} Z ¤ [V_{s2} H V_z F ----------(5–45)

where

¤ Z **0.85**

V_{s1} = nominal shear strength provided by shear reinforcement (in Y J direction).

V_{s2} = nominal shear strength provided by shear reinforcement (in Z J direction).

V_y = nominal shear strength provided by concrete (in Y J direction).

V_z = nominal shear strength provided by concrete (in Z J direction).

To find the nominal shear strength of concrete in (Y *and* Z) directions, a simple shear yield surface is utilized in this study **[17]**

$$\left(\frac{V_y}{V_{cy}}\right)^2 + \left(\frac{V_z}{V_{cz}}\right)^2 = 1 \quad \text{---------- (5 – 46)}$$

Solving equation (5 – 46), one can get

$$V_y = \frac{V_{cy}}{\sqrt{1 + \left(V_z^2 / V_y^2\right)\left(V_{cy}^2 / V_{cz}^2\right)}} \quad \text{---------- (5 – 47)}$$

$$V_z = \frac{V_{cz}}{\sqrt{1 + \left(V_y^2 / V_z^2\right)\left(V_{cz}^2 / V_{cy}^2\right)}} \quad \text{---------- (5 – 48)}$$

where V_{cy} *and* V_{cz} are found from the following expressions

If P = + (compression)

$$V_{cy} = \frac{1}{6}\left(1 + \frac{P_u}{14\,b\,h}\right)\sqrt{f_c'}\,b\,d \quad \text{---------- (5 – 49)}$$

$$V_{cz} = \frac{1}{6}\left(1 + \frac{P_u}{14\,b\,h}\right)\sqrt{f_c'}\,(b - b_1)\,h \quad \text{---------- (5 – 50)}$$

If P = - (tension)

$$V_{cy} = \frac{1}{6}\left(1 - 0.3\,\frac{P_u}{b\,h}\right)\sqrt{f_c'}\,b\,d \quad \text{---------- (5 – 51)}$$

$$V_{cz} = \frac{1}{6}\left(1 - 0.3\,\frac{P_u}{b\,h}\right)\sqrt{f_c'}\,(b - b_1)\,h \quad \text{---------- (5 – 52)}$$

where $P_u = |P|$.

The ratio of the concrete strength in Z direction to the concrete strength in Y direction is assumed to be equal to the ratio of the applied shear force in Z direction to that applied in Y direction

(i.e. $\frac{V_z}{V_y} = \frac{V_{uz}}{V_{uy}}$)

Hence, the required shear reinforcement areas A_{vy} *and* A_{vz} are computed from:

$$A_{vy} = \frac{(V_{uy} - \phi V_y)s}{2\phi f_{yv} d} \quad \text{---------- (5 – 53)}$$

$$A_{vz} = \frac{(V_{uz} - \phi V_z)s}{2\phi f_{yv} (b - b_1)} \quad \text{---------- (5 – 54)}$$

where s is the spacing of stirrups.

5.4.3 Torsion:

For members subjected to a torsional moment in addition to biaxial shear, an additional shear reinforcement is required. The design for torsion is based on a thin walled tube, and space truss analogy is used according to ACI – Code. A member subjected to torsion is idealized as a thin – walled tube with the core concrete cross section in a solid member neglected as shown in Fig. (5 – 1a).

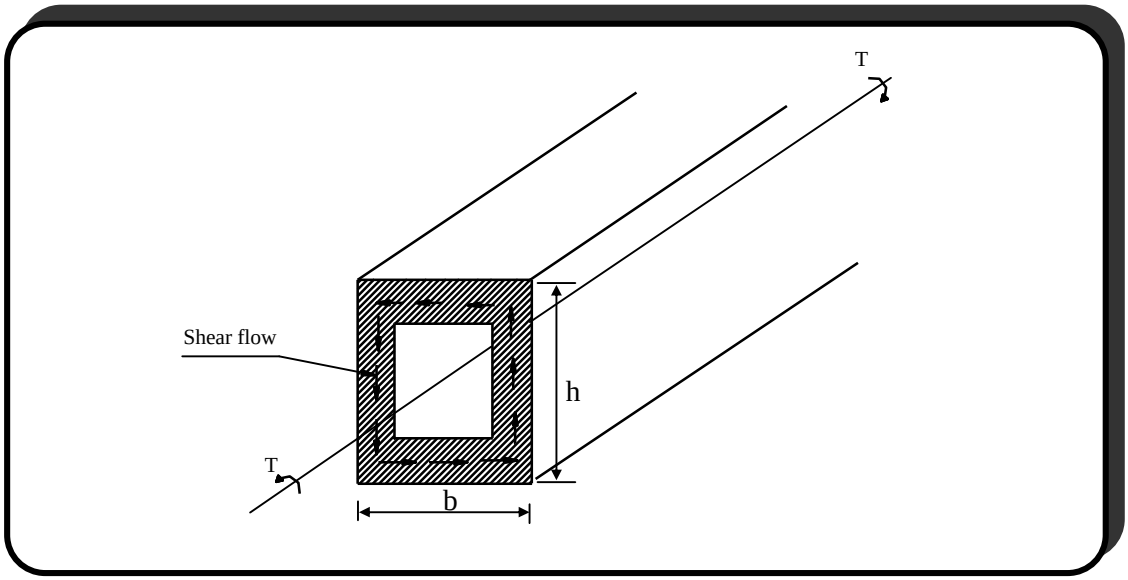

Fig.(5 – 1a): Thin – Walled Tube

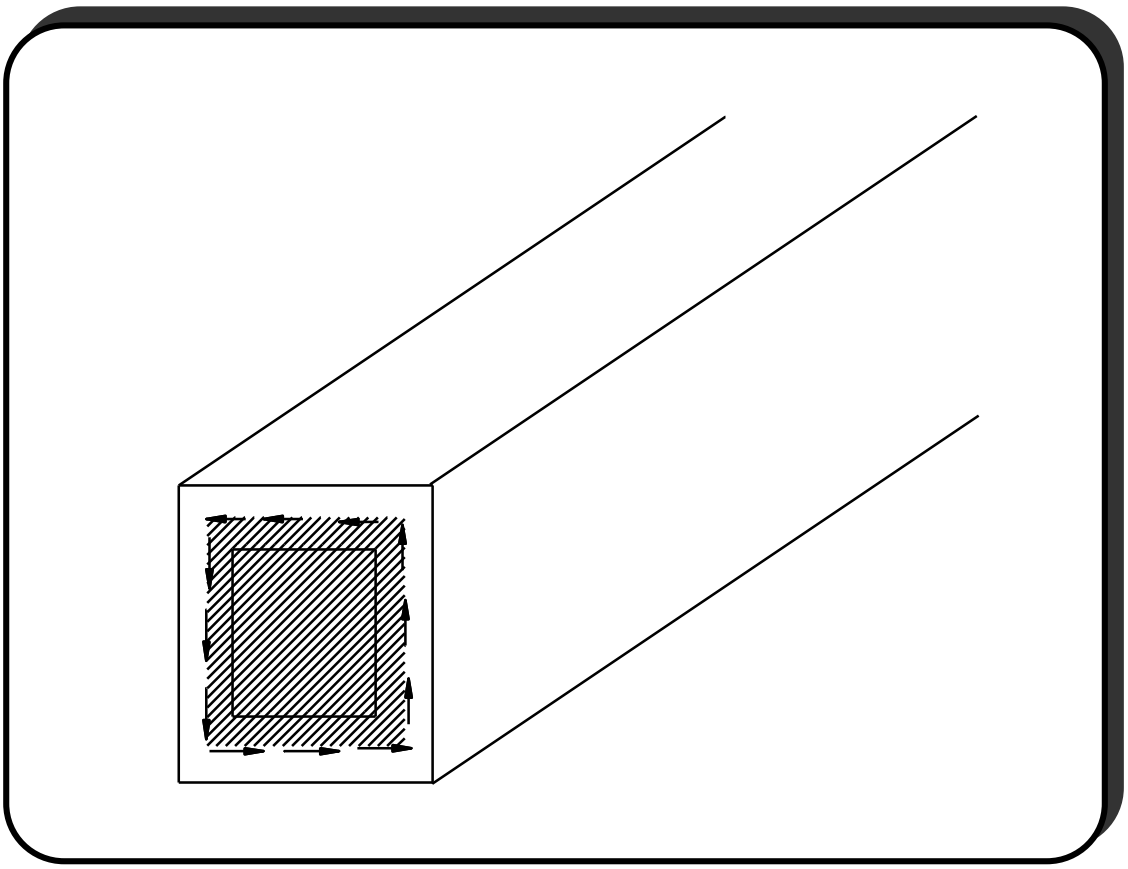

Fig.(5 – 1b): Area enclosed by Shear Flow Path

The reinforcement required for torsion shall be determined from

$$\bar{\phi} T_n \geq T \qquad \text{---------- (5 – 55)}$$

where

$\bar{\phi} = 0.85$

T_n = nominal torsional moment strength.

T = the applied torsional moment found from analysis (elastic or inelastic) under the combination of factored loads.

Hence **[38]**

$$T \leq \bar{\phi} T_n = \bar{\phi} \frac{2 A_o A_t f_{yv}}{S} \qquad \text{---------- (5 – 56)}$$

So

$$A_t = \frac{T S}{\bar{\phi} 2 A_o f_{yv}} \qquad \text{---------- (5 – 57)}$$

where

A_t = area of one leg of a closed stirrup resisting torsion.

S = spacing of transverse torsional reinforcement.

A_o = area enclosed by shear flow path (see Fig.(5 – 1b)) = $.85A_{oh}$

A_{oh} = area enclosed by centerline of the outer most closed transverse torsional reinforcement.

f_{yv} = yield strength of closed transverse torsional reinforcement.

Also, when a member has cracked in torsion its torsional resistance is provided primarily by the closed stirrups and the longitudinal bars located near the surface of the member. Hence, the additional longitudinal reinforcement required for torsion shall be computed from:

$$A_l = \frac{A_t}{S} P_h \left(\frac{f_{yv}}{f_{yl}} \right) \qquad \text{---------- (5 – 58)}$$

where

P_h = perimeter of the centerline of the outer most closed transverse torsional reinforcement.

f_{yl} = yield strength of the longitudinal torsional reinforcement.

The minimum total area of longitudinal torsional reinforcement is obtained from

$$A_{l\,min} = \frac{5\sqrt{f'_c}\,A_{cp}}{12\,f_{yl}} - \left(\frac{A_t}{S} \right) P_h \frac{f_{yv}}{f_{yl}} \qquad \text{---------- (5 – 59)}$$

where

A_{cp} = area enclosed by outside perimeter of concrete cross section ($A_{cp} = bh$ for rectangular cross section).

Thus, for a member subjected to biaxial shear plus torsional moment the total required transverse shear reinforcement (one leg) is:

$$A_{sv} = A_{vy} + A_{vz} + A_t \qquad \text{---------- (5 – 60)}$$

$$= \left[\frac{V_{uy} - \phi V_y}{2\phi f_{yv} d} + \frac{V_{uz} - \phi V_z}{2\phi f_{yv} (b - b_1)} + \frac{T}{2\phi A_o f_{yv}}\right] S$$

So, the required spacing is

$$S_v = \frac{2A_{sv}}{\left[\frac{V_{uy} - \phi V_y}{\phi f_{yv} d} + \frac{V_{uz} - \phi V_z}{\phi f_{yv} (b - b_1)} + \frac{T}{\phi A_o f_{yv}}\right]} \qquad \text{----------(5 – 61)}$$

5.4.4 Other Code Limitations on Shear and Torsion:

a) To reduce unsightly cracking and to prevent crushing of the surface concrete due to inclined compressive stresses due to shear and torsion, the cross – sectional dimensions shall be such that:

$$\sqrt{\left(\frac{V_{uy}}{b\,d}\right)^2 + \left(\frac{T\,P_h}{1.7\,A_{oh}^2}\right)^2} \le \phi\left(\frac{V_y}{b\,d} + \frac{2}{3}\sqrt{f'_c}\right) \qquad \text{---------- (5 – 62)}$$

b) It shall be permitted to neglect torsion effects when the applied torsional moment (T) is:

$$T' = \phi\frac{\sqrt{f'_c}}{12}\left(\frac{A_{cp}^2}{P_{cp}}\right) \qquad \text{----------(5– 63)}$$

where P_{cp} =outside perimeter of concrete cross section.

c) Code limitations on spacing of closed stirrups:

$$S_v \le 600mm \ \ if \ \ V_{s1} \le \frac{1}{3}\sqrt{f'_c}\,b\,d \qquad \text{---------- (5 – 64)}$$

$$S_v \le 300mm \ \ if \ \ V_{s1} > \frac{1}{3}\sqrt{f'_c}\,b\,d \qquad \text{---------- (5 – 65)}$$

$$S_v \le \frac{6 A_{sv} f_y}{b} \quad \text{---------- (5 – 66)}$$

$$S_v \le \frac{d}{2} \text{ if } V_{s1} \le \frac{1}{3}\sqrt{f'_c}\, b d \quad \text{---------- (5 – 67)}$$

$$S_v \le \frac{d}{4} \text{ if } V_{s1} \le \frac{1}{3}\sqrt{f'_c}\, b d \quad \text{---------- (5 – 68)}$$

$$S_v \le \min\left\{\frac{P_h}{8}, 300mm\right\} \quad \text{---------- (5 – 69)}$$

$$V_{s1} \le \frac{2}{3}\sqrt{f'_c}\, b d \quad \text{---------- (5 – 70)}$$

d) Code limitations for tie reinforcement to act as restraint against buckling of longitudinal bars for confinement of concrete are :

$$S_v \le 16 d_b \quad \text{---------- (5 – 71)}$$

$$S_v \le 48 d_{sv} \quad \text{---------- (5 – 72)}$$

$$Sv \le b \quad \text{---------- (5 – 73)}$$

e) An additional practical limitation on minimum tie spacing which is

$$S_v \ge 100mm \quad \text{---------- (5 – 74)}$$

5.4.5 Deflection:

In this study, the center span deflection is considered as the maximum span deflection in the design problem. The deflection (ΔT) is calculated according to the ACI – Code equation as the sum of immediate deflection (ΔL_{immed}) due to service live load and long term deflection $(\Delta_{longterm})$ due to shrinkage and creep i.e.

$$\Delta T = \Delta L_{immed} + \Delta_{long\ term} \quad \text{---------- (5 – 75)}$$

where $\Delta_{long\ term}$ is found through multiplying the immediate deflection due to sustained service load by the following factor **[38]**:

$$\lambda = \frac{\xi}{1 + 50\rho'} \quad \text{---------- (5 – 76)}$$

where ξ is a time dependence factor which has the following values **[38]**:

= 2.0 5 years or more

= 1.4 12 months

= 1.2 6 months

=1.0 3 months

$$\rho' = A_{sc} / b\,d$$

where ρ'=compressive steel ratio.

The computed immediate deflection that is used in the prescribed expression (5 – 75) is based on the elastic analysis at the end of optimization process.

The deflection is controlled by the limiting value of code equal to (overall span of the member) / 240.

5.4.6 Slenderness Effect on the Member Design:

Since the geometric non – linearity is considered in the analysis process, the effect of slenderness on member design as well as minimum eccentricity as specified by ACI – Code will be ignored.

5.5 Optimization:

5.5.1 Decomposition and Multilevel Solution:

The problem that is formulated in the preceding sections can be solved as an integrated unit using any suitable method of non – linear optimization, but this involves real computational difficulties. Some of these may be summarized here **[22]**

1- The problem size (number of variables and constraints) is relatively large even for simple structures. This will greatly increase the computational time which is usually an exponential function of the problem size. In addition, such problem needs a computer of high capacity.

2- The different natures of design variables may produce numerical problems in the solution.

3- The non – linear analysis of structures, being a repetitive nature and involving a solution of set of simultaneous equations, will increase the total computational time (***cpu time***).

These difficulties are largely resolved by decomposing the problem into smaller subproblems. The (multilevel approach) developed by **Kirsch [22]** is adopted here. The approach is more suitable for micro – computer applications and its effectiveness has been already tested and verified in recent works for such type of problems **[15,24,27]**. The problem is subdivided into three levels as given below.

Third Level (Outer Level):

In this level, the design moments and forces are obtained from structural analysis (elastic or inelastic as the case may be). The analysis is repeated when all members are optimized (in second and first levels).

To satisfy the optimization at this level, the convergence criterion on the objective function, which is the total cost of the structure (Z), is

$$\left| \frac{Z^{i} - Z^{i-1}}{Z^{i}} \right| \le e \qquad \text{---------- (5 – 77)}$$

where (Z^{i}) is the total cost of the structure in the ***ith*** iteration and (e) is a prechosen tolerance for the total cost, which is selected depending on a trial test on different types of problems. The value selected and used here is ($e = .001$).

Second Level:

In this level, the independent variables of each member are optimized independently for the computed forces (from third level) using a non – linear optimization method as will be explained later. After each

modification in the independent variables, the solution enters the first level to determine the values of the dependent variables.

First Level:

At this level, the values of the dependent variables are calculated directly using the values of the independent variables and design forces from the 2nd and 3 rd levels respectively.

5.5.2 Method of Optimization:

Since the minimization of the objective function depends on the section resistance (i.e. $P_r, M_{ry} and M_{rz}$) which is an implicit function of the independent design variables and can not be expressed directly as a function of these variables, it cannot be derived with respect to the independent design variables. Hence the gradient method of non –linear optimization such as (SUMT Method) (sequential unconstrained minimization technique) cannot be used in this study. So, the modified direct search method of **Hooke and Jeeves [39]** will be used which uses the function values only. The search consists of a sequence of exploration steps about a base point which if successful are followed by pattern moves. The modification was made on this method to take account of constraints. Indeed it has been suggested that merely giving the objective function a very large value (in a minimization problem) whenever the constraints are violated will suffice (usually $Z = 1*10^{30}$). Certainly this idea has an obvious intuitive appeal and it is easy to program.

The procedure is as follows.

A) Choose an initial base point b_1 and a step length h_j for each variable $X_j, j = 1,2,\ldots n$.

B) Carry out an exploration about b_1. The purpose of this is to acquire knowledge about the local behavior about the function. This knowledge is used to find a likely direction for the pattern move by

which it is hoped to obtain an even greater reduction in the value of the function. The exploration about b_1 proceeds as indicated.

1. Evaluation of (b_1).
2. Each variable is now changed in turn, by adding the step length. Thus, the value of $f(b_1 + h_1 e_1)$ where e_1 is a unit vector in the direction of the x- axis is then calculated. If this reduces the function replace b_1 by $b_1 + h_1 e_1$. if not find $f(b_1 - h_1 e_1)$ and replace b_1 by $b_1 - h_1 e_1$ if the function is reduced. If neither step gives a reduction leave b_1 unchanged and consider changes in X_2, i.e. find $f(b_1 + h_2 e_2)$ etc. when all n variables are considered, a new base point b_2 is obtained.
3. If $b_2 = b_1$ i.e. no function reduction has been achieved, the exploration is repeated about the same point b_1 but with a reduced step length. Reducing the step length (s) to one tenth of its former value appears to be satisfactory in practice.
4. If $b_2 \neq b_1$ a pattern move can be made.

C) Pattern moves utilize the information acquired by exploration and accomplish the function minimization by moving in the direction of the established ‘pattern’. The procedure is as follows.

1- It seems sensible to move further from the base point b_2 in the direction $b_2 - b_1$ since that move already led to a reduction in the function value. So, the function value is evaluated at the next pattern point

$$P_1 = b_1 + 2(b_2 - b_1) \quad \text{---------- (5 – 78)}$$

In general

$$P_i = b_i + 2(b_{i+1} - b_i) \quad \text{---------- (5 – 79)}$$

2- Then continue with exploratory move about $P_1 (P_i)$.

3- If the lowest value at step $C(2)$ is less than the value at the base point $b_2(b_{i+1})$ in general) then a new base point $b_3(b_{i+2})$ has been reached. In this case, repeat $C(1)$. Otherwise abandon the pattern move from $b_2(b_{i+1})$ and continue with an exploration about $b_2(b_{i+1})$.

D) Terminate the process when the step length (s) has been reduced to a predetermined small value, (Usually less than $1*10^{-8}$).

The following flow charts Fig. (5 – 2) represent the method.

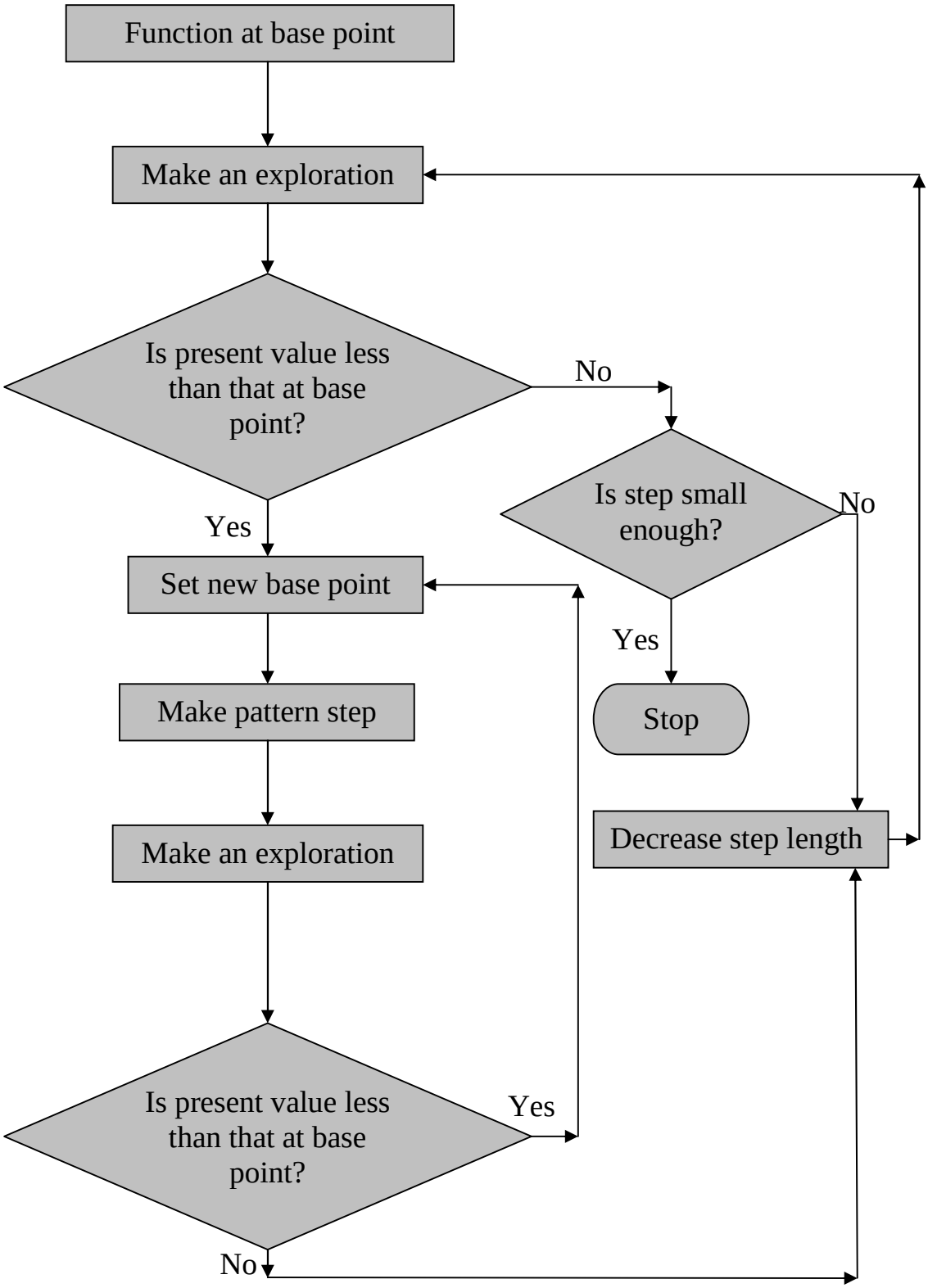

Fig. (5 – 2a): Flow chart for Hooke and Jeeves Method

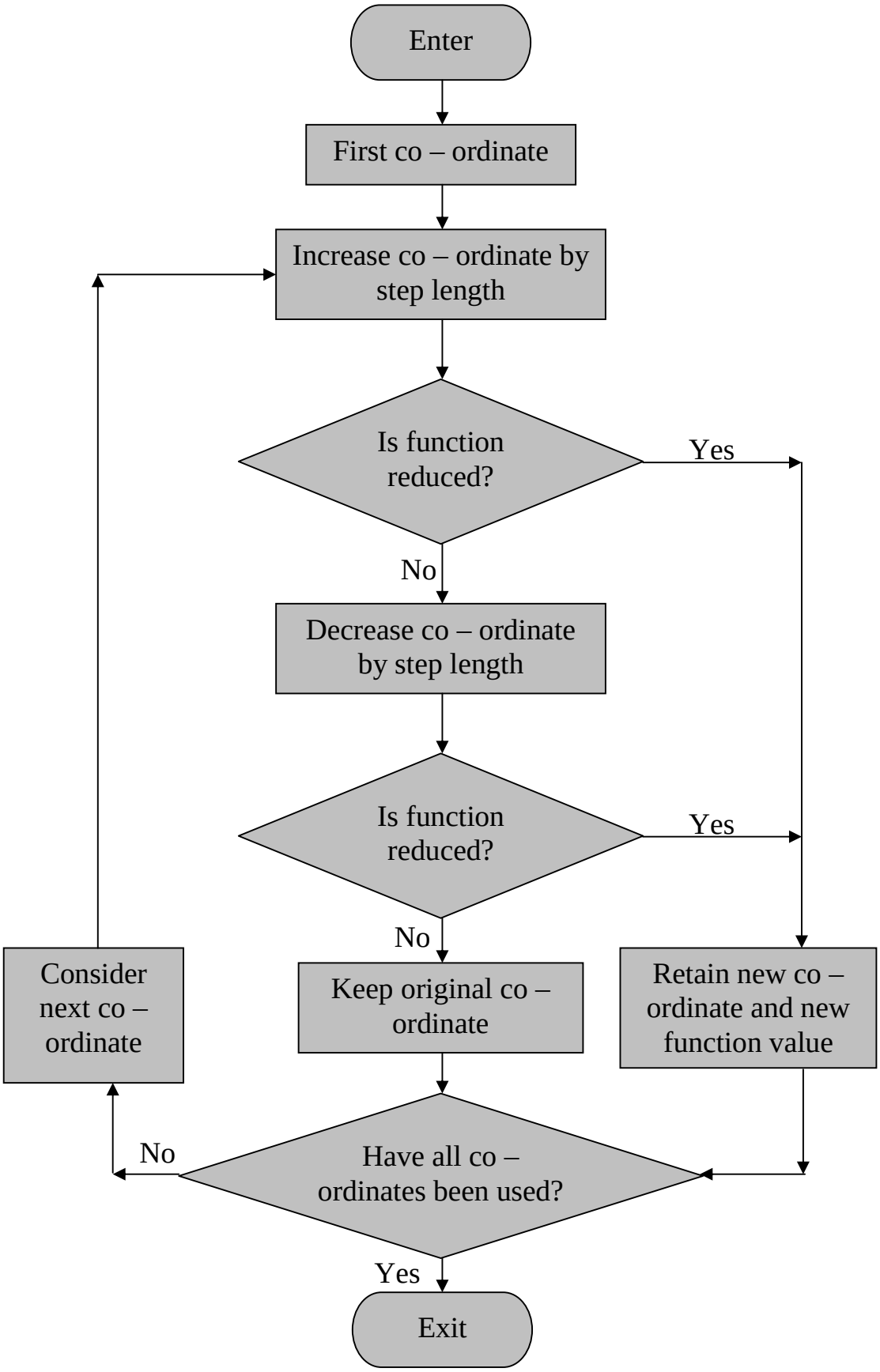

Fig. (5 – 2b): Flow Chart for an Exploration

5.6 Computer Program:

A computer program "**OPSPA**" for carrying out the optimal design of reinforced concrete frames according to the prescribed procedure was written in **FORTRAN 90** language to be used on the **IBM** personal computer or any other compatible microcomputer. The steps of the main program are outlined in the flow chart of Fig. (5 – 3).

It is important to explain here, that the optimal design in the program "**OPSPA**" is based on the non – linear analysis program " **NASPAC** ". In other words, the optimization process is included as a subroutine within the analysis program.

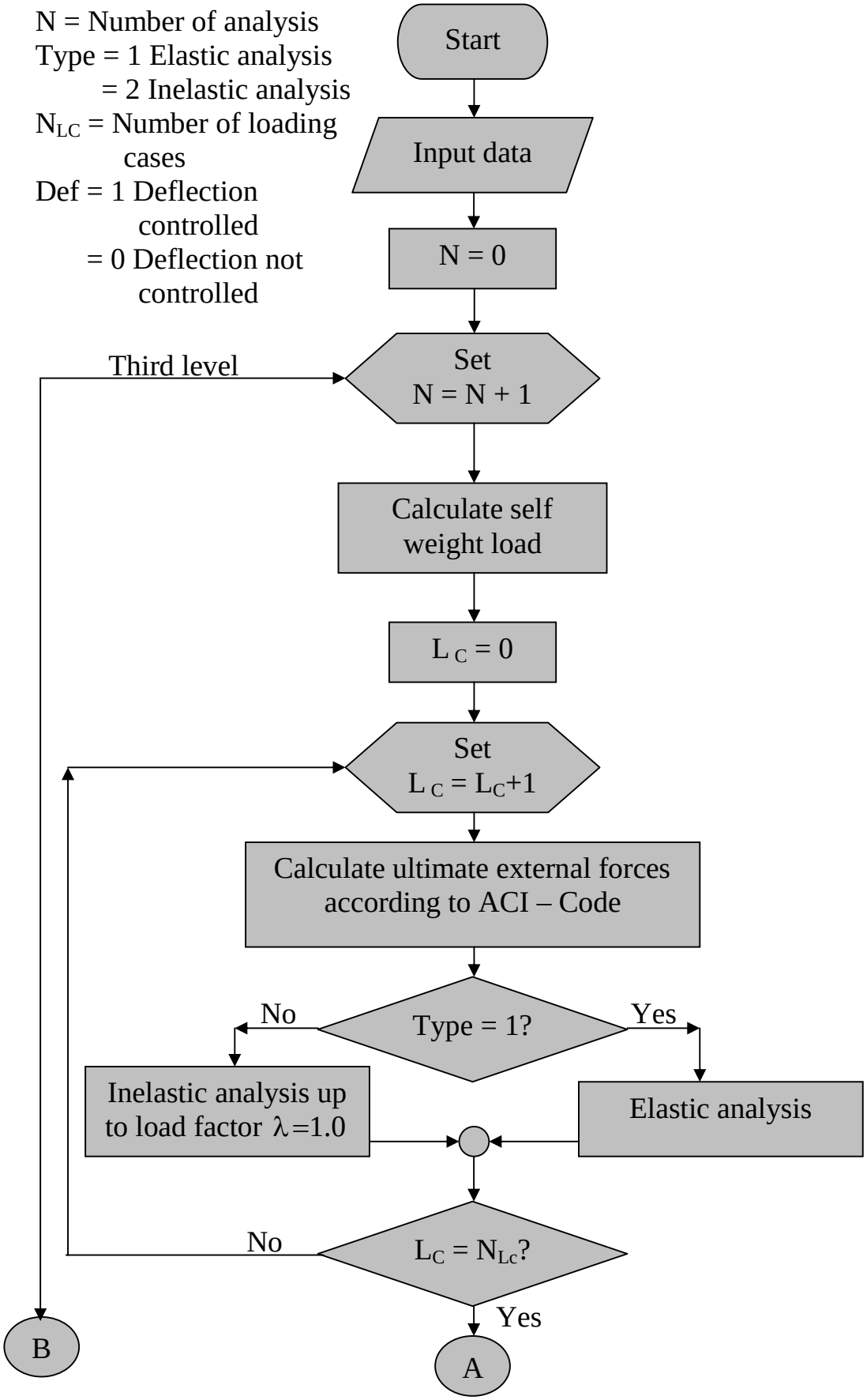

Fig. (5 – 3): Flow Chart of the Program (OPSPA) and Multilevel Approach

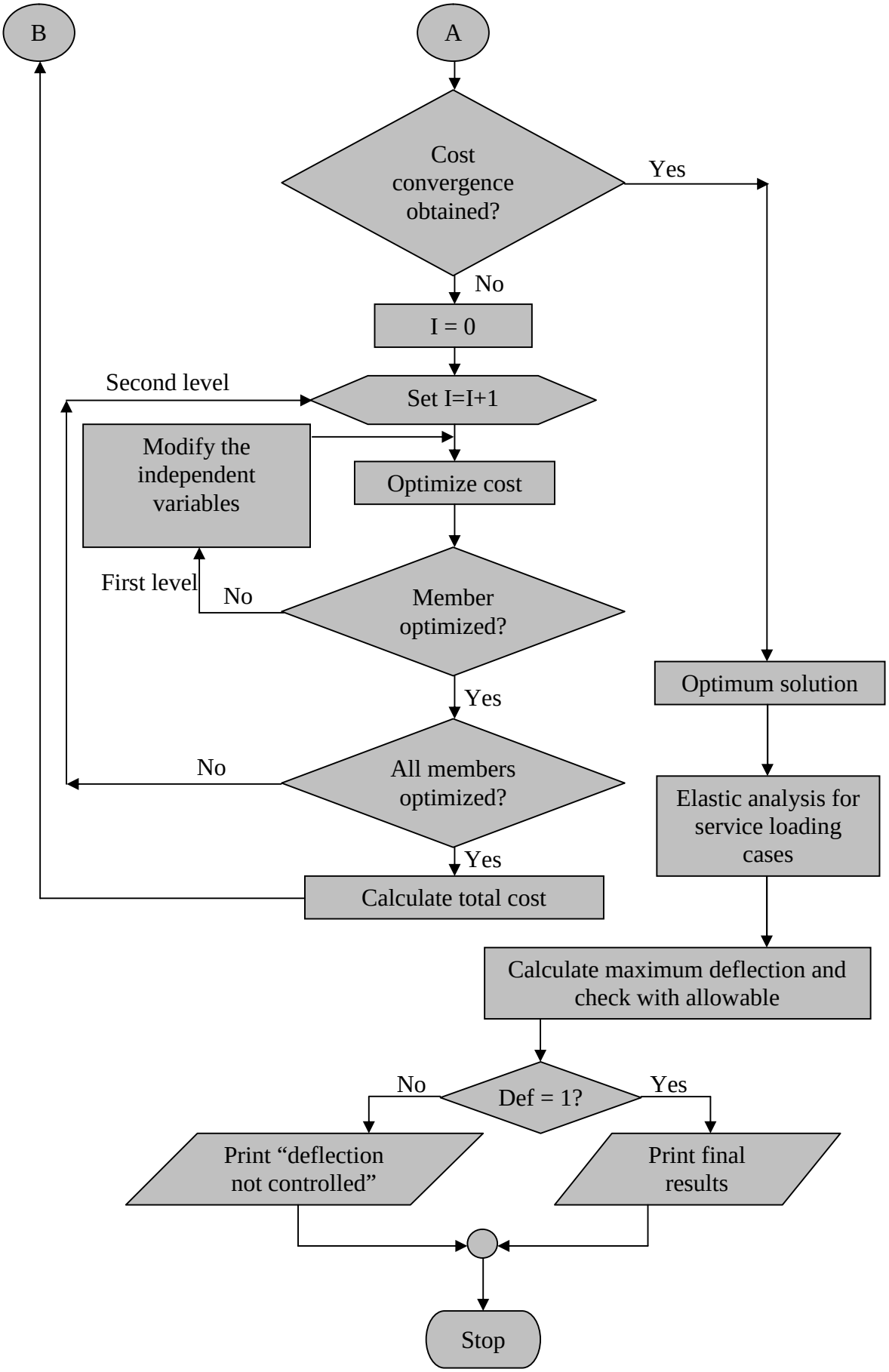

Fig. (5 – 3): Continued

CHAPTER FOUR

FORMULATION OF NON - LINEAR ANALYSIS

4.1 Introduction:

A general non – linear analysis of reinforced concrete frames is formulated in this chapter. The method of analysis is applicable to any reinforced concrete frame. It follows a step – wise linearized incremental procedure based on the displacement stiffness approach which was developed by **Al – Rifaie and Trikha [12]** for the analysis of reinforced concrete plane structures. However, in the present study, such analysis is developed to be capable to carry out non – linear analysis of reinforced concrete space frames. In addition, many effects are considered so as to express the real behavior of the reinforced concrete frames more accurately. The main developments made in this work are, briefly, given as follows:

1- Geometric non – linearity is considered through:

a- Derivation of a non – linear stiffness matrix for a space frame element considering the geometric non – linearity more accurately.

b- Proposing an efficient iteration technique within each load increment for updating the non – linear stiffness matrix and also to predict the possibility of stability failure during any load increment, and

c- Updating the nodal coordinates at the end of each load increment.

2- Possibility of local crushing failure is treated through computing the inelastic rotations, as previously explained, yield and crushing rotations are computed considering the effect of the axial force on the moment capacity of each critical section.

3- The present technique has the ability to analyze structures under uniformly distributed loads and to consider the probability of existence of a third critical section at the point of zero shear along the elastic length of the member in addition to those existing at its two extremities. Also, the fixed end forces for the member under uniformly distributed loads are derived (see chapter (3)) including the effect of shear deformations and geometric non – linearity.

Finally, as a part of this research, a computer Program has been written for solving the following problems:

Problem (A): determination of moments, shear force and axial forces in addition to displacements at critical sections for any reinforced concrete frame subjected to given loads based on non – linear elastic analysis.

Problem (B): same as problem (A) but the analysis is non – linear elastic - plastic.

Problem (C): determining the safety factor (load factor) for the reinforced concrete frame against failure.

4.2 Algorithm for the Proposed Procedure of Analysis:

The adopted solution algorithm which handles the non – linearity in the material and geometry follows a two level process: iterations within increments. The algorithm treats the problem of non – linear behavior as a sequence of linearly elastic problems. Each step of the sequence, represented by a load increment, is based on material and geometry properties appropriate to that step (i.e. the structure stiffness matrix is

updated at the beginning of each step). The procedure of analysis can be given as follows:

1- In any load increment (s), at any iteration (r); the structure is subjected to the external loads [F], and solving the following equation of equilibrium

$$[F] = [K]^{s,r} [D]^{s,r} \quad \text{---------- (4 – 1)}$$

The structure is considered as a linear structure. $[K]^{s, r}$ is the global stiffness matrix of the structure based on the axial forces vector $[P]^{s-1}$ from the previous load increment (**s –** 1) and on the axial forces vector $[P]^{s, r-1}$ if $r \div 1$ **[15],** Where

$$[P]^{s,r-1} = [P]^{s-1} + \Delta P^{s,r-1} + \Delta P^{s,r-2} \quad \text{----- (4 – 2)}$$

(if r = 2; $\Delta P^{s,r-2} = 0$)

where $\lambda = 0.9$ and, $\Delta P^{s,r-1}$ and $\Delta P^{s,r-2}$ are the vectors of change in axial forces found in iterations (r – 1) and (r – 2) respectively.

Equation (4 – 1) can be solved using Gauss – Jordan's Elimination to find the global displacements vector [D].

2- Local axial forces and moments at the member's ends are found from the local nodal displacements that are extracted from the global nodal displacements found from equation (4 – 1). Also, at zero shear point, if it exists, for the element under uniformly distributed load, an additional critical section is indicated at that point.

3- The preceding moments and the axial forces are then used to determine the minimum load (safety) factor (α) among all critical sections which would cause next plastic hinge to be developed according to the corresponding critical section axial force – moment interaction diagram (surface).

4- Repeating steps (1) to (3) until convergence is obtained such that

$$\left|\frac{a^{a\,s,r} - a^{a\,s,r-1}}{a^{a\,s,r}}\right| \le 0.001 \quad \text{---------- (4 – 3)}$$

and the final load factor for increment (s) will be $a^{a\,s} = a^{a\,s,r}$ which is multiplied by element forces and displacements to find the change in them due to load increment (s).

5- At any iteration (r), if $[K]^{s,\,r}$ is singular (i.e. $|K| \le 0$),another iteration equation instead of equation (4 – 2) is to be used for the rest of iterations in load increment (s) which will be the rest of analysis to find $[a^{a\,m,r}]$ and $a^{a}_{final} = \sum_{s=1}^{m} a^{a\,s,r}$. This equation will be **[15]**

$$(P^{s,r-1} = (P^{s-1} + \left(\frac{1}{10}\right)(a\,P^{s,r-1}) + \left(1 - \frac{1}{10}\right)(a\,P^{s,r-2}) \quad \text{--(4– 4)}$$

The factor $[1]$ is reduced by one – tenth every time the singularity problem appears until convergence is obtained as given by equation (4 – 3).

6- At the end of load increment (**s**), the structure stiffness is modified through inserting a plastic hinge in the identified section and updating the nodal coordinates as follows

For node ***N(X,Y,Z);***

$$X^{s+1} = X^{s} + U^{s}_{N[global]}\, a^{a\,s} \quad \text{---------- (4 – 5)}$$

$$Y^{s+1} = Y^{s} + V^{s}_{N[global]}\, a^{a\,s} \quad \text{---------- (4 – 6)}$$

$$Z^{s+1} = Z^{s} + W^{s}_{N[global]}\, a^{a\,s} \quad \text{---------- (4 – 7)}$$

7- Repeating steps (1) to (6) for reanalyzing the updated structure for the applying loads finding another $[a^{a\,s}]$ for each load increment (s) up to collapse.

The final load factor will be

$$\alpha_{final} = \sum_{s=1}^{m} \alpha_s \qquad \text{---------- (4 – 8)}$$

4.3 Distribution of Reinforcement used in the Formulation of the Interaction Surface:

a) Members under axial force plus uniaxial bending:

For members under axial load plus uniaxial bending, the reinforcement may be distributed either equally or not at top and bottom faces.

b) Members under axial force plus biaxial bending:

The reinforced concrete sections shown in Fig. (4 – 1) are considered.

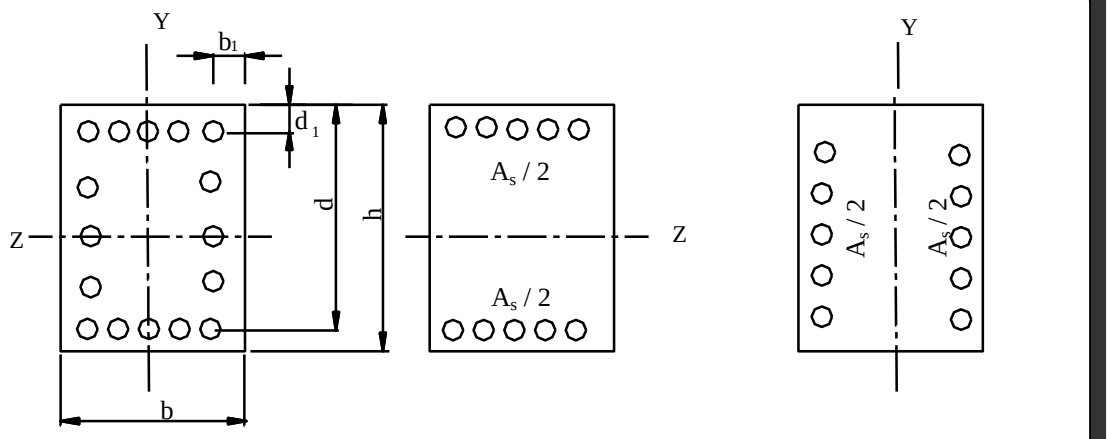

(a)	(b)	(c)
Under Axial Plus Biaxial Bending	**Under Axial Plus Bending about(z-axis)**	**Under Axial Plus Bending about(y-axis)**

Fig.(4 – 1): Member Section for Various Steel Distributions

The section in Fig.(4 – 1a), which is symmetrically distributed about both axes, is assumed to be subjected to axial force plus biaxial bending. If the same section is subjected to axial force plus bending moment about z – axis, all the steel reinforcement should be evenly distributed in faces (b) as suggested by **Pannel [34]** as shown in Fig. (4–1b). Similarly, if the section is under axial force plus bending moment about y – axis, the steel is imagined to flow by even increments from faces (b) to an evenly distributed line in faces (h) as shown in Fig. (4 – 1c).

4.4 Axial Load – Moment Interaction Diagram:

For any reinforced concrete section, the formation of plastic hinge is related to the axial load – moment interaction diagram. Fig.(4 – 2) shows a typical interaction diagram for a reinforced concrete section in its general case (i.e. axial force plus biaxial bending (My, Mz). The interaction is exactly represented by a three – dimensional surface. In the present study and for simplicity, this surface has been idealized by four linear surfaces (planes) defined by six points A, B, $\overline{B}$, C, $\overline{C}$ and D.

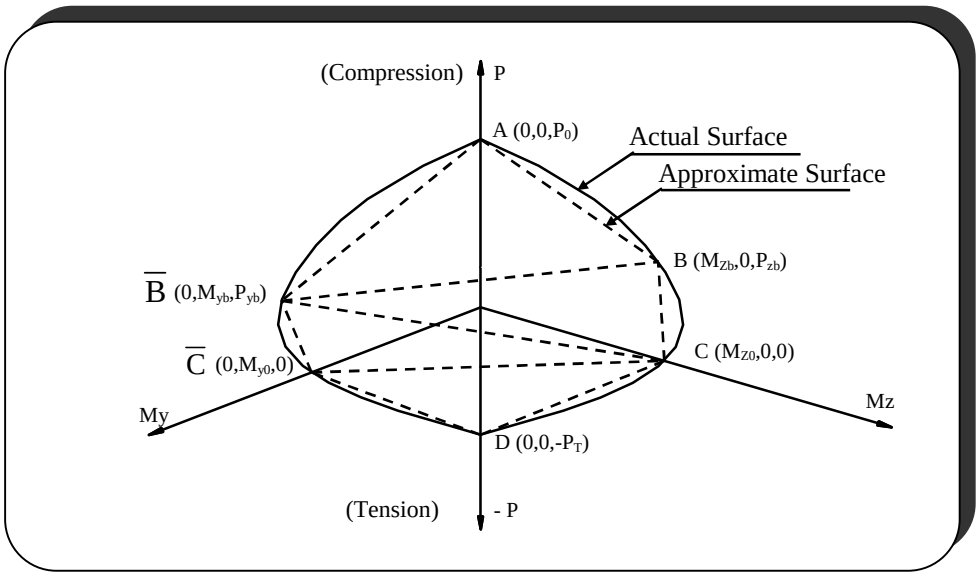

Fig.(4 – 2): Axial Force – Moment Interaction Surface for a Typical Section

To develop the surface, the coordinates of points A, B, $\overline{B}$, C, $\overline{C}$ and D, which are indicated in Fig. (4 – 2), must be determined. Also, in the development of the diagram, the stress – strain curve for concrete in compression is assumed to be parabolic up to the maximum stress (f_c'), which is the cylinder strength, corresponding to a strain of (ε_o), as shown in Fig.(4 – 3), so that **[12]**

$$f_c = f_c'\left[\frac{2\varepsilon_c}{\varepsilon_o} - \left(\frac{\varepsilon_c}{\varepsilon_o}\right)^2\right] \quad \text{---------- (4 – 9)}$$

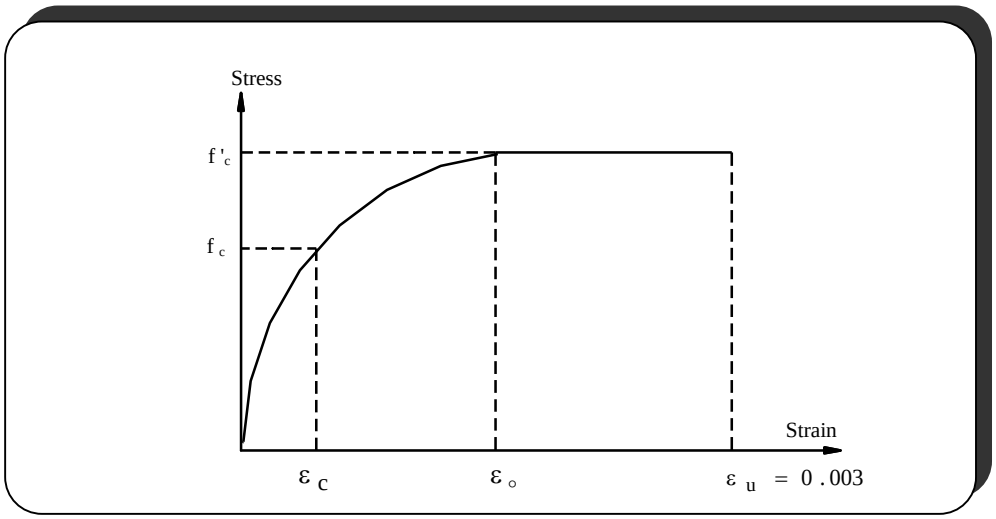

Fig.(4 – 3): Stress – Strain Curve for Concrete

Case (a): Bending About Z – Axis:

Point C corresponds to the yielding of tensile reinforcement under pure flexure with concrete compressive strain ε_c being less than $\varepsilon_o = 0.002$, as shown in Fig. (4 – 4). The analysis of the section gives the following equation for the neutral axis depth c :

$$Ac^3 + Bc^2 + Dc + F = 0 \qquad \text{---------- (4 – 10)}$$

where

$$A = 0.006 E_s \rho'' + \rho'' f_y$$

$$B = 0.000012 \cdot E_s^2 d + 0.006 E_s \rho'' d + 0.000012 \cdot \rho'' E_s^2 d$$

$$D = 0.000024 \cdot E_s^2 d^2 + 0.000012 \cdot \rho'' E_s^2 d h$$

$$F = 0.000012 \cdot E_s^2 d^3 + 0.000012 \cdot \rho'' E_s^2 d_1 d^2$$

in which $\rho = \dfrac{A_{stz}}{bd}$, $\rho'' = \dfrac{A_{scz}}{bd}$

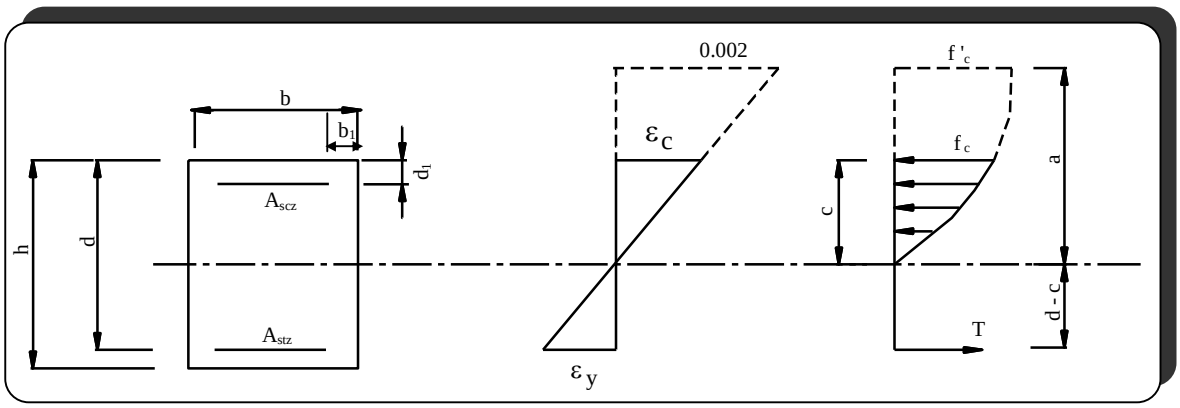

Fig.(4 – 4): Yield Condition Under Pure Flexure

Equation (4 – 10) is solved by Newton – Raphson method to find c. The stress in compression steel is given by

$$f_{sc} = \frac{c - d_1}{d - c} f_y \quad \text{---------- (4 – 11)}$$

The yield moment is given by

$$M_{z_o} = f_c' b c^2 \left[\frac{3a^2 - 4ac}{3a^3}\right](d - c) + \left[\frac{8a^2 c - 3ac^2}{12a^3}\right] A_{sc_z} f_{sc} (d - d_1)$$

------(4 – 12)

where

$$a = \frac{0.002 E_s (d - c)}{f_y}$$

The point B in the diagram corresponds to the balanced state (P_{zb}, M_{zb}) when concrete compressive strain (ε_c) reaches a value of 0.002, simultaneously with tensile steel yielding. At this stage, the neutral axis depth c is given by

$$c = \frac{0.002 d}{0.002 + \varepsilon_y} \quad \text{---------- (4 – 13)}$$

and

$$P_{zb} = 2 f_c' b c/3 + A_{scz} f_{sc} - A_{stz} f_y \quad \text{---------- (4 – 14)}$$

$$M_{zb} = 2 f_c' b c/3 \left(\frac{h}{2} - \frac{3}{8} c\right) + A_{scz} f_{sc} \left(\frac{h}{2} - d_1\right) + A_{stz} f_y \left(\frac{h}{2} - d_1\right)$$

---------- (4 – 15)

where $f_{sc} = 0.002 E_s \frac{(c - d_1)}{c} \le f_y$

Case (b): Bending About Y – Axis:

Proceeding as in case (a) and for pure flexure (point $\bar{C}$) the following equation for neutral axis depth $\bar{c}$ can be obtained:

$$\bar{A}\bar{c}^3 + \bar{B}\bar{c}^2 + \bar{D}\bar{c} + \bar{F} = 0 \quad \text{---------- (4 – 16)}$$

Where

$$\bar{A} = 0.006 E_s \left(\rho' + \rho - \rho_y\right)$$

$$\bar{B} = 0.000012 \cdot E_s^2 (b + b_1) + 0.006 E_c \rho' (b + b_1) + 0.000012 \cdot \rho E_s^2 (b + b_1)$$

$$\bar{D} = 0.000024 \cdot E_s^2 (b + b_1)^2 + 0.000012 \cdot E_s^2 (b + b_1) b$$

$$\bar{F} = 0.000012 \cdot E_s^2 (b + b_1)^3 + 0.000012 \cdot \rho E_s^2 b_1 (b + b_1)^2$$

where $\rho = \dfrac{A_{sty}}{(b + b_1)h}$, $\rho' = \dfrac{A_{scy}}{(b + b_1)h}$

Equation (4 –16) is solved by Newton – Raphson method to find $\bar{c}$. The stress in compression steel can be calculated from the following equation

$$f_{sc} = \frac{\bar{c} + b_1}{b + (b_1 + \bar{c})} f_y \quad \text{---------- (4 – 17)}$$

The yield moment is given by

$$M_{y_o} = f_c' h \bar{c}^2 \left[\frac{3a_1^2 + a_1\bar{c}}{3a_1^3}(b + b_1 + \bar{c}) + \frac{8a_1^2\bar{c} + 3a_1\bar{c}^2}{12a_1^3}\right] \text{---- (4 – 18)}$$
$$+ A_{scy}\left(f_{sc} - f_c'\right)(b + 2b_1)$$

where

$$a_1 = \frac{0.002 E_s (b + (\bar{c} - b1))}{f_y}$$

The point $\bar{B}$ in the diagram corresponds to the balanced state (P_{yb}, M_{yb}). At this stage, the neutral axis depth $\bar{c}$ is given by

$$\bar{c} = \frac{0.002(b + b_1)}{0.002 + \varepsilon_y} \quad \text{---------- (4 – 19)}$$

and

$$P_{yb} = 2 f'_c h\bar{c}/3 + A_{scy} f_{sc} + A_{sty} f_y$$

$$M_{yb} = 2 f'_c h\bar{c}/3 \left(\frac{b}{2} - \frac{3}{8}\bar{c}\right) + A_{scy} f_{sc} \left(\frac{b}{2} - b_1\right) + A_{sty} f_y \left(\frac{b}{2} - b_1\right)$$

---------- (4 – 20)

where

$$f_{sc} = 0.002 E_s \frac{(\bar{c} - b_1)}{\bar{c}} \le f_y$$

Points A and D are determined by the pure compressive strength (P_o) and pure tensile strength P_t of the section, such that

$$P_o = 0.85 f'_c (bh - A_{sT}) + A_{sT} f_y$$ ---------- (4 – 21)

$$P_t = A_{sT} f_y$$ ---------- (4 – 22)

where A_{sT} = total reinforcement in the section

After determining the coordinates of points A, B, $\overline{B}$, C and $\overline{C}$ and by using vector operations, the equations of planes AB$\overline{B}$, B$\overline{B}$C, $\overline{B}$C$\overline{C}$ and C$\overline{C}$D can be derived as follows

Finding the vectors $\vec{V}_2 = \overrightarrow{AB}$ and $\vec{V}_2 = \overrightarrow{A\overline{B}}$ between the points A, B, $\overline{B}$ so that the cross product of the vectors $\vec{V}_1$ and $\vec{V}_2$ represent the normal vector. Hence, the equation of any plane in space is

$$(\vec{V}_1 \times \vec{V}_2) \cdot \overrightarrow{AP_1} = 0$$ ---------- (4 – 23)

where P_1 (M_z, M_y, P) is any point in the plane

Using equation (4 – 23), the equations of planes AB$\overline{B}$,B$\overline{B}$C, $\overline{B}$C$\overline{C}$ and C$\overline{C}$D respectively are:

$$(M_{yb}(P_o - P_{zb}) - M_z)(M_{zb}(P_{yb} - P_o) - M_y) - (M_{zb} - M_{yb})(P - P_o) = 0$$

---------- (4 – 24a)

$$(P_{zb}\,M_{yb}-M_z+M_{zb})(P_{yb}+P_{zb}-M_{z_o}+Mzb)+M_{zb}\,P_{zb}\,M_y$$
$$-(M_{yb}-M_{z_o}+M_{zb})(P+P_{zb})=0$$

---------- (4 – 24b)

$$(+P_{yb}\,M_{y_o}-M_z+M_{zo}\,P_{yb}-M_y+M_{y_o})-(M_{yb}+M_{y_o}-M_{z_o}-P)=0$$

----------(4 – 24c)

$$(P_t\,M_{yo}-M_z)-(P_t\,M_{zo}-M_y)-(M_{zo}M_{yo}-P+P_t)=0$$ ------ (4 – 24d)

4.5 Plastic Hinge Formation:

For any critical section (m), at any stage ($S-1$) of analysis, the total axial force P_s and the total moments $(M_{zs})and(M_{ys})$ are known as a result of analysis of a previous (S) stages. In the current stage ($S-1$), P_1, M_{z1} and M_{y1}, are the axial force and moments caused by applying load at iteration (r) (i.e. for load factor = 1). It is then possible to find minimum load factor (a_m), which would cause a plastic hinge to form at a certain critical section such that the final axial force $(P=P_s-a_m P_1)$ and the moments $(M_z=M_{zs}-a_m M_{z1}\ ,\ M_y=M_{ys}-a_m M_{y1})$ lie on any plane of the interaction surface.

Writing $\overline{M}_{zs}=|M_{zs}|$, $\overline{M}_{ys}=|M_{ys}|$, $\overline{M}_{z1}=|M_{z1}|$, $\overline{P}_s=|P_s|$ and $\overline{P}_1=|P_1|$ then, the load factor (a_m) is calculated as follows:

A- If the force state ($P, M_z and M_y$) lies in the plane $AB\overline{B}$

$$a_m=\frac{M_{zb}(P_{yb}+P_o)\overline{M}_{ys}+M_{yb}(P_o+P_{zb})\overline{M}_{zs}+M_{zb}M_{yb}(\overline{P}_s+P_o)}{M_{yb}\overline{M}_{z1}(P_o+P_{zb})+M_{zb}\overline{M}_{y_1}(P_{yb}+P_o)-M_{zb}M_{yb}\overline{P}_1}$$

---------- (4 – 25a)

B- If the force state ($P, M_z and M_y$) lies in the plane $B\overline{B}C$

$$\alpha_m = \frac{(P_{yb} - P_{zb})(M_{z_o} - M_{zb}) - (M_{zb} P_{zb} - \bar{M}_{ys})(P_{zb} M_{yb} - \bar{M}_{zs}) - (M_{yb} - M_{z_o} - M_{zb})(\bar{P}_s - P_{zb})}{P_{zb} M_{yb} \bar{M}_{z_1} - (P_{yb} - P_{zb})(M_{z_o} - M_{zb}) - (M_{zb} P_{zb} - \bar{M}_{y_1}) + (M_{yb} - M_{z_o} - M_{zb})(\bar{P}_1}$$

---------- (4 – 25b)

C- If the force state (P, M_z and M_y) lies in the plane $\bar{B}C\bar{C}$

$$\alpha_m = \frac{P_{yb} M_{y_o} \bar{M}_{zs} - M_{z_o} P_{yb} (\bar{M}_{ys} - M_{y_o}) - M_{z_o} \bar{P}_s (M_{yb} - M_{y_o})}{M_{z_o} (M_{yb} - M_{y_o}) (\bar{P}_1 - P_{yb} M_{y_o} \bar{M}_{z_1} - P_{yb} M_{z_o} \bar{M}_{y_1}}$$

---------- (4 – 25c)

D- If the axial force P is tensile, α_m necessary for a hinge to form is obtained by considering plane $C\bar{C}D$ so that

$$\alpha_m = \frac{(P_t - \bar{P}_s)(M_{z_o} M_{y_o}) - P_t M_{y_o} \bar{M}_{zs} - P_t M_{z_o} \bar{M}_{ys}}{M_{z_o} M_{y_o} \bar{P}_1 - P_t M_{y_o} \bar{M}_{z_1} - P_t M_{z_o} \bar{M}_{y_1}}$$ -----(4 – 25d)

The sign of each of P_s, Mz_s, My_s, P_1, M_{z_1}, and M_{y_1} must be taken into consideration to include local unloading and to express the actual behavior of the structure more accurately. To do this:

a- If the sign of $(\bar{M}_{zs})$ is opposite to the sign of (M_{z1}), one should put either $(\bar{M}_{zs} - |M_{zs}|)$ or $(\bar{M}_{z_1} - |M_{z_1}|)$ to be used in the expressions (4– 25a) through (4 – 25d). The bending moment about Y axis can be treated in the same way.

b- If the sign of (P_s) is opposite to the sign of (P_1), one may put either $(\bar{P}_s - |P_s|)$ or $(\bar{P}_1 - |P_1|)$ to be used in the expressions (4 – 25a) through (4 – 25d).

Since, it is not possible to know beforehand the plane in which (P, M_z and M_y) may lie, the determination of (α_m) is essentially a trial and a check procedure and the computer program copes with different possibilities.

4.6 Moment – Rotation Law:

The moment – rotation law of a reinforced concrete section is one of the main features in the inelastic analysis of reinforced concrete frames since the redistribution of moments depends on the amount of inelastic rotation which occurs in the section after the formation of a plastic hinge in that section.

In general, there are many previously suggested linearized moment – rotation laws as given in Fig. (4 – 5)

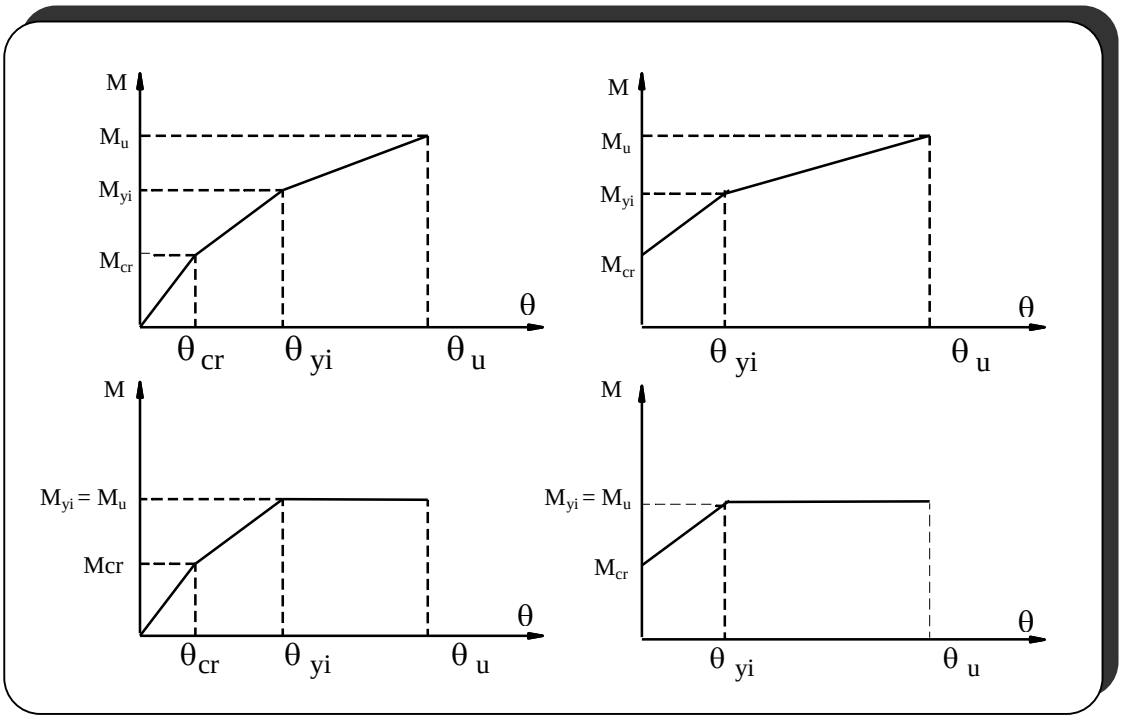

Fig.(4 – 5): Several Idealized Moment – Rotation Laws

However, the one adopted in the present work is a bilinear moment – rotation law as shown in Fig. (4 – 6).

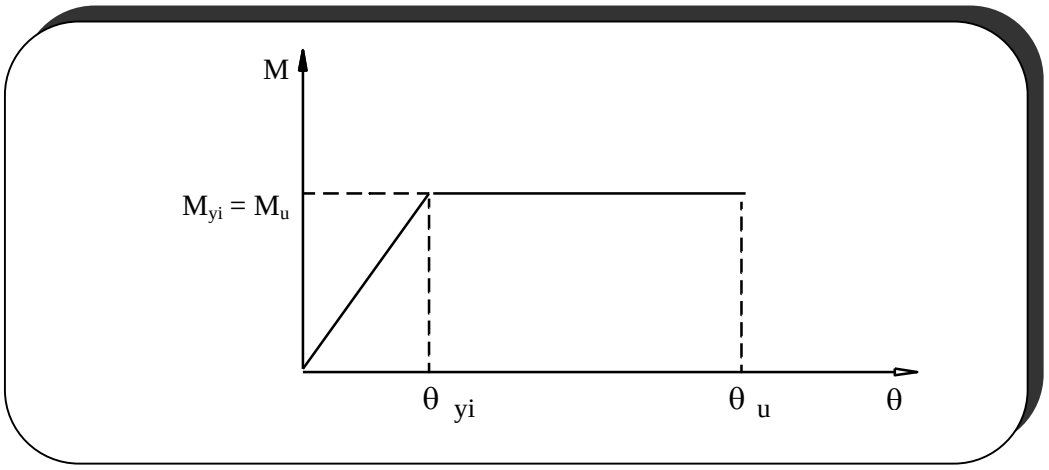

Fig.(4 – 6): Adopted Moment – Rotation Law

The yield moment (M_{yi}) and the corresponding rotation (θ_{yi}) are found from analysis at the instant when a plastic hinge is formed at a certain section. The ultimate moment (M_u) is assumed to be the same as (M_{yi}) since the section is assumed to be not capable to resist any additional moment after plastic hinge formation.

To calculate the ultimate rotation (i.e. θ_u) corresponding to crushing state, the following equation can be used for any critical section of any member **[35]**:

$$\theta_u = \frac{\varepsilon_u}{c} L_P \qquad \text{---------- (4 – 26)}$$

where $\varepsilon_u = 0.003$, L_p = length of plastic hinge (i.e. length of plastic zone forming a plastic hinge) and c = distance from extreme compression fiber to the neutral axis of the section (at ultimate condition).

For the case, $M_{yi} = M_u = 0$ (i.e. the member under pure axial force), if

a- The axial force is compressive then

$\theta_y = \theta_u = 0$ and crushing failure happens suddenly

or

b- The axial force is tensile then

$\bar{}_{u}$ ì ã and no possibility of crushing failure.

4.6.1 Length of Plastic Hinge (L_P):

The length of a plastic hinge can be defined as the equivalent length of a plastic hinge over which the plastic curvature is considered to be constant. There are many empirical expressions for the length of plastic hinge (L_P) on one side of critical section as **[35]**

$$L_P = 0.5\bar{d} + 0.05Z \quad \text{---------- (4 – 27)}$$

where

Z = distance from the point of maximum moment to the nearest point of zero moment.

$\bar{d}$ the normal distance from the extreme point in compression to the extreme lower reinforcing bar in tension.

To simplify the calculation of L_P, it is taken as **[24]**

$$L_P = 0.75\bar{d} \quad \text{---------- (4 – 28)}$$

It may be noted that, the length of the plastic hinge region for internal critical section is taken as twice of (L_P) calculated from equation (4 – 29), as follows **[24]**:

$$L_P = 2[0.75\bar{d}] \quad \text{---------- (4 – 29)}$$

4.6.2 Location of Neutral Axis (c):

a- <u>Members subjected to uniaxial loads (Axial compression plus uniaxial bending)</u>

A section is considered for a reinforced concrete member subjected to axial force plus uniaxial moment, as shown in Fig. (4 – 7)

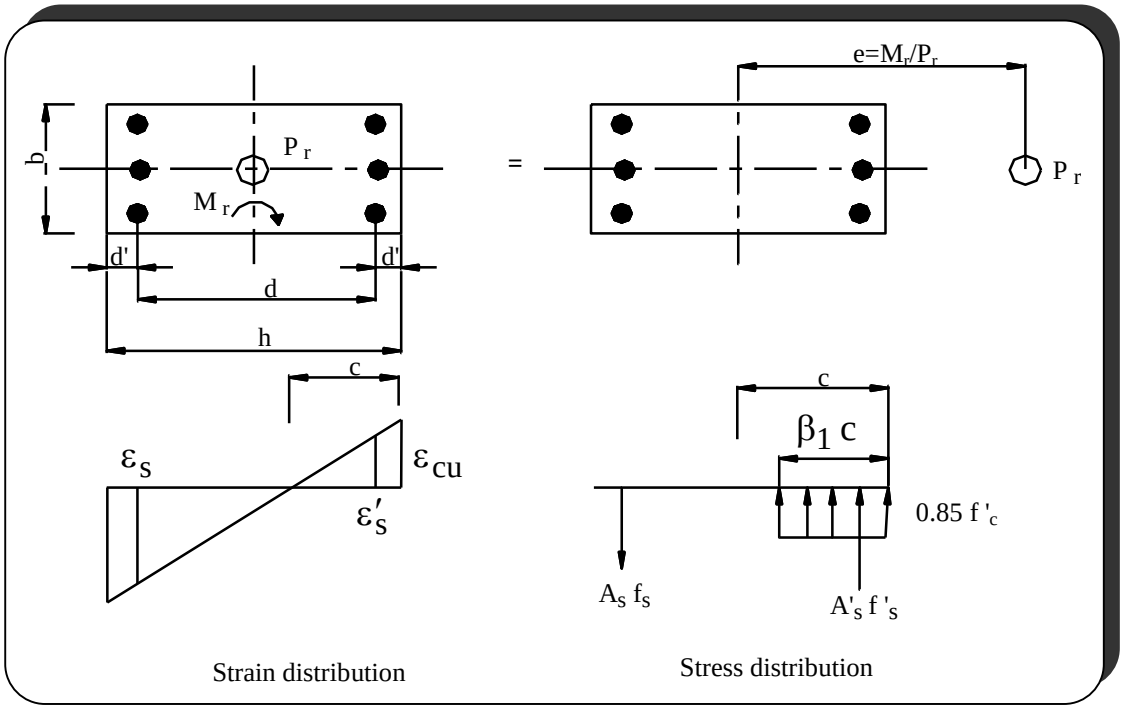

Fig.(4 – 7): Strain Distribution and Internal Forces for Member with Uniaxial Loads

Under the balanced strain condition, the member fails at the yielding of tension steel which occurs simultaneously with extreme compression fibers reaching the limit strain of ε_{cu}. The position of the neutral axis for the balanced condition is:

$$c_b = \frac{\varepsilon_{cu}\, d}{\varepsilon_{cu} + \varepsilon_y} \qquad \text{---------- (4 – 30)}$$

where c_b = the position of the neutral axis from the extreme fibers that reach ε_{cu}, and ε_{cu} = the ultimate strain of concrete in compression. Knowing the position of neutral axis, the axial and the bending resistance of the member under a balanced strain condition can be obtained as

$$P_{rb} = 0.85\, f'_c\, \beta_1 c_b\, b + A'_s\,(f'_s - 0.85\, f'_c) - A_s\, f_y \qquad \text{---------- (4 – 31)}$$

$$M_{rb} = 0.85\, f'_c\, \beta_1 c_b\, b\left(\frac{h}{2} - \frac{\beta_1 c_b}{2}\right) + A'_s\,(f'_s - 0.85\, f'_c)\left(\frac{h}{2} - d'\right) + A_s\, f_y\left(d - \frac{h}{2}\right) \qquad \text{---(4 – 32)}$$

The eccentricity in this case is:

$$e_b = \frac{M_{rb}}{P_{rb}} \quad \text{---------- (4 – 33)}$$

When the eccentricity of the applied loads is smaller than (e_b), the member will fail in compression failure mode (i.e. Concrete strain reaches the maximum strain ε_{cu} before steel on the tension side reaches yield strain). The position of the neutral axis can be found by solving the following equation

$$F_1 c^3 + F_2 c^2 + F_3 c + F_4 = 0 \quad \text{---------- (4 – 34)}$$

where F_i (i = 1 – 4) are coefficients. If the compression steel has yielded (i.e. $f_s' = f_y$), then

$$F_1 = 0.425 f_c' b \beta_1^2 \quad \text{---------- (4 – 35)}$$

$$F_2 = 0.85 f_c' b \beta_1 \left(e - \frac{h}{2}\right) \quad \text{---------- (4 – 36)}$$

$$F_3 = A_s E_s \varepsilon_{cu} \left(e + \frac{h}{2} - d'\right) - A_s' \left(f_y - 0.85 f_c'\right) \left(\frac{h}{2} - e - d'\right) \quad \text{---- (4 – 37)}$$

$$F_4 = -A_s E_s \varepsilon_{cu} \left(h - d'\right) \left(e + \frac{h}{2} - d'\right) \quad \text{---------- (4 – 38)}$$

If the compression steel has not yielded, $f_s' < f_y$, then F_1 and F_2 have the same expressions as equations (4 – 35) and (4 – 36). F_3 and F_4 can be calculated as follows:

$$F_3 = A_s E_s \varepsilon_{cu} \left(e + \frac{h}{2} - d'\right) - A_s' E_s \varepsilon_{cu} \left(\frac{h}{2} - e - d'\right) - 0.85 A_s' f_c' \left(\frac{h}{2} - e - d'\right) \quad \text{---------- (4 – 39)}$$

$$F_4 = A_s' E_s \varepsilon_{cu} d' \left(\frac{h}{2} - e - d'\right) - A_s E_s \varepsilon_{cu} d \left(e + \frac{h}{2} - d'\right) \quad \text{------- (4 – 40)}$$

When eccentricity of the applied loads is greater than e_b, the member will fail in tension failure mode. Steel on the tension side will yield first. The location of the neutral axis can be determined by solving equation (4 – 34), with coefficient Fi calculated as described below. If the compression steel has yielded, then

$$F_1 = 0 \quad \text{---------- (4 – 41)}$$

$$F_2 = 0.425 f_c' b \beta_1^2 \quad \text{---------- (4 – 42)}$$

$$F_3 = 0.85 f_c' b \beta_1 \left(e - \frac{h}{2}\right) \quad \text{---------- (4 – 43)}$$

$$F_4 = A_s' \left[f_y - 0.85 f_c' \left(e - \frac{h}{2} + d'\right) - A_s f_y \left(e + \frac{h}{2} - d'\right)\right] \quad \text{---------- (4 – 44)}$$

If the compression steel has not yielded, then F_1 and F_2 can be determined from equations (4 – 35) and (4 – 36) respectively, and F_3 and F_4 can be obtained as follows:

$$F_3 = A_s' E_s \varepsilon_{cu} \left(e - \frac{h}{2} + d'\right) - 0.85 A_s' f_c' \left(e - \frac{h}{2} + d'\right) - A_s f_y \left(e + \frac{h}{2} - d'\right) \quad \text{-------- (4 – 45)}$$

$$F_4 = A_s' E_s \varepsilon_{cu} \left(e - \frac{h}{2} + d'\right) \quad \text{---------- (4 – 46)}$$

For members subjected to axial tension plus uniaxial bending, the location of the neutral axis c can be determined from the same equation (4 – 34) but with coefficients as described below. If the compression steel (i.e. as in this case) has yielded, then

$$F_1 = 0 \quad \text{---------- (4 – 47)}$$

$$F_2 = -0.425 f_c' b \beta_1^2 \quad \text{---------- (4 – 48)}$$

$$F_3 = 0.85 f'_c b \beta_1 \left(e + \frac{h}{2}\right) \quad \text{---------- (4 – 49)}$$

$$F_4 = A_s' [f_y - 0.85 f'_c] \left(e + \frac{h}{2} - d'\right) + A_s f_y \left(e - \frac{h}{2} + d'\right) \quad \text{-------- (4 – 50)}$$

If the compression steel has not yielded, the coefficient F_i is as follows

$$F_1 = -0.425 f'_c b c^2 \quad \text{---------- (4 – 51)}$$

$$F_2 = 0.85 f'_c b \beta_1 \left(e + \frac{h}{2}\right) \quad \text{---------- (4 – 52)}$$

$$F_3 = A_s' [\varepsilon_{cu} E_s - 0.85 f'_c] \left(e + \frac{h}{2} - d'\right) + A_s f_y \left(e - \frac{h}{2} + d'\right) \quad \text{--------(4 – 53)}$$

$$F_4 = -A_s \varepsilon_{cu} E_s \left(e + \frac{h}{2} - d'\right) \quad \text{---------- (4 – 54)}$$

β_1, as defined in ACI – Code **[38]**, is given as follows

$$\beta_1 = 0.85 \quad if \quad f'_c \le 30\ MPa \quad \text{---------- (4 – 55)}$$

$$\beta_1 = 0.85 - 0.05 \frac{f'_c - 30}{7} \quad if \quad f'_c > 30\ MPa \quad \text{---------- (4 – 56)}$$

However, β_1 is not less than 0.65

b- <u>Members with biaxial loads (Axial compression plus biaxial bending)</u>

When a rectangular section is subjected to biaxial loads i.e. axial force P_f, bending moments M_{fz}, M_{fy} about Z and Y axes respectively, the position of the neutral axis can be found by using the iteration method for solving equilibrium equations. Assuming that the maximum compressive strain in concrete occurs at the corner O, as shown in Fig. (4 – 8) and taking the moments about the axes oX_1 and oY_1, respectively, the following equations can be established:

$$M_1 = \sum_{i=1}^{n} f_{si} A_{si} Y_i + e_z \left(\frac{h}{2}\right) + 0.85 f'_c Q_{cx} + A_c e_z \left(\frac{h}{2}\right) = 0$$

---------- (4 – 57a)

$$M_2 = \sum_{i=1}^{n} f_{si} A_{si} X_i + e_y \left(\frac{b}{2}\right) + 0.85 f'_c Q_{cy} + A_c e_y \left(\frac{b}{2}\right) = 0$$

---------- (4 – 57b)

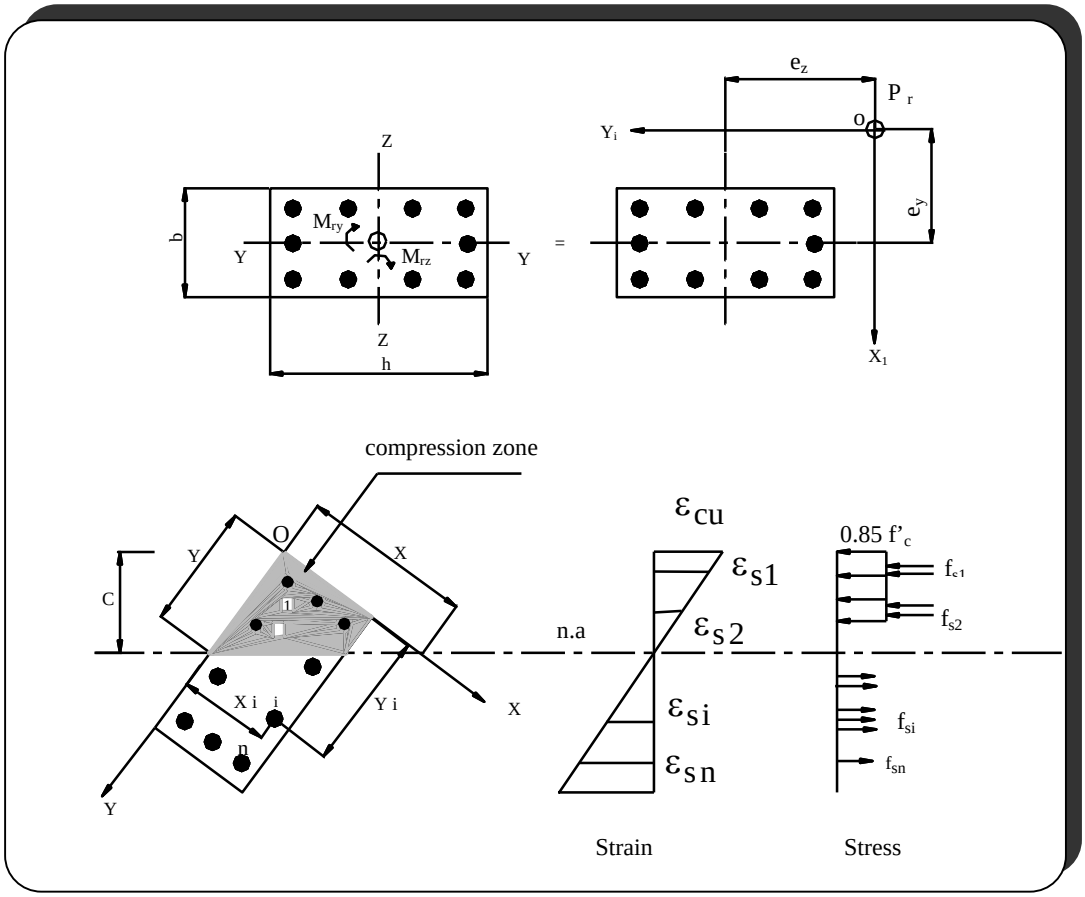

Fig.(4 – 8): Strain and Stress Distribution for a Member with Biaxial Loads

where

A_{si} , f_{si} = area and stress of the ith reinforcing bar

X_i , Y_i = coordinates of the *ith* reinforcing bar in the X , Y coordinate system.

A_c , Q_{cx} and Q_{cy} = area and the first moments of compression zone about reference axes X and Y , respectively.

e_z, e_y = eccentricities of the applied loads. $e_z = M_{fz}/P_f$, $e_y = M_{fy}/P_f$

P_f , M_{fz} and M_{fy} are the force state at the section under considerations obtained from analysis (factored loads) .

P_r , M_{rz} and M_{ry} are the ultimate axial and bending moment resistance of the section. When $(b/X + h/Y) \le 1$, part of the section of concrete is in compression and the neutral axis goes through the section, as shown in Fig. (4 – 8). A_c , Q_{cx} and Q_{cy} can be expressed as:

$$A_c = (1 + K_1^2 + K_2^2)\frac{XY}{2} \qquad \text{---------- (4 – 58)}$$

$$Q_{cx} = (1 + K_1^3 + 3K_2^2 + 2K_2^3)\frac{XY^2}{6} \qquad \text{---------- (4 – 59)}$$

$$Q_{cy} = (1 + 2K_1^3 + 3K_1^2 + K_2^3)\frac{X^2Y}{6} \qquad \text{---------- (4 – 60)}$$

where

$K_1 = (X + b)/X$ *for* $X < b$ *, and* $K_1 = 0$ *for* $X \ge b$

$K_2 = (Y + h)/Y$ *for* $Y < h$ *, and* $K_2 = 0$ *for* $Y \ge h$

When $(b/X + h/Y) \ge 1$, the whole section is in compression,

Hence,

$$A_c = bh \quad , \quad Q_{cx} = \frac{bh^2}{2} \quad , \quad Q_{cy} = \frac{b^2h}{2} \qquad \text{---------- (4 – 61)}$$

Stress in reinforcing bars can be found according to the similar triangles of strain distribution and the relationship between the stress and strain :

$$f_{si} = E_s \varepsilon_{cu}\left(\frac{X_i}{X} + \frac{Y_i}{Y} - 1\right) \quad |f_{si}| \le f_y \qquad \text{----------(4 – 62)}$$

It can be seen from equation (4 – 57) that the resultant moments M_1 and M_2 about oX_1 and oY_1 are implicit functions of the position coordinates X and Y of the neutral axis. The simultaneous equations can be solved by

Newton – Raphson method. Expanding the equation and keeping only the linear terms **[25]**:

$$M_1(X,Y) = M_1(X_0,Y_0) + \frac{\partial M_1(X_0,Y_0)}{\partial X}dX + \frac{\partial M_1(X_0,Y_0)}{\partial Y}dY$$

---------- (4 – 63a)

$$M_2(X,Y) = M_2(X_0,Y_0) + \frac{\partial M_2(X_0,Y_0)}{\partial X}dX + \frac{\partial M_2(X_0,Y_0)}{\partial Y}dY$$

---------- (4 – 63b)

where

$M_1(X_0,Y_0), M_2(X_0,Y_0)$ = moments calculated from equation (4 – 57) with initial estimation values X_0 and Y_0.

And $(dX = X - X_0, dY = Y - Y_0)$ are the increments of the neutral axis coordinates.

Equation (4 – 63) can be solved for dX and dY, and new coordinates of the neutral axis can be found as $X = X_0 + dX, Y = Y_0 + dY$. The same procedure is repeated until equation (4 – 57) convergence to the desired accuracy (always $M_1(X,Y)$, $M_2(X,Y) \le 0.0001$).

For members subjected to axial tensile force plus biaxial bending, the location of the neutral axis can be determined in the same previous way but A_c, Q_{cx}, Q_{cy} and f_{si} have the following expressions:

$$A_c = bh - (1 - K_1^2 - K_2^2)\frac{XY}{2} \quad \text{---------- (4 – 64)}$$

$$Q_{cx} = \frac{bh^2}{2} - (1 - K_1^3 - 3K_2^2 + 2K_2^3)\frac{XY^2}{6} \quad \text{---------- (4 – 65)}$$

$$Q_{cy} = \frac{b^2h}{2} - (1 - K_2^3 - 3K_1^2 + 2K_1^3)\frac{X^2Y}{6} \quad \text{---------- (4 – 66)}$$

$$f_{si} = E_s \varepsilon_{cu}\left(\frac{1}{b/X + h/Y - 1}\right)\left(1 - \frac{Xi}{X} - \frac{Yi}{Y}\right) \quad |f_{si}| \le f_y \quad \text{--(4 – 67)}$$

where

X_i, Y_i = coordinates of the *ith* reinforcing bar in X, Y coordinate system as shown in Fig. (4 – 9)

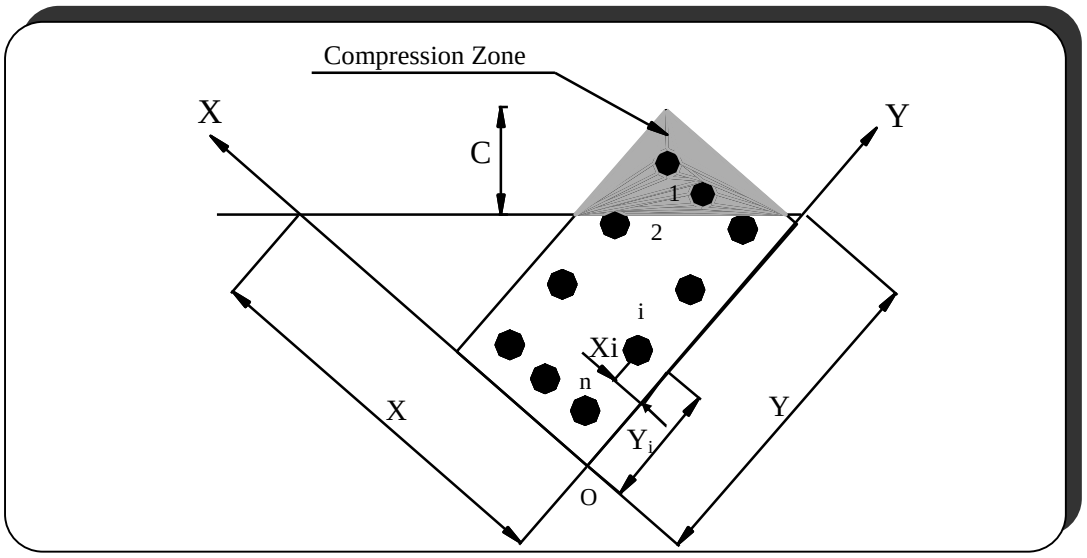

Fig.(4 – 9): Location of Neutral Axis for Axial Tension Plus Biaxial Bending.

4.7 Inelastic Rotations:

It is necessary to find an expression for computing the inelastic rotations $(\theta_{y\,inel})$ *and* $(\theta_{z\,inel})$ at any critical section after plastic hinge formation. Such rotations will be added to the yield rotations (i.e. $\theta_{y\,i}$ *and* $\theta_{z\,i}$) and the resulting rotation ϕ_{yz} can be computed using the following equation:

$$\theta_{z\,y} = \sqrt{\theta_{y_{to}}^2 + \theta_{z_{to}}^2} \qquad \text{---------- (4 – 68)}$$

where

$$\theta_{y_{to}} = \theta_{y\,i} + \theta_{y_{inel}} \qquad \text{---------- (4 – 69a)}$$

$$\theta_{z_{to}} = \theta_{z\,i} + \theta_{z_{inel}} \qquad \text{---------- (4 – 69b)}$$

The resulting rotation θ_{yz} will be compared with θ_u and check for crushing failure.

The inelastic rotations can be found as follows:

a)

In this case, there is a plastic hinge at left extremity of the elastic length. The inelastic rotations in this section is found as explained in chapter three:

$$\theta_{y\,a_{inel}} = \frac{L}{S_4 - 4EI_y}\left[S_8\left(\frac{6EI_y}{L^2}\right)w_a + S_8\left(\frac{6EI_y}{L^2}\right)w_b + S_5\left(\frac{2EI_y}{L}\right) - \theta_{y\,b}\right] \quad \text{------(4 – 70)}$$

$$\theta_{z\,a_{inel}} = \frac{L}{S_2 - 4EI_z}\left[S_6\left(\frac{6EI_z}{L^2}\right)v_a + S_6\left(\frac{6EI_z}{L^2}\right)v_b + S_3\left(\frac{2EI_z}{L}\right) - \theta_{z\,b}\right] \quad \text{-------- (4 – 71)}$$

b)

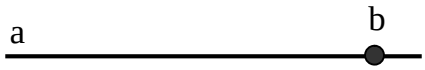

In this case, the plastic hinge is at right extremity so,

$$\theta_{y\,b_{inel}} = \frac{L}{S_4 - 4EI_y}\left[S_8\left(\frac{6EI_y}{L^2}\right)w_a + S_8\left(\frac{6EI_y}{L^2}\right)w_b + S_5\left(\frac{2EI_y}{L}\right) - \theta_{y\,a}\right] \quad \text{-----(4 – 72)}$$

$$\theta_{z\,b_{inel}} = \frac{L}{S_2 - 4EI_z}\left[S_6\left(\frac{6EI_z}{L^2}\right)v_a + S_6\left(\frac{6EI_z}{L^2}\right)v_b + S_3\left(\frac{2EI_z}{L}\right) - \theta_{z\,a}\right] \quad \text{----(4 – 73)}$$

c) 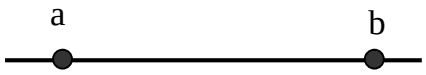

The element in this case has two plastic hinges at its extremities, the inelastic rotations can be found as follows

$$\theta_{a_{inel}} = \theta_{b_{inel}} = \frac{w_a + w_b}{L} \qquad \text{---------- (4 – 74)}$$

$$\phi_{a_{inel}} = \phi_{b_{inel}} = \frac{v_a + v_b}{L} \qquad \text{---------- (4 – 75)}$$

where

w_a, w_b, v_a and v_b are the deflections in Z and Y directions respectively at points (a) and (b).

4.8 Cross – Section Properties:

To express the behavior of reinforced concrete frames more accurately, for sections within elastic the cracking limit, the effective moments of inertia ($I_{ez\ and}\ I_{ey}$) and the cracked cross – sectional area are adopted in the present work. The effective moment of inertia about either axis ($I_{ez}\ or\ I_{ey}$) can be expressed in the following form using the moments of inertia I_g and I_{cr} of the gross section and of the cracked section, respectively, **[36]**

$$I_e = \left(\frac{P_{cr}}{P}\right)^3 I_g + \left[1 - \left(\frac{P_{cr}}{P}\right)^3\right] I_{cr} \leq I_g \qquad \text{---------- (4 – 76)}$$

in which (if the bending is about z – axis):

$$P_{cr} = \frac{1}{2} f_c\, bx + Asc\ fsc + A_{st}\ f_{st}$$

$$f_c = \frac{x}{(h - x)} f_r$$

$$f_{sc} = (n - 1)\frac{(x - d_1)}{(h - x)} f_r$$

$$f_{st} = n\frac{(d - x)}{(h - x)} f_r$$

$$f_r = 0.7\sqrt{f_c'}$$

where $0 \le P_{cr}/P \le 1$, P_{cr} = the force corresponding to the cracking stage, P = the axial force at the stage the section properties are calculated, f_r = modulus of rupture, n = modular ratio ($n = \frac{E_s}{E_c}$) and f_c, f_{sc}, f_{st} are the stresses at extreme compression fiber of concrete and at the level of compression and tension reinforcement respectively.

It is important to mentioned here that:

a) If $M = 0$ and $: P > 0$ (compressive) then $I_e = I_g$

b) If $M = 0$ and $P < 0$ (tensile) then $I_e = I_{cr}$

To obtain I_{crz} (assuming bending about Z - axis) of reinforced concrete members subjected to combined bending and axial force, it is necessary first to calculate the neutral axis location (x) using the given ratio of bending moment to axial force (e), and second to determine the location of the center of gravity (y) of the transformed section, so, for the section shown in Fig.(4 – 10):

$$\frac{b}{6e_z}x_z^3 + \left(\frac{b}{2} - \left(\frac{h}{2e_z} - x_z^2 + \left(nA_{st}\left(\frac{d - h/2}{e_z} + 1\right) + (n - 1)A_{sc}\left(\frac{d_1 - h/2}{e_z} + 1\right)\right)\right)\right)$$

$$- x_z - \left(nA_{st}\left(\frac{d^2 + d(e_z - h/2)}{e_z}\right) + (n - 1)A_{sc}\left(\frac{d_1^2 + d_1(e_z - h/2)}{e_z}\right)\right) = 0$$

------(4 – 77)

$$y = \frac{b x_z^2/2 + n A_{st} d + (n - 1) A_{sc} d_1}{b x_z + n A_{st} + (n - 1) A_{sc}} \quad \text{---------- (4 – 78)}$$

$$I_{cr\,z} = \frac{b\,x_z^3}{12} + b\,x_z\left(y - \frac{x_z}{2}\right)^2 + n\,A_{st}\,(d - y)^2 + (n-1)\,A_{sc}\,(y - d_1)^2$$

---------- (4 – 79)

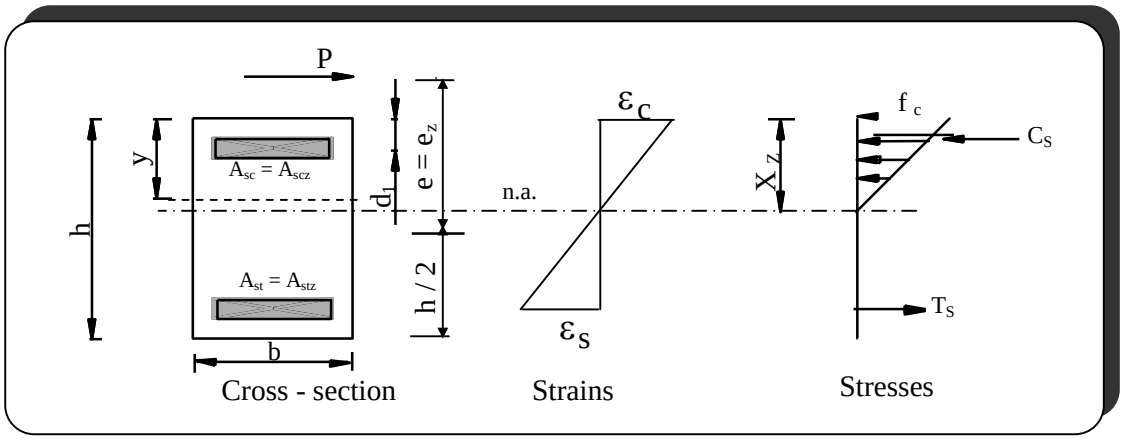

Fig. (4 – 10): Stress and Strain Distribution in Cracked Section (bending is about z – axis)

Proceeding the same previous procedure, for bending about Y – axis and for the section shown in Fig.(4 – 11), then:

$$\frac{h\,x_y^3}{6e_y} + \left(\frac{h}{2} - 1\right)\frac{b}{2e_y}\,x_y^2 + \left[nA_{st}\left(\frac{b/2 - b_1}{e_y} + 1\right) + (n-1)A_{sc}\left(\frac{b_1 - b/2}{e_y} + 1\right)\right]$$

$$(x_y - n\,A_{st}\left[\frac{(b - b_1)^2 + (b - b_1)(e_y - b/2)}{e_y}\right]$$

$$+ (n-1)A_{sc}\left[\frac{b_1^2 + b_1(e_y - b/2)}{e_y}\right] = 0$$

--------- (4 – 80)

$$z = \frac{h\,x_y^2/2 + n\,A_{st}(b - b_1) + (n-1)A_{sc}\,b_1}{h\,x_y + n\,A_{st} + (n-1)A_{sc}}$$

---------- (4 – 81)

$$I_{cr\,y} = \frac{h\,x_y^3}{12} + h\,x_y \left(z - \frac{x_y}{2} \right)^2 + n\,A_{st} \left(b - b_1 - z \right)^2 + (n-1) A_{sc} \left(z - b_1 \right)^2$$

---------- (4 – 82)

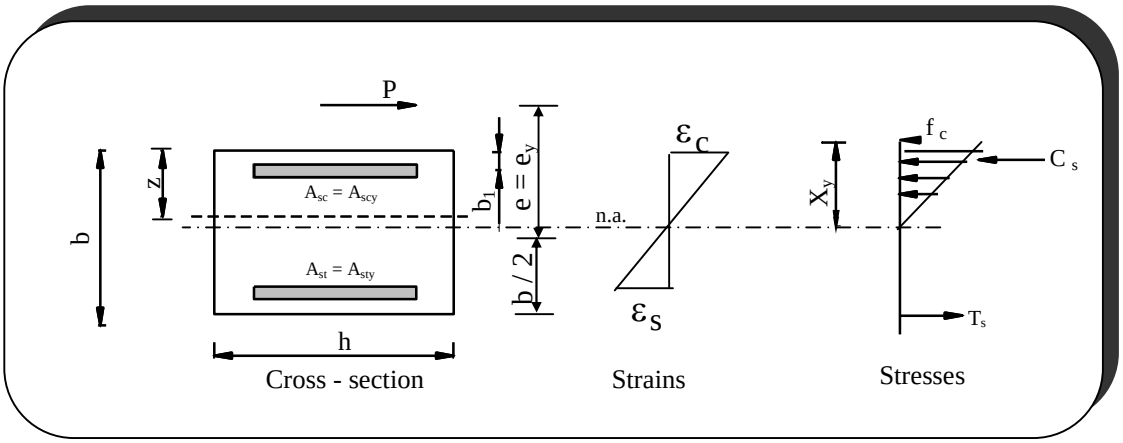

Fig. (4 – 11): Stress and Strain Distribution in Cracked Section (bending is about y – axis)

Also, the adopted (cracked) cross – sectional area for the section (A_{cr}) can be obtained as follows:

$$A_{cr1} = b\,x_z + n\,A_{stz} + (n-1) A_{sc\,z}$$ ---------- (4 – 83a)

$$A_{cr2} = h\,x_y + n\,A_{st\,y} + (n-1) A_{sc\,y}$$ ---------- (4 – 83b)

$$A_{cr} = \frac{A_{cr1} + A_{cr2}}{2}$$ ---------- (4 – 84)

To obtain the cross – sectional properties for the member, the average properties for member ends are taken.

4.9 Failure Criteria:

In the present study, failure of reinforced concrete frames is declared if:

a) Complete or partial collapse mechanism is reached and indicated theoretically by singular structure stiffness matrix (i.e. $|K| \approx 0$), where $|K|$ is the determinate of the structure stiffness matrix.

b) Beam mechanism failure is reached when three plastic hinges are existing in one element.

c) Local crushing failure is indicated when the total rotation (resulting rotation θ_{yz}) of any critical section at any load increment reaches the computed crushing rotation of that section θ_u.

4.10 Computer Program:

A computer program "**NASPAC**" was written, as a part of this work, for the analysis of reinforced concrete space frames based on the prescribed procedure. The program is written in **FORTRAN 90** language for the **IBM** personal computer and compatible microcomputers. The flow chart of this program is given in Fig.(4 – 12) to outline the main steps in the program.

Type = 1 elastic analysis
= 2 inelastic analysis
SN = 1 singular stiffness matrix
= 0 non – singular stiffness matrix

$$DEF = \left| \frac{a^{a\,r} - a^{a\,r-1}}{a^{a\,r}} \right|$$

(for iteration loop)
≤ 0.001 convergence
> 0.001 not
Crus = 1 if $\bar{}_{total} < \bar{}_{u}$
= 0 if not

$$Res = \left[\frac{\sum_{i=1}^{n} (P_i - f_i)^2}{\sum_{i=1}^{n} (P_i)^2} \right]^{1/2}$$

$Res \le 0.001$ convergence (elastic analysis) **[37]**
> 0.001 not
{P}= applied load vector
{f}= internal load vector

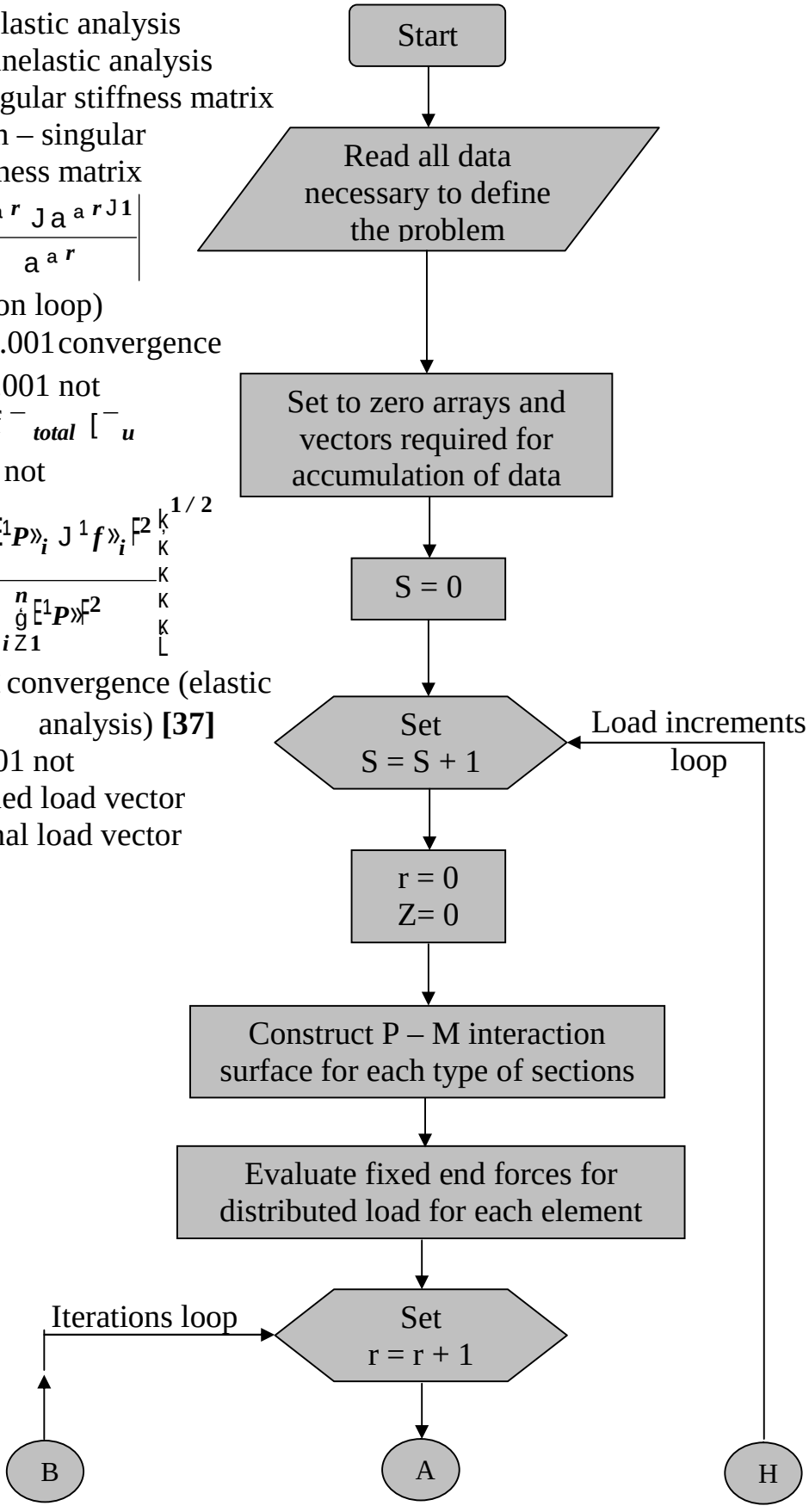

Fig. (4 – 12): Flow Chart of the Program (NASPAC)

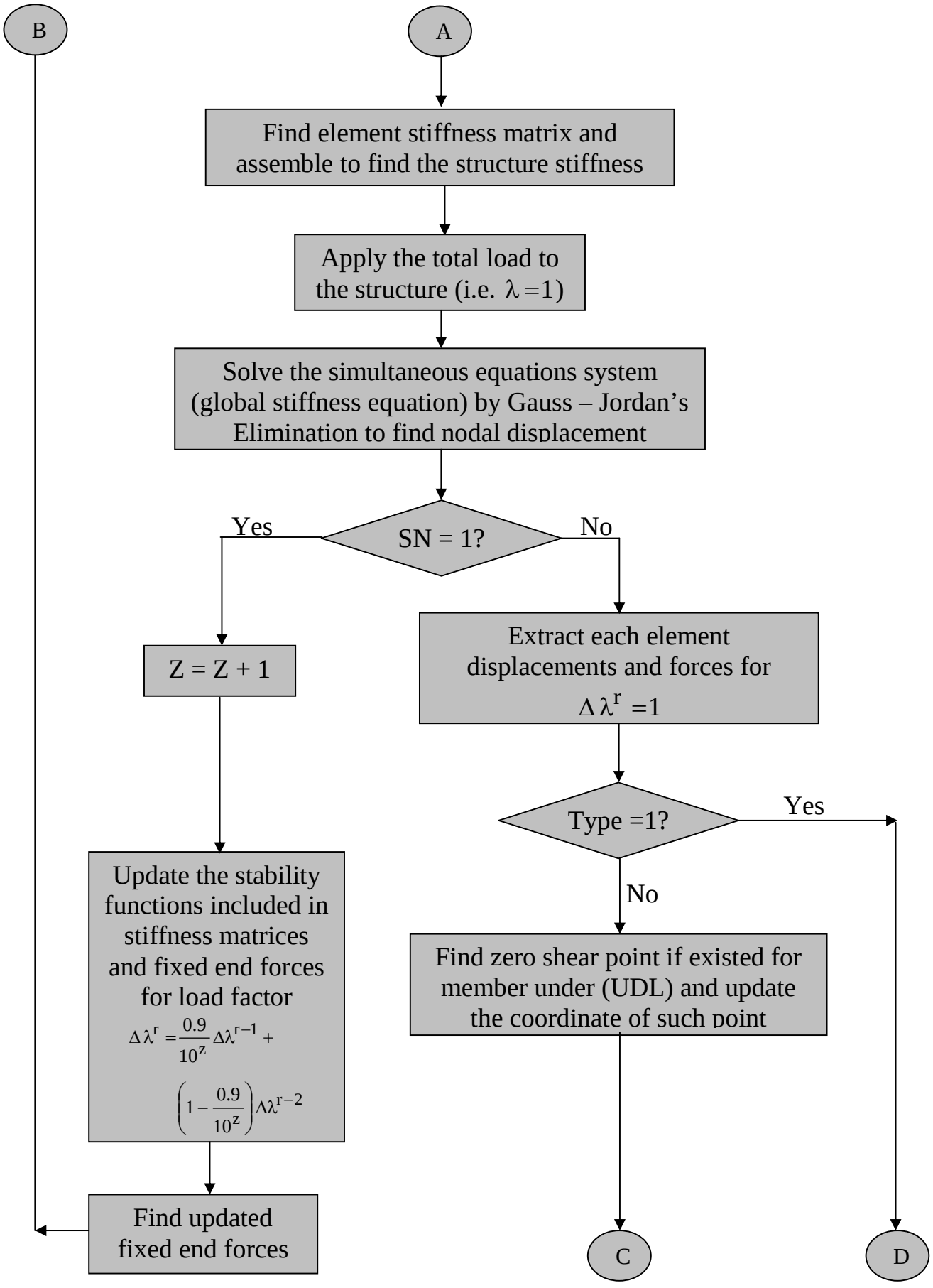

Fig. (4 – 12): Continued

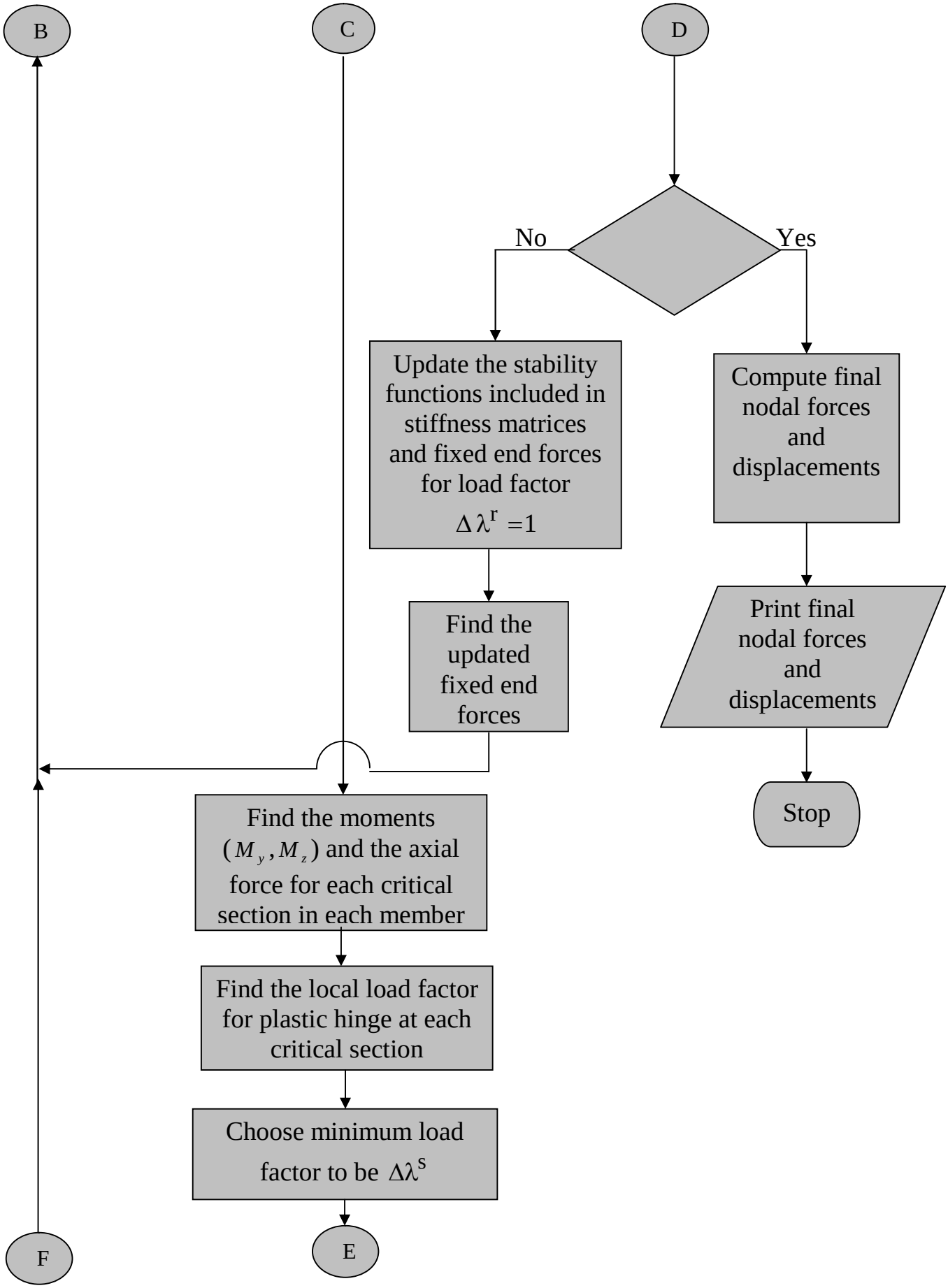

Fig. (4 – 12): Continued

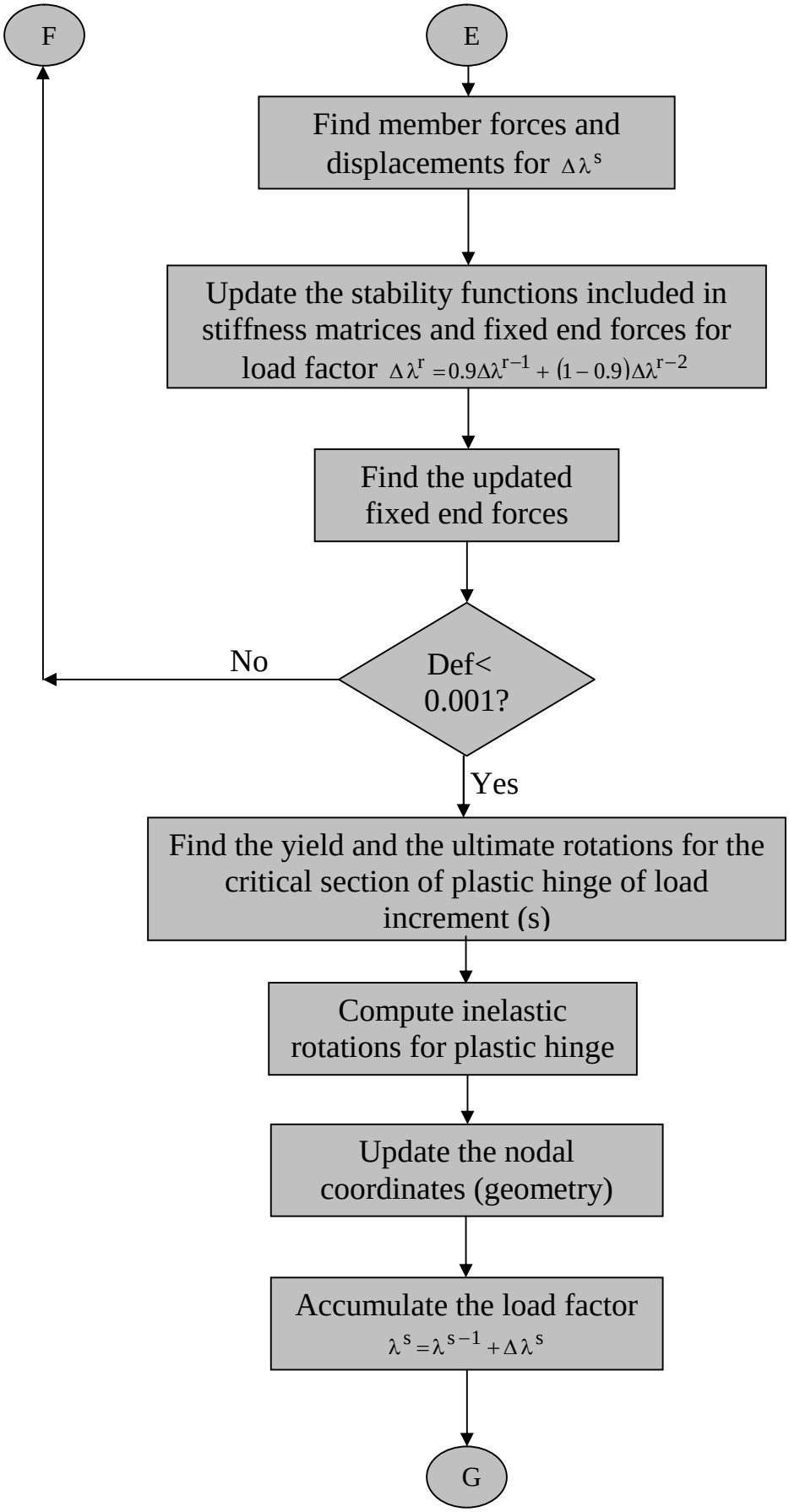

Fig. (4 – 12): Continued

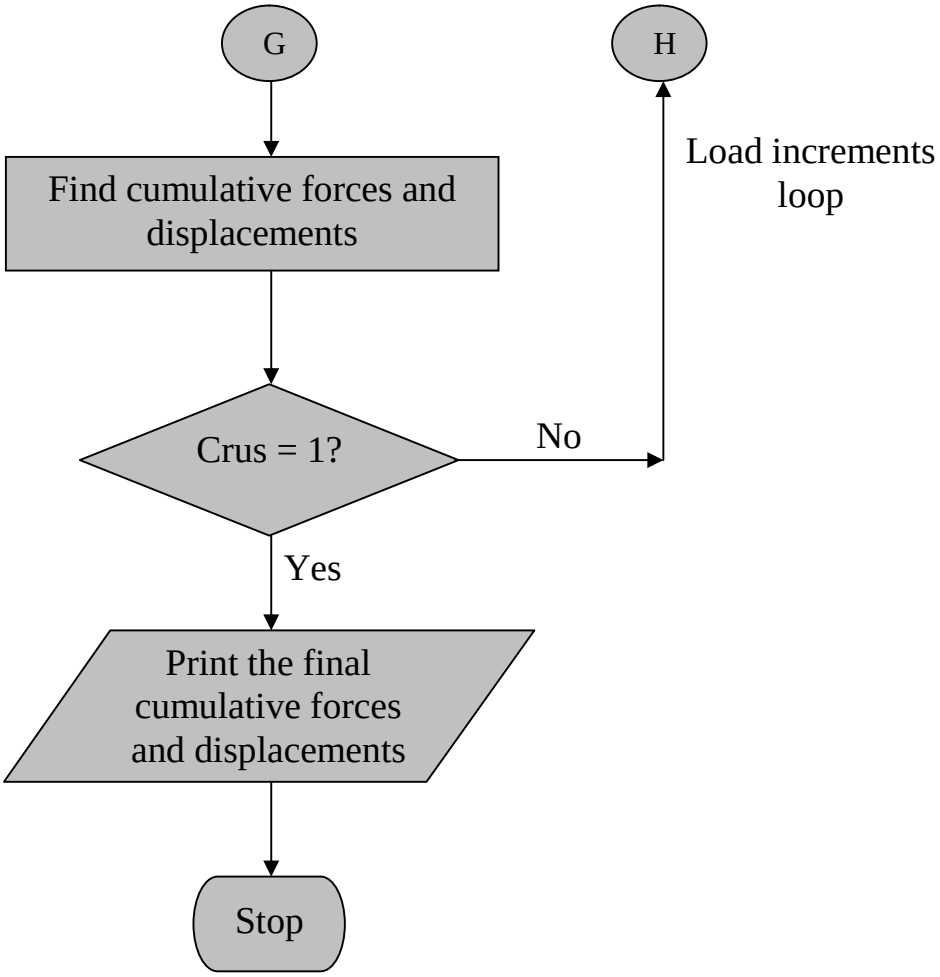

Fig. (4 – 12): Continued

CHAPTER ONE

INTRODUCTION

1.1 General:

Many structural design problems have several solutions and some may have an infinite number of solutions. The purpose of optimization is to find the best possible solution among many potential solutions satisfying the chosen criteria. In structural design, engineers have based their designs on working stress or ultimate strength criteria and on minimum weight or minimum cost as objectives, since they are seeking lighter and more economical design taking into account function, safety and serviceability.

With the increase in the availability of advanced computers and of the developments in mathematical programming methods, the engineering design using the digital computers have improved progressively resulting in efficient and economical structural systems.

The advantages of optimization are best recognized when dealing with highly structural forms. Reinforced concrete plane and space frames have been the subject of considerable studies in this respect.

1.2 Non-linear Analysis:

A literature survey indicates that a substantial amount of work has been done on the elastic and inelastic behavior of R.C. plane and steel space frames. Therefore, presentation of analytical algorithm that attempts to predict the non-linear behavior of R.C. space frames is desirable.

In most civil engineering structures, the forming members are either long and slender or short and stocky. In the former type, the effect of axial force on the response of the member is important, while in the latter type, the effect of shear force on the response of the member is important.

Accordingly, most of the developments reported in the literature in chapter two account for the effect of one of them, but not both, on the flexural behavior of frame members.

In the present study, explicit expressions for stability functions for three-dimensional frame elements, in terms of member length, cross-sectional properties, axial force and end moments are derived .The combined effect of axial force, shear force and bending moments are considered in the derivation of the stability functions. Material non-linearity and inelastic behavior of space frames are important features and they are included well in the present study. The analysis is based on plastic hinge model using stiffness method.

In the present non-linear analysis, the possibility of local crushing failure and stability failure, in addition to plastic collapse mechanism, are also considered. A simplified axial force-moment interaction surface for the detection of plastic hinge formation is suggested. A step-by-step incremental algorithm is followed.

1.3 Structural Optimization:

A general mathematical model of the structural optimization problem can be presented in the following form:

A certain function (z) called the objective function,

$$z = f(x_i) \qquad i = 1,2,\ldots,n$$

which is usually the weight or the cost or amount of reinforcement of the structure involves (n) design variables [x_i], and it is minimized subjected to inequality constraints,

$$g_j(x_i) \leq 0 \qquad j = 1,2,\ldots,m$$

and /or equality constraints,

$$g_j(x_i) = 0 \qquad k = 1,2,\ldots,s$$

The vector [x] of the design variables will have optimum values when the objective function reaches its minimum value.

The constraints reflect the design and functional requirements .It can be seen from a survey of research work **[1]** on optimal design of civil engineering structural systems that only a few papers have been published on the cost optimization of reinforced concrete structures .All but two of them deal with two-dimensional frames. As such there is a need to perform research on cost optimization of realistic three-dimensional structures, especially large structures with hundreds of members where optimization can result in substantial saving.

1.4 Experimental work:

Several experimental investigations of the non-linear behavior of reinforced concrete frames are presented and reviewed in chapter two. However, there is no clear experimental investigation on the non-linear behavior of three-dimensional frames.

Consistent with the purpose of the present work, one model of reinforced concrete space frame was tested in laboratory. The details of dimensions, reinforcement, material, --- etc are presented in chapter six, and the results are given in chapter seven. The aims of the experimental study are mainly:

1-To investigate the actual non-linear behavior of R.C. space frames.

2-To ensure the validity and efficiency of the proposed theoretical analysis which is also applied on several reinforced concrete frames that were tested or analyzed by others.

1.5 Scope of the Present Study:

In the present study, the non-linear behavior and optimal design of reinforced concrete space frames are treated in detail.

In chapter two, the previous works dealing with the analysis of frames, optimal design of reinforced concrete frames and experimental tests on reinforced concrete frames are reviewed. The non-linear stiffness matrices for several three-dimensional frame elements are given in chapter three.

In chapter four, the steps of the proposed algorithm for the analysis approach on reinforced concrete frames are explained. The formulation of the design optimization problem involving the objective function, design variables, constraints and the optimization method used in the present study is given in chapter five. In chapter six, the experimental investigation is presented. The application and the presentation of the results with discussion are given in chapter seven. Chapter eight gives the conclusions and recommendations for future work.

CHAPTER SIX

EXPERIMENTAL WORK

6.1 Introduction:

As a part of the present study, an experimental investigation is carried out in the structural laboratory of the Civil Engineering Department at the University of Babylon. One model of reinforced concrete space frame was cast and tested up to failure. The aims of the test are:

a) To assess the validity of the new proposed theoretical procedure for the non – linear analysis of reinforced concrete space frames.

b) To investigate the more appropriate section properties, whether to be for gross section or effective section that may be adopted in the theoretical method of analysis.

6.2 Description of the Tested Model:

The experimental program includes the preparation and testing of one model of a reinforced concrete space frame. The shape and dimensions of the model are given in Fig. (6 – 1a). All the members of the model have the same reinforcement and dimensions. The main reinforcement is consisting of four deformed bars (bar diameter ¤ =8 mm) which are equally distributed on member section (percentage of reinforcement ° = 2.0 %). Ties (lateral reinforcement) are distributed in each member as shown in Fig. (6 – 1b) and Fig. (6 – 1c) using plain bars of (6 mm) diameter (with spacing c/c=100 mm).

The model was loaded by four concentrated loads as indicated in Fig. (6 – 1) and tested up to failure.

6.3 Concrete Mix:

6.3.1 Materials:

a) Cement: Ordinary Portland cement of Kufa factory was used for the model.

b) Aggregate: Al – Akhaidher washed sand and Al – Nibaie washed gravel were used for the model. However the sand was sieved on (4.75 mm) sieve size, while the gravel was sieved on (19 mm) sieve size.

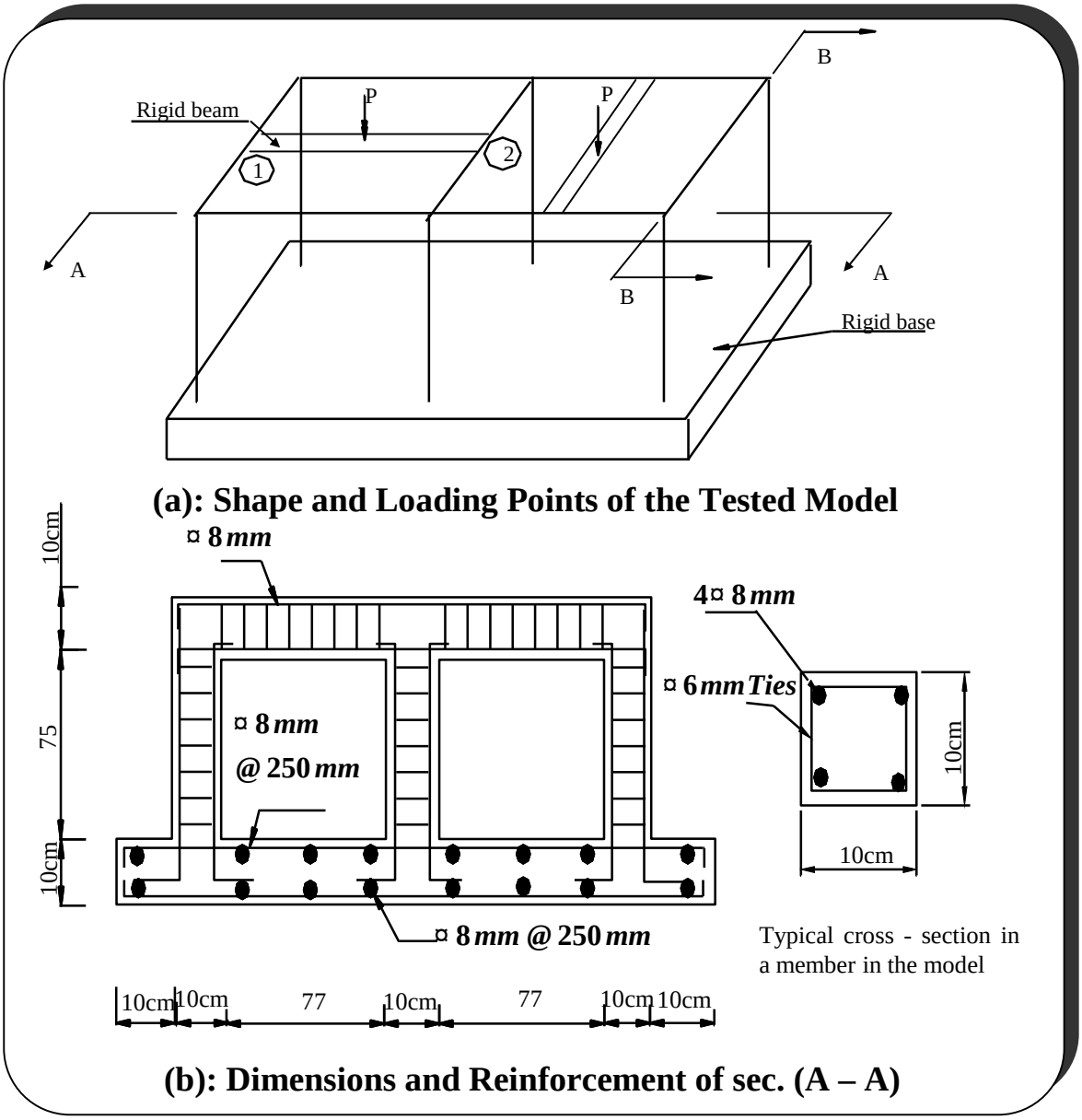

Fig. (6 – 1) Dimensions and Details of Reinforcement for the tested Model

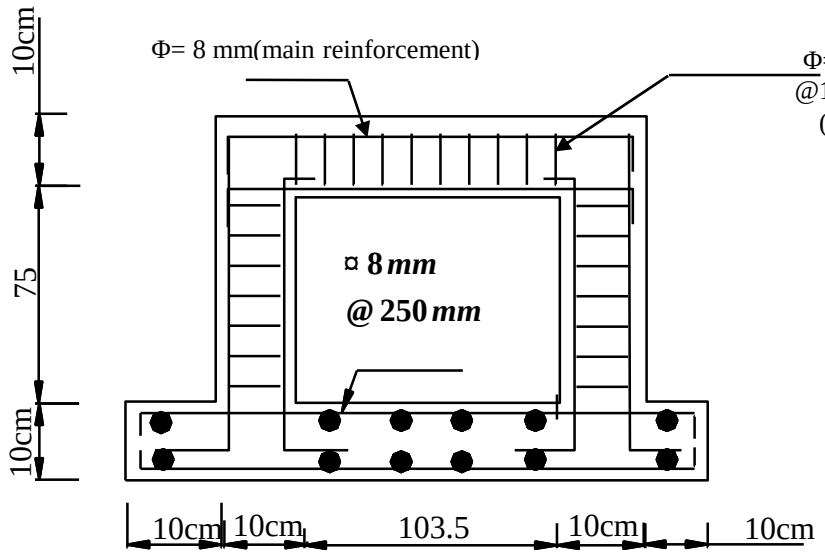

(c): Dimensions and Reinforcement of sec. (B – B)

Fig. (6 – 1): Continued

6.3.2 Mix Proportions:

The following mix proportions by weight were used for the model as:

Cement : sand : aggregate = 1 : 1.5 : 3

Water / cement = 0.55

6.4 Reinforcing Steel Bars:

Deformed bars with diameter ¤ 8mm were used for longitudinal reinforcement and $(\phi 6\,\text{mm})$(spacing=100 mm) plain bars for closed ties as shear and confining reinforcement. The strength properties of the reinforcing bars are given in Table (6 – 1).

6.5 Casting and Curing of the Tested Model:

The tested model was cast in wooden form stiffened with battens to maintain the model shape. The model form was sprayed by a lubricating

oil before casting which would facilitate the removal of the form after hardening of the concrete. Concrete was mixed mechanically for about two minutes. As soon as the mixing was completed, concrete was cast on the form and compacted by using a vibrating rod. The formwork was removed at 24 hours after casting. The model was then covered with wet burlap and polythene sheeting and was stored for twenty – eight days. The burlap and polythene covers were removed at age of (28 days) and the model was left dry. Next, the model was painted white for clear identification of cracks during test.

6.6 Control Specimens:

Three control specimens of (150 mm) standard cubes were cast for the model. The cubes rather than cylinders were used because cubes have the property that one can make the test in the direction normal to the casting direction. The control specimens were cast in three layers, compacting each layer for ten seconds using a vibrating table. After casting and compacting, the top surfaces of the specimens were smoothed. After one day, the moulds were removed off and the control specimens were stored beside the model under the same conditions. The control specimens were tested under uniaxial compression at 28 days age. The average compressive strength of the specimens was $f'_c = 26.3\ MPa$.

6.7 Measurements:

6.7.1 Deflection:

Dial gages with capacity of (25.4mm) and accuracy of (0.025mm) were used to measure the deflection of the model at ends (1) and (2) (see Fig. (6 – 1a)) at the lower chord. The dial gages were fixed in such away that they were in contact with the lower chord.

Table (6 – 1): Strength Properties of the Used Steel Reinforcement

Bar Diam. (mm)	f_y (MPa)	f_u (MPa)	Uses
¤ 8	445.63	600.96	**Main reinf.**
ϕ6	350	440	**Ties**

6.7.2 Loads:

A load cell with capacity of (70 Tons) was used to measure the loads applied by two jacks which transmitted the loads to four points using two rigid beams as shown in Fig. (6 – 1a).

6.7.3 Concrete Strains:

The longitudinal strains of concrete were measured for the model at its joints faces using a mechanical strain gage having a gage length of (200 mm). Groups of demec points were attached to the previously cleaned surface of the concrete over a gage length of (200 mm). Each group consisted of 4 pairs of demec points distributed as shown in Fig. (6 – 2). Because of symmetry, only one half of the model was considered.

6.8 Testing:

The model was tested using a load cell of maximum capacity of (70 Tons) at the age of (36 days). Fig. (6 – 3) shows the details of the test set up which consisted of a rigid steel frame with I – section. The frame was designed as a self – equilibrating system. In addition, rigid steel beams were used to transmit the applied loads. The model was subjected to four

concentrated loads applied via two hydraulic jacks. The load of each jack was distributed on two points using a rigid beam. The testing began by applying loads via the hydraulic jacks with appropriate increments of load. A load increment of (275 kg) was applied to the model until failure. The readings of the deflections and strains versus loads were recorded simultaneously for each load increment.

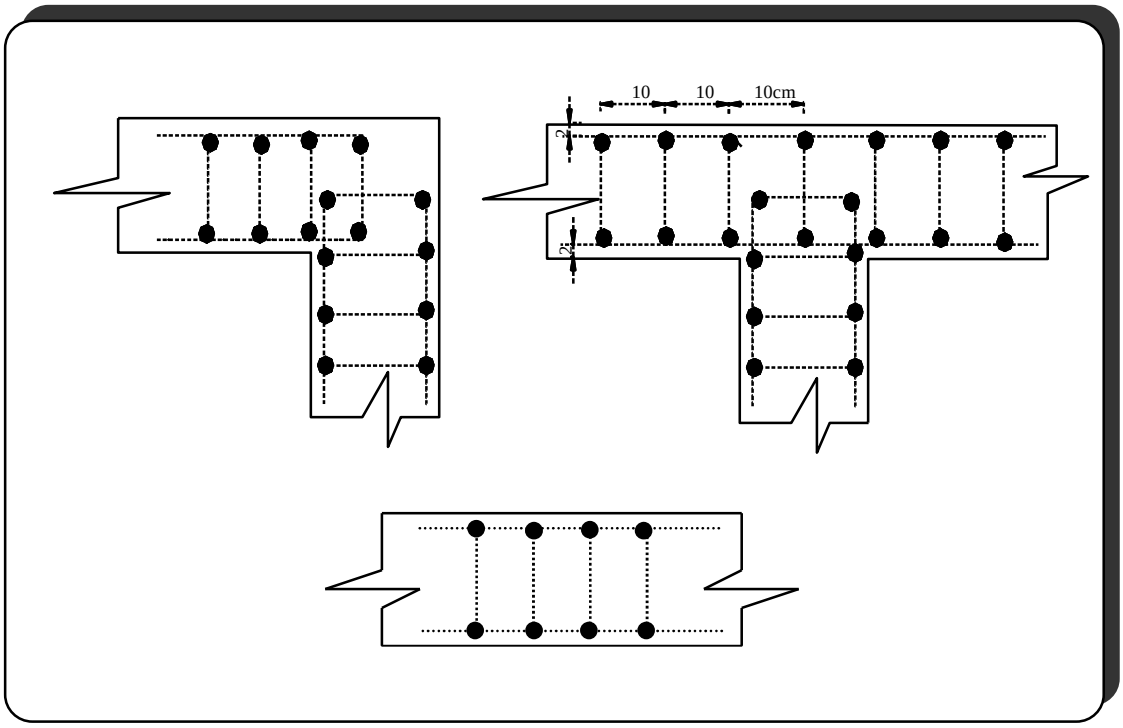

Fig. (6 – 2): Locations of Demec Points for Measuring Concrete Strains

Fig. (6 – 3): Setup of Flexural Test on Model

CHAPTER THREE

FORMULATION OF STIFFNESS MATRICES FOR 3D FRAME ELEMENT

3.1 General:

In this chapter, a complete formulation of stiffness matrices for a three – dimensional frame element is presented. The stiffness matrices presented here are based on that previously derived by **Ekhande et al [33]**. They derived explicit expressions for stability functions for three – dimensional frame element, in terms of member length, cross – sectional properties, axial force and end moments taking into account the interaction between axial force and both bending moments carried by such members as a geometric non – linearity effect. These stability functions did not include the effect of shear deformations. In the present study, new more accurate expressions for stability functions are derived by considering; (1) the interaction between axial force and bending moments (2) the bowing effect and (3) the shear deformations. In addition, the derived element stiffness matrices consider the material non – linearity through including different combination of plastic hinges in each element. The possible locations of plastic hinges are: the left extremity , the right extremity of the elastic length of the element and the point of zero shear if existed for element under distributed load.

For the case of element under uniformly distributed load, modified fixed end reactions are derived considering both of shear deformations and geometric non – linearity effects.

3.2 Formulation of Stiffness Matrix for a Prismatic Elastic Element:

Members carrying both axial force and bending moments are subjected to an interaction between these effects. The lateral deflection of a member causes an additional bending moment when subjected simultaneously to an applied axial force. In a like manner, the presence of bending moments affects the axial stiffness of the member due to an apparent shortening of the member caused by the bending deformations. Hence, these effects are important when the deformations are large and they should be treated carefully in deriving the element stiffness matrix.

The basic differential equation for this problem **[11]** is

$$\frac{dy}{dx} = \frac{dy_m}{dx} + \frac{\bar{B}V_x}{AG} \qquad \text{---------- (3 – 1)}$$

Where $\frac{\bar{B}V_x}{AG} = \frac{dys}{dx}$

$\bar{B}$ = shear shape factor which is for a rectangular section **[11]**

$\bar{B} = \frac{12 + 11\nu}{10 + 11\nu}$ and for concrete section ($\nu = 0.17$) **[15]**, $\bar{B} = 1.185$

By differentiating with respect to x;

$$\frac{d^2y}{dx^2} = \frac{d^2y_m}{dx^2} + \frac{\bar{B}V_x'}{AG} = +\frac{M_x}{EI} + \frac{\bar{B}V_x'}{AG} \qquad \text{---------- (3 – 2)}$$

where prime denotes differentiation with respect to x.

The deformation of a finite element in a two dimensional strut is shown in Fig.(3 – 1).

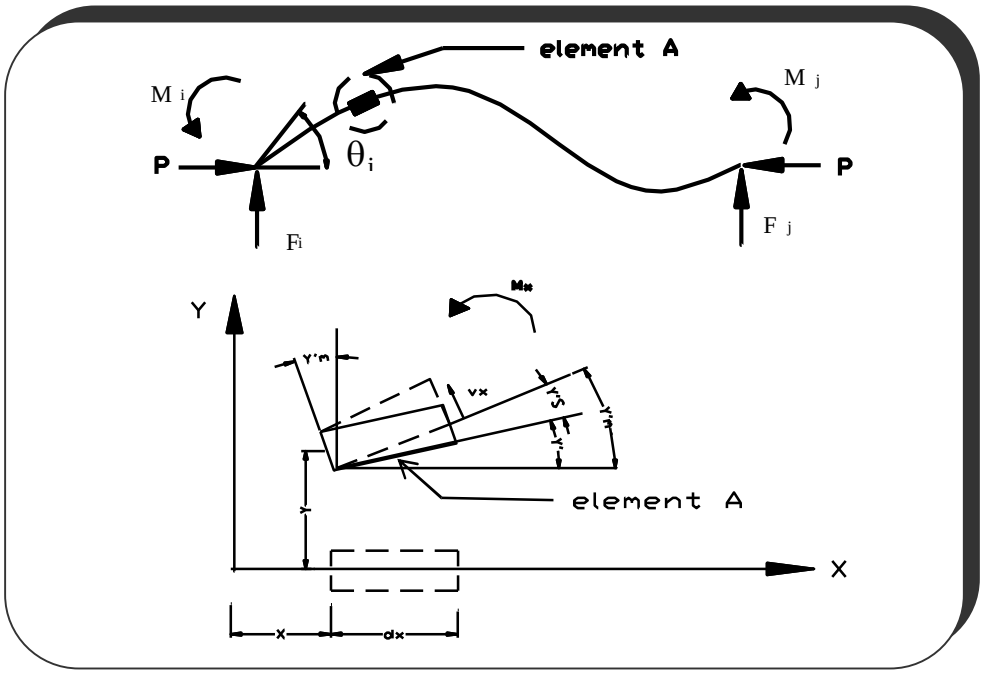

Fig. (3 – 1)Shear Deformations of a finite Beam Element

3.2.1 Effect of Flexure on Axial Stiffness (Bowing Effect):

The axial stiffness of the elment in the absence of end moments is given by EA / L, and the axial deformation due to the axial force P is given by PL / AE. However, the end moments produce an additional axial deformation in the element. In order to include the effect of flexure on axial deformation, the axial stiffness of the element must be modified. Writing the modified axial stiffness as $S_1(EA / L)$ where S_1 is a modification factor or the stability function for the effect of flexure on axial stiffness, the expression for S_1 is derived as follows:

Referring to Fig.(3 – 2a) and (3 – 2b),then

$$ds^2 = dx^2 + dy^2 + dz^2 \quad \text{---------- (3 – 3a)}$$

which can be arranged as

$$\left(\frac{ds}{dx}\right)^2 = 1 + \left(\frac{dy}{dx}\right)^2 + \left(\frac{dz}{dx}\right)^2 \quad \text{---------- (3 – 3b)}$$

Shortening due to bending is $d\phi_b = ds - dx$

$$\varepsilon = \frac{d\phi_b}{dx} = \frac{ds}{dx} - 1 \quad \text{---------- (3 – 4a)}$$

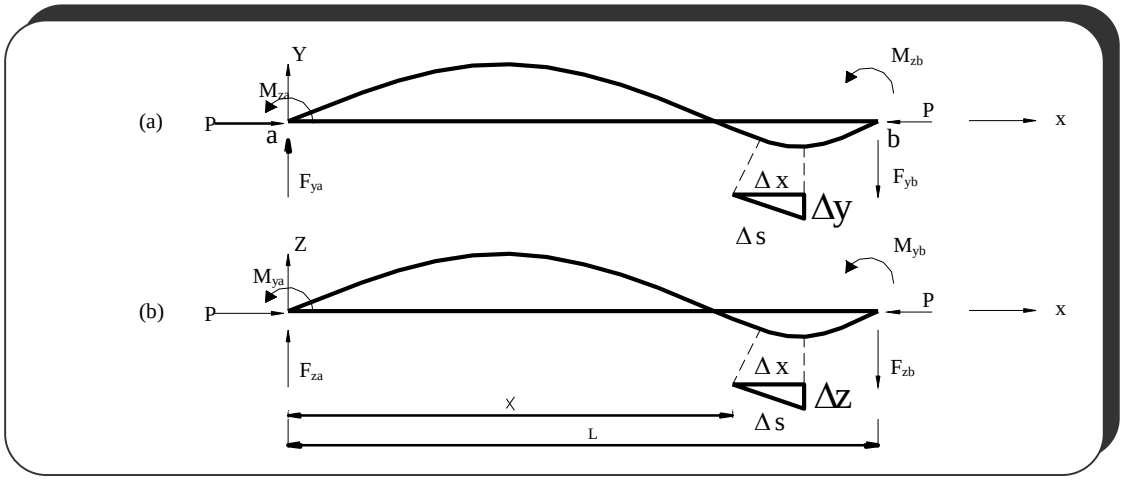

Fig.(3 – 2): Effect of Flexure on Axial Stiffness:
(a) Bending in x – y Plane; (b) Bending in x – z Plane

Using Taylor's expansion and neglecting higher order terms, the following equation can be obtained

$$\frac{d\phi_b}{dx} = \frac{1}{2}\left(\frac{dy}{dx}\right)^2 + \left(\frac{dz}{dx}\right)^2 \quad \text{---------- (3 – 4b)}$$

Therefore the shortening of the element due to bending is

$$\phi_b = \int_0^L \frac{d\phi_b}{dx}\,dx \quad \text{---------- (3 – 5a)}$$

$$= \frac{1}{2}\int_0^L \left(\frac{dy}{dx}\right)^2 + \left(\frac{dz}{dx}\right)^2 dx \quad \text{---------- (3 – 5b)}$$

Total shortening of the element, ϕ_t = shortening due to axial load (ϕ_a) + shortening due to bending (ϕ_b):

$$\phi_t = \frac{PL}{EA} + \frac{1}{2}\int_0^L \left(\frac{dy}{dx}\right)^2 + \left(\frac{dz}{dx}\right)^2 dx \quad \text{---------- (3 – 6a)}$$

$$\phi_t = \frac{PL}{EA}\left[1 + \frac{EA}{2PL}\int_0^L \left(\frac{dy}{dx}\right)^2 + \left(\frac{dz}{dx}\right)^2 dx\right] \quad \text{---------- (3 – 6b)}$$

$$\text{or } \phi_t = \frac{P}{S_1\left(\frac{EA}{L}\right)} \quad \text{---------- (3 – 6c)}$$

Where $S_1 = \dfrac{1}{1 + \dfrac{EA}{2PL}\int_0^L \left(\dfrac{dy}{dx}\right)^2 + \left(\dfrac{dz}{dx}\right)^2 dx}$ ---------- (3 – 7)

Referring to Fig.(3–1) and Fig.(3–2a), and from equilibrium requirements, the following equations can be obtained

$V_x = F_{ya} + Py\alpha m$ ---------- (3 – 8)

From equation (3 – 1)

$y\alpha m = \dfrac{dy}{dx} + \dfrac{\bar{B}V_x}{AG}$

Substituting the value of $y\alpha m$ into equation (3 – 8); then

$V_x = F_{ya} + Py\alpha = \dfrac{1}{1 + \dfrac{\bar{B}P}{AG}}$

Hence, by differentiation

$V_x\alpha = + Py\alpha\alpha = \dfrac{1}{1 + \dfrac{\bar{B}P}{AG}}$ ---------- (3 – 9)

Also, from Fig.(3 – 2a)

$M_x = M_{za} + \dfrac{M_{za} + M_{zb}}{L}x + Py$ ---------- (3 – 10)

writing $\sim^2 = \dfrac{P}{EI_Z}$ ---------- (3 – 11)

and

$k_v = \dfrac{1}{\left[1 + \dfrac{\bar{B}P}{AG}\right]}$ ---------- (3 – 12)

then by substituting equations (3 – 9), (3 – 10), (3 – 11) and (3 – 12) into equation (3 – 2) and rearranging the terms, then

$$k_v\ y'' + \alpha^2 y = \frac{\alpha^2}{P}\left[\frac{x}{L}(M_{za} + M_{zb}) - M_{za}\right] \quad \text{---------- (3 – 13)}$$

The solution for equation (3 – 13) is given by the summation of complementary function and particular integral:

$$y = A\cos\left(\frac{\alpha x}{\sqrt{k_v}}\right) + B\sin\left(\frac{\alpha x}{\sqrt{k_v}}\right) + \left[\frac{x}{PL}(M_{za} + M_{zb}) - \frac{M_{za}}{P}\right] \quad \text{----(3-14a)}$$

Substituting the boundary condition $y = 0$ at $x = 0$ and $x = L$, then

$$A = \frac{M_{za}}{P}$$

$$B = -\frac{1}{P}\left[\frac{M_{za}\left(\cos\left(-L/\sqrt{k_v}\right) + M_{zb}\right)}{\sin\left(-L/\sqrt{k_v}\right)}\right] \quad \text{---------- (3 – 14b)}$$

The slope of the element in the $X - Y$ plane is given by

$$\left(\frac{dy}{dx}\right) = -\left(A\alpha/\sqrt{k_v}\right)\sin\left(\frac{\alpha x}{\sqrt{k_v}}\right) + \left(B\alpha/\sqrt{k_v}\right)\cos\left(\frac{\alpha x}{\sqrt{k_v}}\right) + \frac{1}{PL}(M_{za} + M_{zb}) \quad \text{----(3 – 14c)}$$

Similarly, the equation of the element for bending in the $X - Z$ plane is given by

$$z = C\cos\left(\frac{\alpha x}{\sqrt{k_v}}\right) + D\sin\left(\frac{\alpha x}{\sqrt{k_v}}\right) + \left[\frac{x}{PL}(M_{ya} + M_{yb}) - \frac{M_{ya}}{P}\right] \quad \text{----(3 –15a)}$$

where $\alpha^2 = \dfrac{P}{EI_y}$ ---------- (3 – 15b)

Substituting the boundary conditions $z = 0$ at $x = 0$ and $x = L$, then

$$C = \frac{M_{ya}}{P}$$

$$D = -\frac{1}{P}\left[\frac{M_{ya}\left(\cos\left(\alpha L/\sqrt{k_v}\right) + M_{yb}\right)}{\sin\left(\alpha L/\sqrt{k_v}\right)}\right] \quad \text{---------- (3 – 15c)}$$

The slope of the element in the XZ plane is given by

$$\left(\frac{dz}{dx}\right)_{XZ} = C_1/\sqrt{k_v}\,\sin\left(\frac{x}{\sqrt{k_v}}\right) + D_1/\sqrt{k_v}\,\cos\left(\frac{x}{\sqrt{k_v}}\right) \quad \text{----(3 – 15d)}$$

$$+\frac{1}{PL}(M_{ya} + M_{yb})$$

Now, the integral in equation (3 – 7) can be evaluated. The final result of the integration is

$$\int_0^L \left(\frac{dy}{dx}\right)^2 dx = \frac{A_2^2\tilde{}^2}{2k_v}\left[L - \frac{\sqrt{k_v}}{2\tilde{}}\sin\left(\frac{2\tilde{}L}{\sqrt{k_v}}\right)\right] + \frac{AB\tilde{}}{2\sqrt{k_v}}\left[\cos\left(\frac{2\tilde{}L}{\sqrt{k_v}}\right) - 1\right] +$$

$$\frac{B^2\tilde{}^2}{2k_v}\left[L + \frac{\sqrt{k_v}}{2\tilde{}}\sin\left(\frac{2\tilde{}L}{\sqrt{k_v}}\right)\right] + \frac{2}{PL}(M_{za} + M_{zb})\left[A_2\cos\left(\frac{\tilde{}L}{\sqrt{k_v}}\right) - 1\right] + B\sin\left(\frac{\tilde{}L}{\sqrt{k_v}}\right)$$

$$+\frac{1}{P^2L}(M_{za} + M_{zb})^2$$

$$= H_y \quad \text{---------- (3 – 16a)}$$

and

$$\int_0^L \left(\frac{dz}{dx}\right)^2 dx = \frac{C_2^2\ {}^2}{2k_v}\left[L - \frac{\sqrt{k_v}}{2}\sin\left(\frac{2\ L}{\sqrt{k_v}}\right)\right] + \frac{CD}{2\sqrt{k_v}}\left[\cos\left(\frac{2\ L}{\sqrt{k_v}}\right) - 1\right] +$$

$$\frac{D^2\ {}^2}{2k_v}\left[L + \frac{\sqrt{k_v}}{2}\sin\left(\frac{2\ L}{\sqrt{k_v}}\right)\right] + \frac{2}{PL}(M_{ya} + M_{yb})\left[C_2\cos\left(\frac{L}{\sqrt{k_v}}\right) - 1\right] + D\sin\left(\frac{L}{\sqrt{k_v}}\right)$$

$$+\frac{1}{P^2L}(M_{ya} + M_{yb})^2$$

$$= H_z \quad \text{---------- (3 – 16b)}$$

Therefore equation (3 – 7) becomes

$$S_1 = \frac{1}{1 + \frac{EA}{2PL}(H_y + H_z)} \quad \text{---------- (3 – 17)}$$

A similar approach can be used to derive an expression for S_1 for the element with axial tensile force P. The final expression is as follows:

$$S_1 = \frac{1}{1 - \frac{EA}{2PL}(H_y + H_z)} \quad \text{---------- (3 – 18)}$$

where

$$H_y = \frac{E^2\alpha^2}{2k_v}\left[\frac{\sqrt{k_v}}{2\alpha}\sinh\left(\frac{\alpha L}{\sqrt{k_v}}\right)\left(L + \frac{EF\alpha}{2\sqrt{k_v}}\right)\cosh\left(\frac{2\alpha L}{\sqrt{k_v}}\right) - 1 + \frac{F^2\alpha^2}{2k_v}\right]$$
$$\left[L + \frac{\sqrt{k_v}}{2\alpha}\sinh\left(\frac{\alpha L}{\sqrt{k_v}}\right) - \frac{2}{PL}\right]\left[M_{za} + M_{zb}\right]\left[E\cosh\left(\frac{\alpha L}{\sqrt{k_v}}\right) - 1\right] \quad \text{--(3–19a)}$$
$$+ F\sinh\left(\frac{\alpha L}{\sqrt{k_v}}\right) + \frac{1}{P^2L}\left[M_{za} + M_{zb}\right]^2$$

$$H_z = \frac{G^2\beta^2}{2k_v}\left[\frac{\sqrt{k_v}}{2}\sinh\left(\frac{\beta L}{\sqrt{k_v}}\right)\left(L + \frac{GH}{2\sqrt{k_v}}\right)\cosh\left(\frac{2\beta L}{\sqrt{k_v}}\right) - 1 + \frac{H^2\beta^2}{2k_v}\right]$$
$$\left[L + \frac{\sqrt{k_v}}{2}\sinh\left(\frac{\beta L}{\sqrt{k_v}}\right) - \frac{2}{PL}\right]\left[M_{ya} + M_{yb}\right]\left[G\cosh\left(\frac{\beta L}{\sqrt{k_v}}\right) - 1\right] \quad \text{--(3–19b)}$$
$$+ H\sinh\left(\frac{\beta L}{\sqrt{k_v}}\right) + \frac{1}{P^2L}\left[M_{ya} + M_{yb}\right]^2$$

$$\begin{Bmatrix} E = \dfrac{M_{za}}{P} \\ F = \dfrac{1}{P}\left(\dfrac{M_{za}\cosh(L/\sqrt{k_v})}{\sinh(L/\sqrt{k_v})} + M_{zb}\right) \\ G = \dfrac{M_{ya}}{P} \\ H = \dfrac{1}{P}\left(\dfrac{M_{ya}\cosh(L/\sqrt{k_v})}{\sinh(L/\sqrt{k_v})} + M_{yb}\right) \end{Bmatrix} \quad \text{---------- (3 – 19c)}$$

3.2.2 Effect of Axial Force on Flexural Stiffness:

3.2.2.1 Bending in X – Y Plane:

Referring to Fig.(3 – 2a), the differential equation of the element bending in the x–y plane is given by equation (3 – 13) for which the solution is given by equation (3 – 14a). the end slopes of the element are obtained by applying the following end conditions:

$$\left(\frac{dy}{dx}\right)_{x=0} = -\theta_{za} + \frac{\bar{B}V_x}{AG} = -\theta_{za} + \frac{\bar{B}}{AG}\left(\frac{M_{za}+M_{zb}}{L} + P\theta_{za}\right) \quad \text{-----(3 – 20a)}$$

$$\left(\frac{dy}{dx}\right)_{x=L} = -\theta_{zb} + \frac{\bar{B}V_x}{AG} = -\theta_{zb} + \frac{\bar{B}}{AG}\left(\frac{M_{za}+M_{zb}}{L} + P\theta_{zb}\right) \quad \text{-----(3 – 20b)}$$

Substituting the values of $\left(\frac{dy}{dx}\right)$ at $(x = 0)$ and $(x = L)$ from equation (3 – 14c) into equations (3 –20a) and (3 –20b) and by rearranging the terms, the following equations in a matrix form can be obtained:

$$\begin{bmatrix} M_{za} \\ M_{zb} \end{bmatrix} = \begin{bmatrix} S_2(4EI_Z/L) & S_3(2EI_Z/L) \\ S_3(2EI_Z/L) & S_2(4EI_Z/L) \end{bmatrix} \begin{bmatrix} -\theta_{za} \\ -\theta_{zb} \end{bmatrix} \quad \text{----------(3 – 21a)}$$

When P is compressive, then S_2 and S_3 functions take the following form:

$$S_2 = \frac{-L(-L\sqrt{k_v}\cos(-L/\sqrt{k_v}) + \sin(-L/\sqrt{k_v}))}{4(2\sqrt{k_v}\cos(-L/\sqrt{k_v}) + (-Lk_v\sin(-L/\sqrt{k_v}) + 2\sqrt{k_v})} \quad \text{---(3 – 21b)}$$

$$S_3 = \frac{-L(\sin(-L/\sqrt{k_v}) + (-L\sqrt{k_v}))}{2(2\sqrt{k_v}\cos(-L/\sqrt{k_v}) + (-Lk_v\sin(-L/\sqrt{k_v}) + 2\sqrt{k_v})} \quad \text{---(3 – 21c)}$$

For members subject to axial tensile force P and bending in the X – Y plane, P is replaced by – P in equation (3 – 13). Solving the resulting differential equation, one can get again equation (3 – 21a), where

$$S_2 = \frac{-L(\sinh(-L/\sqrt{k_v}) + (-L\sqrt{k_v}\cosh(-L/\sqrt{k_v}))}{4(2\sqrt{k_v}\cosh(-L/\sqrt{k_v}) + -Lk_v\sinh(-L/\sqrt{k_v}) + 2\sqrt{k_v})} \quad \text{-----(3 – 21d)}$$

$$S_3 = \frac{-L(-L\sqrt{k_v}) + \sinh(-L/\sqrt{k_v}) +}{2(2\sqrt{k_v}\cosh(-L/\sqrt{k_v}) + -Lk_v\sinh(-L/\sqrt{k_v}) + 2\sqrt{k_v})} \quad \text{---(3 – 21e)}$$

3.2.2.2 Bending in X – Z Plane:

Referring to Fig. (3 – 2b) and following the same procedure previously mentioned, the stability functions for bending in the x – z plane can be derived. The relationship between end moments and end slopes is given by

$$\begin{bmatrix} M_{ya} \\ M_{yb} \end{bmatrix} = \begin{bmatrix} S_4(4EI_Y/L) & S_5(2EI_Y/L) \\ S_5(2EI_Y/L) & S_4(4EI_Y/L) \end{bmatrix} \begin{bmatrix} \theta_{ya} \\ \theta_{yb} \end{bmatrix} \quad \text{----------(3 – 22a)}$$

where S_4 and S_5 are as follows:

For axial compression:

$$S_4 = \frac{L(-L\sqrt{k_v}\cos(-L/\sqrt{k_v}) + \sin(-L/\sqrt{k_v}))}{4\left(2\sqrt{k_v}\cos(-L/\sqrt{k_v}) + \left(-Lk_v\sin(-L/\sqrt{k_v})\right) + 2\sqrt{k_v}\right)} \quad \text{----(3– 22b)}$$

$$S_5 = \frac{L(\sin(-L/\sqrt{k_v}) + (-L\sqrt{k_v}))}{2(2\sqrt{k_v}\cos(-L/\sqrt{k_v}) + (-Lk_v\sin(-L/\sqrt{k_v}) + 2\sqrt{k_v})} \quad \text{----(3 – 22c)}$$

For axial tension:

$$S_4 = \frac{L\left(\sinh\left(L/\sqrt{k_v}\right)\right)\left(L\sqrt{k_v}\right)\left(\cosh\left(L/\sqrt{k_v}\right)\right)}{4\left(2\sqrt{k_v}\cosh\left(L/\sqrt{k_v}\right)\right)-\left(Lk_v\sinh\left(L/\sqrt{k_v}\right)\right)2\sqrt{k_v}} \quad \text{----(3– 22d)}$$

$$S_5 = \frac{L\left(L\sqrt{k_v}\right)\sinh\left(L/\sqrt{k_v}\right)}{2\left(2\sqrt{k_v}\cosh\left(L/\sqrt{k_v}\right)\right)-\left(Lk_v\sinh\left(L/\sqrt{k_v}\right)\right)2\sqrt{k_v}} \quad \text{----(3–22e)}$$

in which $^2 = \frac{P}{EI_y}$

3.2.3 Effect of Axial Force on Stiffness against Translation:

If both of the ends of the element are restrained against rotation, but one end is translated through a distance a relative to other, the flexural and shear stiffnesses of the element against this translation are affected by the axial force P.

3.2.3.1 Translation in X – Y Plane:

1) Stability function for the effect of axial force on flexural stiffness about Z – axis against translation a_y:

Referring to Fig. (3 – 3) and using the slope – deflection equation:

$$M_{za} = S_2\left(\frac{4EI_Z}{L}\right)\left(\frac{a_y}{L}\right) + S_3\left(\frac{2EI_Z}{L}\right)\left(\frac{a_y}{L}\right) \quad \text{---------- (3 – 23a)}$$

$$= \frac{6EI_Z}{L^2}a_y\left(\frac{2}{3}S_2 + \frac{1}{3}S_3\right) \quad \text{---------- (3 – 23b)}$$

$$= S_6\frac{6EI_Z}{L^2}a_y \quad \text{----------(3 – 23c)}$$

where $S_6 = \frac{2}{3}S_2 + \frac{1}{3}S_3$ ---------- (3 – 23d)

is the stability function for the effect of axial force (including the effect of shear deformations) on flexural stiffness (about the Z axis) against translation a_y. Substituting the values of S_2 and S_3 from equations (3 –

21b) and (3 – 21c) when the axial force is compressive and from equation equations (3 – 21d) and (3 – 21e) when the axial force is tensile, the following expression for S_6 can be obtained:

When P is compressive:

$$S_6 = \frac{-\phi^2 L^2 \sqrt{k_v}(\cos(-L/\sqrt{k_v}) - 1)}{6(2\sqrt{k_v}\cos(-L/\sqrt{k_v}) + Lk_v \sin(-L/\sqrt{k_v}) - 2\sqrt{k_v})} \quad \text{--- (3 – 23e)}$$

When P is tensile:

$$S_6 = \frac{-\phi^2 L^2 \sqrt{k_v}(1 - \cosh(-L/\sqrt{k_v}))}{6(2\sqrt{Kv}\cosh(-L/\sqrt{k_v}) - Lk_v \sinh(-L/\sqrt{k_v}) - 2\sqrt{k_v})} \quad \text{---(3 – 23f)}$$

2) <u>Stability function for the effect of axial force on shear stiffness against translation</u> a *y* :

Referring once again to Fig. (3 – 3)

$$F_{ya} = \frac{\acute{g}\ M}{L} \quad \text{---------- (3 – 24a)}$$

where

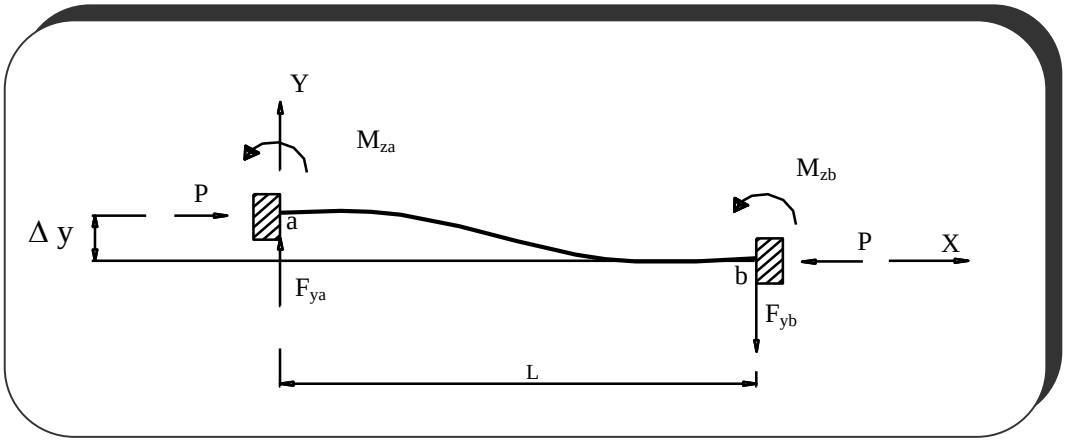

Fig. (3 – 3): Effect of Axial Force on Stiffness against Translation.

$$\acute{g}\ M = M_{za} + M_{zb} - P\,ay \quad \text{---------- (3 – 24b)}$$

and $$M_{za} = S_2 \frac{4EI_Z}{L}\left(\frac{ay}{L}\right) + S_3 \frac{2EI_Z}{L}\left(\frac{ay}{L}\right) \quad \text{---------- (3 – 24c)}$$

$$M_{Zb} = S_3 \frac{2EI_Z}{L}\left(\frac{a_y}{L}\right) + S_2 \frac{4EI_Z}{L}\left(\frac{a_y}{L}\right) \qquad \text{---------- (3 – 24d)}$$

Thus

$$F_{ya} = \left(\frac{12}{L}\right) S_2 \left(\frac{8EI_Z}{L^3}\right) + S_3 \left(\frac{4EI_Z}{L^3}\right) - \left(\frac{P}{L}\right) a_y \qquad \text{---------- (3 – 24e)}$$

Letting $\sim^2 = \dfrac{P}{EI_Z}$,then

$$F_{ya} = \left(\frac{12}{L}\right) S_2 \left(\frac{8EI_Z}{L^3}\right) + S_3 \left(\frac{4EI_Z}{L^3}\right) - \frac{\sim^2 EI_Z}{L} a_y$$

$$= \frac{12EI_Z}{L^3}\left(\frac{2}{3}\right) S_2 + \frac{1}{3} S_3 - \frac{\sim^2 L^2}{12}\left(\frac{1}{L}\right) a_y = S_7 \left(\frac{12EI_Z}{L^3}\right) \qquad \text{---(3 – 24f)}$$

where $S_7 = \dfrac{2}{3} S_2 + \dfrac{1}{3} S_3 - \dfrac{\sim^2 L^2}{12}$ ---------- (3 – 24g)

is the stability function for the effect of axial force on shear stiffness against translation a_y .Substituting for S_2 and S_3 from equations (3 – 21b) and (3 – 21c) when the axial force is compressive.

$$S_7 = \frac{\sim^2 L^2 \sqrt{k_v}\left(\cos\left(\sim L/\sqrt{k_v}\right) - 1\right)}{6\left(2\sqrt{k_v}\cos\left(\sim L/\sqrt{k_v}\right) + \sim L k_v \sin\left(\sim L/\sqrt{k_v}\right) - 2\sqrt{k_v}\right)} - \frac{\sim^2 L^2}{12}$$

----------(3 – 24h)

When the axial force P is tensile, P is replaced by $-P$ in equation (3 – 24b) and by taking values of S_2 and S_3 from (3 – 21d) and (3 – 21e); the following expression for S_7 can be obtained:

$$S_7 = \frac{\sim^2 L^2 \sqrt{k_v}\left(1 - \cosh\left(\sim L/\sqrt{k_v}\right)\right)}{6\left(2\sqrt{k_v}\cosh\left(\sim L/\sqrt{k_v}\right) - \sim L k_v \sinh\left(\sim L/\sqrt{k_v}\right) - 2\sqrt{k_v}\right)} + \frac{\sim^2 L^2}{12}$$

--------- (3 – 24i)

3.2.3.2 Translation in X – Z Plane:

1) Stability function for effect of axial force on flexural stiffness against translation a_z:

Proceeding as in the previous section, the stability function for the effect of axial force on flexural stiffness against translation a_z is given by

$$S_8 = \frac{2}{3}S_4 + \frac{1}{3}S_5 \quad \text{---------- (3 – 25a)}$$

Substituting the values of S_4 and S_5 from equations (3 – 22b) and (3 – 22d) when the axial force is compressive, and from equations (3 – 22c) and (3 – 22e) when the axial force is tensile,then the following expressions for S_8 are obtained:

When P is compressive:

$$S_8 = \frac{2L^2\sqrt{k_v}(\cos(L/\sqrt{k_v}) - 1)}{6(2\sqrt{k_v}\cos(L/\sqrt{k_v}) + Lk_v\sin(L/\sqrt{k_v}) - 2\sqrt{k_v})} \quad \text{---(3 – 25b)}$$

When P is tensile:

$$S_8 = \frac{2L^2\sqrt{k_v}(1 - \cosh(L/\sqrt{k_v}))}{6(2\sqrt{k_v}\cosh(L/\sqrt{k_v}) - Lk_v\sinh(L/\sqrt{k_v}) - 2\sqrt{k_v})} \quad \text{---(3– 25c)}$$

2) Stability function for effect of axial force on shear stiffness against translation Δz:

Proceeding as in the previous section, the stability function S_9 for the effect of axial force on shear stiffness against translation a_z is given by

$$S_9 = \frac{2}{3}S_4 + \frac{1}{3}S_5 - \frac{2L^2}{12} \quad \text{when the axial force is compressive --(3 – 26a)}$$

$$S_9 = \frac{2}{3}S_4 + \frac{1}{3}S_5 + \frac{2L^2}{12} \quad \text{when the axial force is tensile -------(3 – 26b)}$$

Substituting the values of S_4 and S_5 from equations (3 – 22b) and (3 – 22d) when the axial force is compressive, and from equations (3 – 22c)

and (3 – 22e) when the axial force is tensile,then the following expressions for S_9 are obtained:

When P is compressive:

$$S_9 = \frac{\phi L^2\sqrt{k_v}\left(\cos\left(L/\sqrt{k_v}\right)-1\right)}{6\left(2\sqrt{k_v}\cos\left(L/\sqrt{k_v}\right)+Lk_v\sin\left(L/\sqrt{k_v}\right)-2\sqrt{k_v}\right)}-\frac{\phi L^2}{12}$$

----------(3 – 26c)

When P is tensile:

$$S_9 = \frac{\phi L^2\sqrt{k_v}\left(1-\cosh\left(L/\sqrt{k_v}\right)\right)}{6\left(2\sqrt{k_v}\cos\left(L/\sqrt{k_v}\right)-Lk_v\sinh\left(L/\sqrt{k_v}\right)-2\sqrt{k_v}\right)}+\frac{\phi L^2}{12}$$

----------(3 – 26d)

3.2.4 Torsional Stiffness:

The derivation of the torsional constant (J_m) is given in Appendix (A).

Hence, the non – linear tangent stiffness matrix for a three – dimensional frame element becomes:

$$\begin{bmatrix}
S_1\frac{AE}{L} & & & & & & & & & & & \\
0 & S_7\frac{12EI_Z}{L^3} & & & & & & & & & & \\
0 & 0 & S_9\frac{12EI_y}{L^3} & & & & & & sym & & & \\
0 & 0 & 0 & \frac{GJ_m}{L} & & & & & & & & \\
0 & 0 & S_8\frac{6EI_y}{L^2} & 0 & S_4\frac{4EI_y}{L} & & & & & & & \\
0 & S_6\frac{6EI_Z}{L^2} & 0 & 0 & 0 & S_2\frac{4EI_z}{L} & & & & & & \\
-S_1\frac{AE}{L} & 0 & 0 & 0 & 0 & 0 & S_1\frac{AE}{L} & & & & & \\
0 & -S_7\frac{12EI_Z}{L^3} & 0 & 0 & 0 & S_6\frac{6EI_z}{L^2} & 0 & S_7\frac{12EI_Z}{L^2} & & & & \\
0 & 0 & -S_9\frac{12EI_y}{L^3} & 0 & S_8\frac{6EI_y}{L^2} & 0 & 0 & 0 & S_9\frac{12EI_y}{L^3} & & & \\
0 & 0 & 0 & -\frac{GJ_m}{L} & 0 & 0 & 0 & 0 & 0 & \frac{GJ_m}{L} & & \\
0 & 0 & -S_8\frac{6EI_y}{L^2} & 0 & S_5\frac{2EI_y}{L} & 0 & 0 & 0 & -S_8\frac{6EI_y}{L^2} & 0 & S_4\frac{4EI_y}{L} & \\
0 & -S_6\frac{6EI_Z}{L^2} & 0 & 0 & 0 & S_3\frac{2EI_z}{L} & 0 & -S_6\frac{6EI_Z}{L^2} & 0 & 0 & 0 & S_2\frac{4EI_z}{L}
\end{bmatrix}$$

For $P = 0$ (i.e. no axial force), it is easy to find the following expressions for the stability functions S_1 through S_9 as

$$S_1 = 1.0 \qquad \text{----------(3-27)}$$

$$S_2 = \frac{(4+\Phi_z)}{(4+\Phi_z)} \qquad \text{----------(3-28)}$$

$$S_3 = \frac{(2-\Phi_z)}{(2+\Phi_z)} \qquad \text{----------(3-29)}$$

$$S_4 = \frac{(4+\Phi_y)}{(4+\Phi_y)} \qquad \text{----------(3-30)}$$

$$S_5 = \frac{(2-\Phi_y)}{(2+\Phi_y)} \qquad \text{----------(3-31)}$$

$$S_6 = \frac{1}{(1+\Phi_z)} \qquad \text{----------(3-32)}$$

$$S_7 = \frac{1}{(1+\Phi_z)} \qquad \text{----------(3-33)}$$

$$S_8 = \frac{1}{(1+\Phi_y)} \qquad \text{----------(3-34)}$$

$$S_9 = \frac{1}{(1+\Phi_y)} \qquad \text{----------(3-35)}$$

where

$$\Phi_z = \frac{12\bar{B}EI_z}{AGL^2} \quad , \quad \Phi_y = \frac{12\bar{B}EI_y}{AGL^2}$$

As $(\sim)$ and $(\ )$ approach to zero, computation difficulties arise in finding the stability functions S_1 through S_9 from their prescribed general expressions. To avoid such difficulties, linear interpolation is suggested to be used in the ranges $0 \le \sim \le \frac{0.2}{L}$ and $0 \le \ \le \frac{0.2}{L}$ as follows

For $P \le -\frac{0.2}{L}P_E$ and $P \ge \frac{0.2}{L}P_E$ (for axial compressive or axial tensile force) the value of any stability function S can be calculated from the following equation

$$\begin{cases} S = S_0 + (S_0 + S_{0.1})\dfrac{-L}{0.2} & \textit{for bending in x - y plane} \\ S = S_0 + (S_0 + S_{0.1})\dfrac{L}{0.2} & \textit{for bending in x - z plane} \end{cases} \text{----------(3 – 36)}$$

where

S_0 = value of stability function for zero axial force $P = 0$,

$S_{0.1}$ = value of stability function for $P = \frac{0.2}{L}P_E$

3.3 Formulation of Stiffness Matrices for a Prismatic Element in the Presence of a Plastic Hinge:

Three cases for the location of plastic hinges were considered as follows:

3.3.1 Plastic Hinge at Left Extremity:

The element shown in Fig.(3 – 4) is considered.

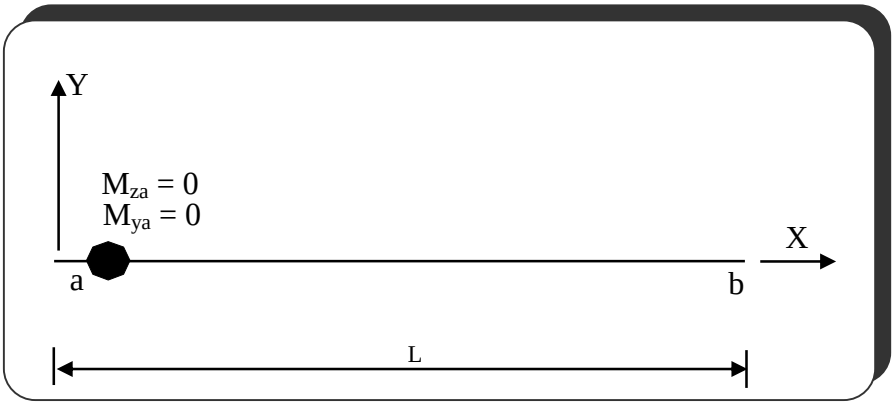

Fig. (3 – 4); Frame Element with Plastic Hinge at Left Extremity

From the conditions of joint a (i.e. where plastic hinge existed) and utilizing the previously derived stiffness matrix for the element with no

plastic hinge, the following equilibrium equations for the additional bending moments (i.e. after plastic hinge formation)are obtained:

$$M_{ya} = S_8\left(\frac{6EI_y}{L^2}\right)w_a + S_4\left(\frac{4EI_y}{L^2}\right)\theta_{ya} + S_8\left(\frac{6EI_y}{L^2}\right)w_b + S_5\left(\frac{2EI_y}{L}\right)\theta_{yb} \quad \text{----------(3 – 37a)}$$

$$M_{za} = S_6\left(\frac{6EI_z}{L^2}\right)v_a + S_2\left(\frac{4EI_z}{L}\right)\theta_{za} + S_6\left(\frac{6EI_z}{L^2}\right)v_b + S_3\left(\frac{2EI_z}{L}\right)\theta_{zb} \quad \text{----------(3 – 37b)}$$

Hence, the values of the inelastic rotations (θ_{ya}) and (θ_{za}) are obtained as follows

$$\theta_{ya} = \frac{L}{S_4\left[4EI_y\right]}\left[S_8\left(\frac{6EI_y}{L^2}\right)w_a - S_8\left(\frac{6EI_y}{L^2}\right)w_b - S_5\left(\frac{2EI_y}{L}\right)\theta_{yb}\right] \quad \text{-----(3 – 37c)}$$

$$\theta_{za} = \frac{L}{S_2\left[4EI_z\right]}\left[-S_6\left(\frac{6EI_z}{L^2}\right)v_a + S_6\left(\frac{6EI_z}{L^2}\right)v_b - S_3\left(\frac{2EI_z}{L}\right)\theta_{zb}\right] \quad \text{-----(3 – 37d)}$$

Substituting the values of (θ_{ya}) and (θ_{za}) back into the stiffness equations similar to equations (3 – 37a) and (3 – 37b) defining other reactions, the modified stiffness matrix takes the following form

$$
\begin{bmatrix}
S_1\frac{AE}{L} & & & & & & & & & & \\
0 & \bar{S}_7\frac{EI_Z}{L^3} & & & & & & & & & \\
0 & 0 & \bar{S}_9\frac{EI_y}{L^3} & & & & & sym & & & \\
0 & 0 & 0 & \frac{GJ_m}{L} & & & & & & & \\
0 & 0 & 0 & 0 & 0 & & & & & & \\
0 & 0 & 0 & 0 & 0 & 0 & & & & & \\
-S_1\frac{AE}{L} & 0 & 0 & 0 & 0 & 0 & S_1\frac{AE}{L} & & & & \\
0 & -\bar{S}_7\frac{EI_Z}{L^3} & 0 & 0 & 0 & 0 & 0 & \bar{S}_7\frac{EI_Z}{L^3} & & & \\
0 & 0 & -\bar{S}_9\frac{EI_y}{L^3} & 0 & 0 & 0 & 0 & 0 & \bar{S}_9\frac{EI_y}{L^3} & & \\
0 & 0 & 0 & -\frac{GJ_m}{L} & 0 & 0 & 0 & 0 & 0 & \frac{GJ_m}{L} & \\
0 & 0 & \bar{S}_8\frac{EI_y}{L^2} & 0 & 0 & 0 & 0 & 0 & \bar{S}_8\frac{EI_y}{L^2} & 0 & \bar{S}_4\frac{EI_y}{L} \\
0 & \bar{S}_6\frac{EI_Z}{L^2} & 0 & 0 & 0 & 0 & 0 & -\bar{S}_6\frac{EI_Z}{L^2} & 0 & 0 & 0 & \bar{S}_2\frac{EI_z}{L}
\end{bmatrix}
$$

where

$$\bar{S}_2 = 4S_2 - \frac{(S_3)^2}{S_2} \quad , \quad \bar{S}_4 = 4S_4 - \frac{(S_5)^2}{S_4} \quad , \quad \bar{S}_6 = 6S_6 - \frac{3(S_6 \cdot S_3)}{S_2}$$

$$\bar{S}_7 = 12S_7 - \frac{9(S_6)^2}{S_2} \quad , \quad \bar{S}_8 = 6S_8 - \frac{3(S_8 \cdot S_5)}{S_4} \quad , \quad \bar{S}_9 = 12S_9 - \frac{9(S_8)^2}{S_4}$$

3.3.2 Plastic Hinge at Right Extremity:

Proceeding as in the previous section and following the same procedure, the stiffness matrix for the element shown in Fig.(3 – 5), in which the plastic hinge exists at right extremity is as follow:

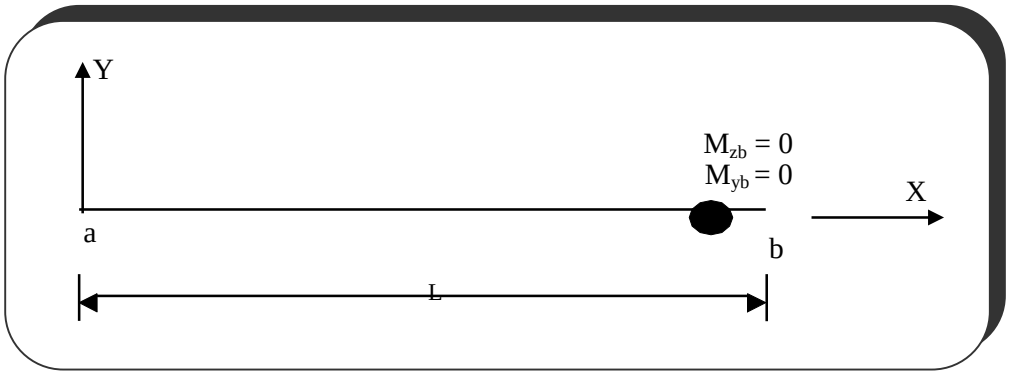

Fig.(3 – 5): Frame Element with Plastic Hinge at Right Extremity

$$
K_2 = \begin{bmatrix}
S_1\frac{AE}{L} & & & & & & & & & & \\
0 & \bar{S}_7\frac{EI_Z}{L^3} & & & & & & & & & \\
0 & 0 & \bar{S}_9\frac{EI_y}{L^3} & & & & & & sym & & \\
0 & 0 & 0 & \frac{GJ_m}{L} & & & & & & & \\
0 & 0 & \bar{S}_8\frac{JEI_y}{L^2} & 0 & \bar{S}_4\frac{EI_y}{L} & & & & & & \\
0 & \bar{S}_6\frac{EI_Z}{L^2} & 0 & 0 & 0 & \bar{S}_2\frac{EI_z}{L} & & & & & \\
-S_1\frac{AE}{L} & 0 & 0 & 0 & 0 & 0 & S_1\frac{AE}{L} & & & & \\
0 & -\bar{S}_7\frac{JEI_Z}{L^2} & 0 & 0 & 0 & \bar{S}_6\frac{JEI_z}{L^2} & 0 & \bar{S}_7\frac{EI_Z}{L^3} & & & \\
0 & 0 & -\bar{S}_9\frac{JEI_y}{L^3} & 0 & \bar{S}_8\frac{EI_y}{L^2} & 0 & 0 & 0 & \bar{S}_9\frac{EI_y}{L^3} & & \\
0 & 0 & 0 & -\frac{JGJ_m}{L} & 0 & 0 & 0 & 0 & 0 & \frac{GJ_m}{L} & \\
0 & 0 & 0 & 0 & 0 & 0 & 0 & 0 & 0 & 0 & 0 \\
0 & 0 & 0 & 0 & 0 & 0 & 0 & 0 & 0 & 0 & 0
\end{bmatrix}
$$

Same expressions for $\bar{S}_2, \bar{S}_4, \bar{S}_6, \bar{S}_7, \bar{S}_8, \bar{S}_9$ as defined previously in section 3.3.1 are valid.

3.3.3 Plastic Hinge at Both Extremities:

The element of this case is shown in Fig. (3 – 6).From equilibrium requirements:

$$F_{ya} = \frac{M_{za} + M_{zb}}{L} = 0 \ , \ F_{yb} = 0$$

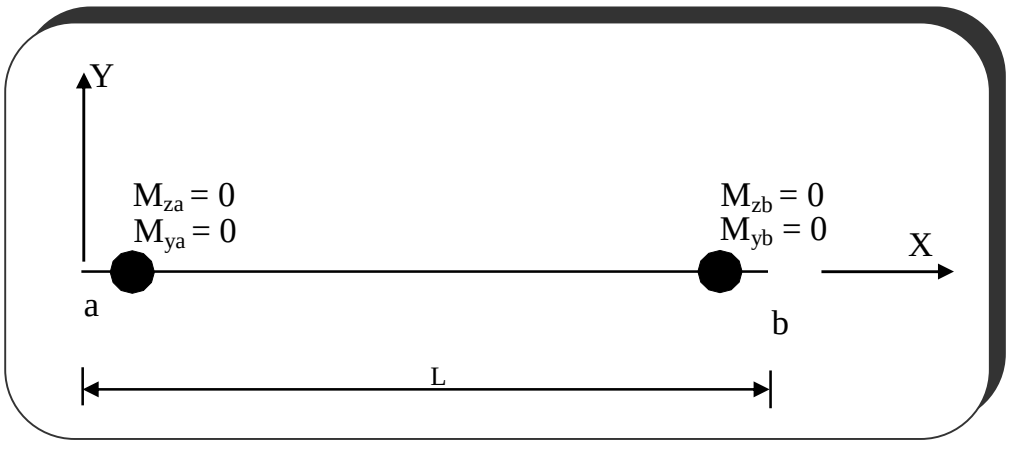

Fig.(3 – 6): Frame Element with Plastic Hinge at both Extremities

Similarly

$$F_{za} = \frac{M_{ya} + M_{yb}}{L} = 0 \quad , \quad F_{zb} = 0$$

Hence, the stiffness matrix will be

$$[K_3] = \begin{bmatrix} \frac{AE}{L} & & & & & & & & & & & \\ 0 & 0 & & & & & & & & & & \\ 0 & 0 & 0 & & & & & sym & & & & \\ 0 & 0 & 0 & \frac{GJ_m}{L} & & & & & & & & \\ 0 & 0 & 0 & 0 & 0 & & & & & & & \\ 0 & 0 & 0 & 0 & 0 & 0 & & & & & & \\ -\frac{AE}{L} & 0 & 0 & 0 & 0 & 0 & \frac{AE}{L} & & & & & \\ 0 & 0 & 0 & 0 & 0 & 0 & 0 & 0 & & & & \\ 0 & 0 & 0 & 0 & 0 & 0 & 0 & 0 & 0 & & & \\ 0 & 0 & 0 & -\frac{GJ_m}{L} & 0 & 0 & 0 & 0 & 0 & \frac{GJ_m}{L} & & \\ 0 & 0 & 0 & 0 & 0 & 0 & 0 & 0 & 0 & 0 & 0 & \\ 0 & 0 & 0 & 0 & 0 & 0 & 0 & 0 & 0 & 0 & 0 & 0 \end{bmatrix}$$

For the three cases described, the sign of the axial force (i.e. axial tensile or axial compressive force) would be taken into account in the expressions of the stability functions S_1 through S_9 as previously derived.

3.4 Fixed End Forces due to Uniformly Distributed Load over the Length of the Element:

a) <u>Bending in X – Y plane</u>:

Considering the element shown in Fig. (3 – 7), subjected to a uniform load w_y and fixed at both ends, the basic differential equations (3 – 1) and (3 – 2) can be used to solve the problem.

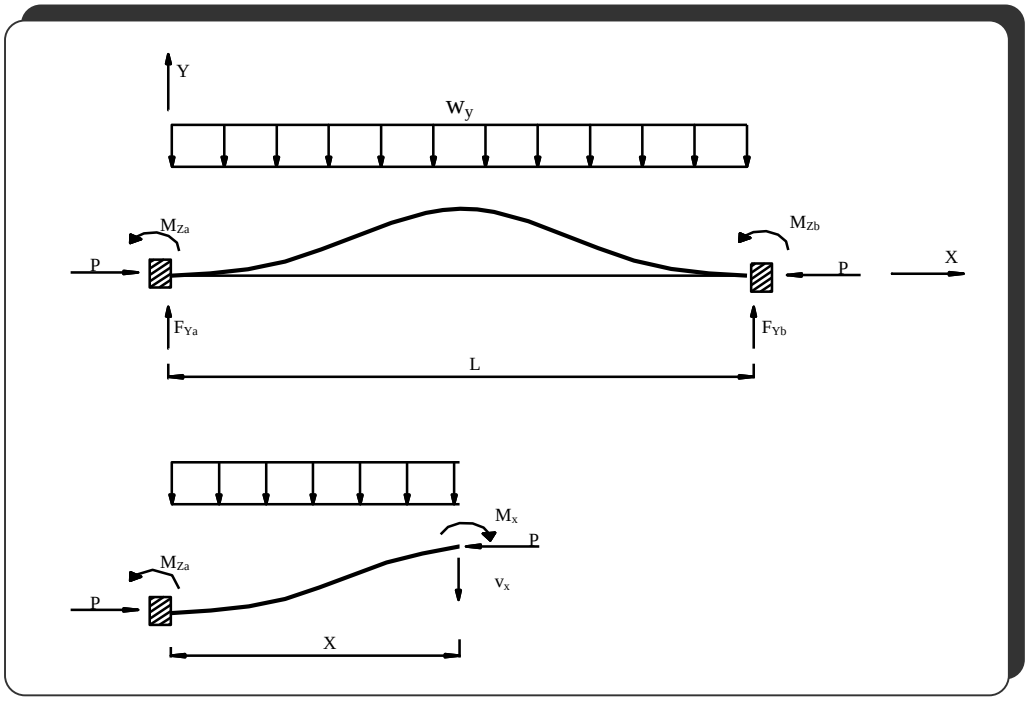

Fig. (3 – 7): Fixed End Forces due to Uniformly Distributed Load acting on a Frame Element in (x – y) Plane.

From symmetry and equilibrium requirements,

$$F_{ya} = F_{yb} = \frac{W_y \, L}{2} \qquad \text{---------- (3 – 38a)}$$

The equilibrium equations for a section at distance (x) from the left support are:

$$M_x = M_{za} + Py + F_{ya}\, x + \frac{W_y \, x^2}{2} \qquad \text{---------- (3 – 38b)}$$

$$Vx = Fya + W_y \, x + Py \qquad \text{---------- (3 – 38c)}$$

Then, from equations (3 – 1) and (3 – 38c), the following expression for V_x is obtained

$$V_x = \left[F_{ya} + W_y \, x + Py\right] \left[\frac{1}{1 + \frac{\bar{B}P}{AG}}\right] \qquad \text{---------- (3 – 38d)}$$

Hence, by differentiation

$$V'_x = W_y + Py' \left[\frac{1}{1 - \frac{\bar{B}P}{AG}}\right] \qquad \text{---------- (3 – 38e)}$$

Writing $\sim^2 = \frac{P}{EI_Z}$, $Kv = \frac{1}{1 - \frac{\bar{B}P}{AG}}$ and substituting the values of (M_x, V_x') from equations (3 – 38b) and (3 – 38e) into equation (3 – 2), the following equation is obtained,

$$k_v\, y'' + \sim^2 y = \frac{\sim^2}{P}\left[M_{Za} + \frac{W_y Lx}{2} + \frac{W_y x^2}{2}\right] + \frac{\bar{B} W_y}{(AG - \bar{B}P)}$$

----------(3 – 39a)

The solution of this differential equation will be

$$y = A_1 \cos\left(\sim x/\sqrt{k_v}\right) + B_1 \cos\left(\sim x/\sqrt{k_v}\right) + \frac{W_y x^2}{2P}$$

----------(3 – 39b)

$$- \frac{W_y Lx}{2P} - \frac{W_y}{\sim^2 P}\left[k_v - \frac{\bar{B}P}{AG}\right] + k_v - \frac{\sim^2 M_{Za}}{W_y}$$

Applying the boundary conditions at $x = 0$ and $x = L$; $y = 0$ to find

$$A_1 = \frac{+ W_y}{\sim^2 P}\left[k_v - \frac{\bar{B}Pk_v}{AG}\right] + \frac{\sim^2 M_{Za}}{W_y}$$

$$B_1 = \frac{W_y}{\sim^2 P}\left[k_v - \frac{\bar{B}Pk_v}{AG}\right] + \frac{\sim^2 M_{Za}}{W_y}\left[\frac{\cos\left(\sim L/\sqrt{k_v}\right) + 1}{\sin\left(\sim L/\sqrt{k_v}\right)}\right]$$

Then, by differentiating equation (3 – 39b), then,

$$y' = \frac{+\sim}{\sqrt{k_v}} A_1 \sin\left(\sim x/\sqrt{k_v}\right) + \frac{\sim}{\sqrt{k_v}} B_1 \cos\left(\sim x/\sqrt{k_v}\right) + \frac{W_y x}{P} - \frac{W_y L}{2P}$$

----------(3 – 39c)

Finally, using the boundary condition at $x = 0;\ y = \frac{\bar{B} W_y L}{2AG}$ to find the expression for the fixed end moments $(M_{za})\ and\ (M_{zb})$ as follows

$$M_{za} = M_{zb} = \frac{W_y \left[\frac{1}{\sqrt{k_v}} - \left[\frac{1}{2} \left(1 + \frac{\bar{B} E I_z}{AG} k_v \right) \cos\frac{L}{2}\sqrt{k_v} + \frac{1}{2} \left(\frac{L}{2} \right) \left(1 + \frac{\bar{B} E I_z}{AG} k_v \right) \sin\frac{L}{2}\sqrt{k_v} \right] \right]}{\frac{1}{\sqrt{k_v}} \left[\cos\frac{L}{2}\sqrt{k_v} + 1 \right]}$$

---------- (3 – 40)

Similarly, when the axial force is tensile, then from symmetry,

$$F_{ya} = F_{yb} = \frac{w_y L}{2}$$ ---------- (3 – 41a)

The equilibrium equations for a section at distance (x) from the left end (see Fig.(3 – 8)) will be:

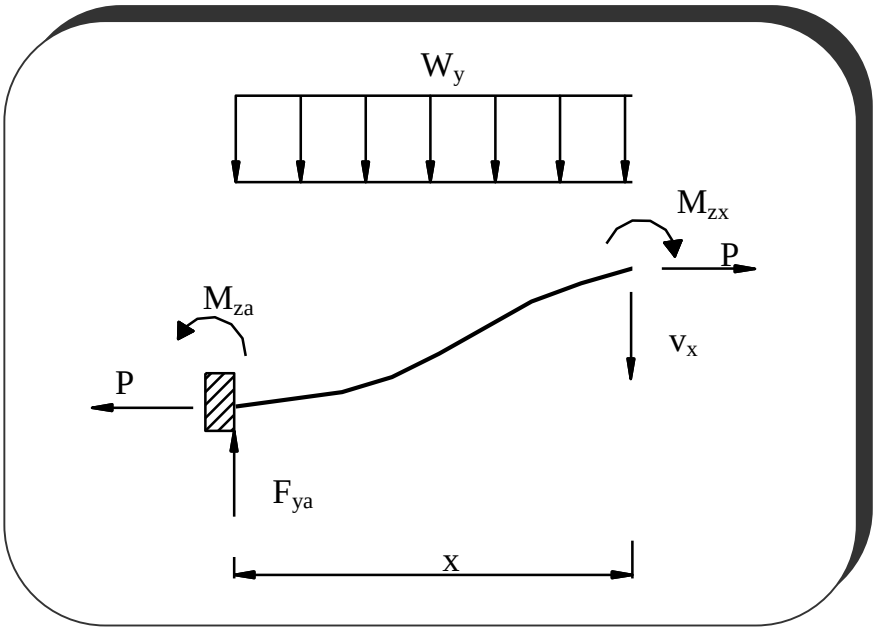

Fig. (3 – 8)Fixed end Forces for Axial Tensile Force

$$M_x = M_{za} + P y + F_{ya}\, x - \frac{W_y x^2}{2} \qquad \text{----------(3 – 41b)}$$

$$V_x = F_{ya} - W_y\, x + P y' \qquad \text{---------- (3 – 41c)}$$

Again, in the same way, utilizing equations (3 – 1) and (3 – 41c), one obtains

$$V_x = \left[F_{ya} - W_y\, x + P y'\right] \frac{1}{\left(1 + \frac{\bar{B} P}{AG}\right)} \qquad \text{---------- (3 – 41d)}$$

Hence, by differentiation

$$V_x' = \left[-W_y + P y''\right] \frac{1}{\left(1 + \frac{\bar{B} P}{AG}\right)} \qquad \text{---------- (3 – 41e)}$$

Then, from equations (3 – 2), (3 – 41b) and (3 – 41e), the following differential equation is obtained

$$k_v\, y'' - \sim^2 y = \frac{\sim^2}{P}\left(M_{za} - \frac{W_y L x}{2} + \frac{W_y x^2}{2} - \frac{\bar{B} P W_y}{\sim^2 AG} k_v\right) \text{------(3– 42a)}$$

where

$$\sim^2 = \frac{P}{EI_Z}\ ,\ k_v = \frac{1}{\left(1 + \frac{\bar{B} P}{AG}\right)}$$

The solution of this differential equation will be

$$y = A_2 \cosh\left(\frac{\sim x}{\sqrt{k_v}}\right) + B_2 \sinh\left(\frac{\sim x}{\sqrt{k_v}}\right) + \frac{W_y x^2}{2P} + \frac{W_y L x}{2P} + \frac{W_y}{\sim^2 P}\left(k_v + \frac{\bar{B} P k_v}{AG} + \frac{\sim^2 M_{za}}{W_y}\right) \qquad \text{---- (3 – 42b)}$$

The boundary conditions at $x = 0$; $y = 0$ and at $x = L$; $y = 0$ lead to the following:

$$A_2 = \frac{-W_y}{\sim^2 P}\left[k_v - \frac{\bar{B}P k_v}{AG} - \frac{\sim^2 M_{za}}{W_y}\right]$$

$$B_2 = \frac{W_y}{\sim^2 P}\left[k_v - \frac{\bar{B}Pk_v}{AG} - \frac{\sim^2 M_{za}}{W_y}\right]\left[\frac{\cosh(\sim L/\sqrt{k_v})}{\sinh(\sim L/\sqrt{k_v})} - 1\right]$$

and by differentiation of equation (3 – 42b), then

$$y' = \frac{\sim}{\sqrt{k_v}} A_2 \sinh\left(\frac{\sim x}{\sqrt{k_v}}\right) + \frac{\sim}{\sqrt{k_v}} B_2 \cosh\left(\frac{\sim x}{\sqrt{k_v}}\right) - \frac{W_y x}{P} + \frac{W_y L}{2P} \qquad \text{----------(3 – 42c)}$$

The expression for M_{za} and M_{zb} (when P is tensile) is found through applying the boundary condition at x = 0, $y' = \frac{-\bar{B} W_y L}{2AG}$ .Hence, this expression may be written as follows,

$$M_{za} = -M_{zb} = \frac{W_y\left[\left(\frac{L}{2}\right)\left(1 - \frac{\bar{B}EI_z\sim^2}{AG}\right)\sinh(\sim L/\sqrt{k_v}) - \sqrt{k_v}/\sim\left(1 - \frac{\bar{B}EI_z\sim^2}{AG}\right)\left[\cosh(\sim L/\sqrt{k_v}) - 1\right]\right]}{\sim\sqrt{k_v}\left[\cosh(\sim L/\sqrt{k_v}) - 1\right]}$$

---------- (3 – 43)

It is easy to show that by using L 'Hopital's Rule, the fixed end moment as $P \to 0$ (tensile or compressive) has the following value:

$$M_{za} = -M_{zb} = \frac{W_y L^2}{12} \qquad \text{---------- (3 – 44)}$$

b) <u>Bending in X – Z plane:</u>

Proceeding as in the previous section and replacing ~ by , the following equations for the fixed end moments due to a uniformly

distributed load W_z for both axial tensile force or axial compressive force can be obtained:

For axial compressive force:

$$M_{ya} = M_{yb} = \frac{W_z\left[\sqrt{k_v}\left/\left[1+\left(\frac{\bar{B}EI_z}{AG}\right)^2 k_v\right]\right.\cos\left(L\sqrt{k_v}\right)-1\right]+\left(\frac{L}{2}\right)\left[1+\left(\frac{\bar{B}EI_z}{AG}\right)^2 k_v\right]\sin\left(L\sqrt{k_v}\right)}{\left(\sqrt{k_v}\right)\left[\cos\left(L\sqrt{k_v}\right)-1\right]} \quad \text{---------- (3 – 45)}$$

For axial tensile force:

$$M_{ya} = M_{yb} = \frac{W_z\left[\left(\frac{L}{2}\right)\left[1-\left(\frac{\bar{B}EI_z}{AG}\right)^2 k_v\right]\sinh\left(L\sqrt{k_v}\right)\left/\left[1-\left(\frac{\bar{B}EI_z}{AG}\right)^2 k_v\right]\right.\cosh\left(L\sqrt{k_v}\right)-1\right]}{\left(\sqrt{k_v}\right)\left[\cosh\left(L\sqrt{k_v}\right)-1\right]} \quad \text{---------- (3 – 46)}$$

where $k^2 = \frac{P}{EI_y}$

Also, as $P \to 0$ (tensile or compressive), utilizing L 'Hopital's Rule:

$$M_{ya} = M_{yb} = \frac{W_z L^2}{12} \quad \text{---------- (3 – 47)}$$

As $\sim k \to 0$, computational problems arises in finding the fixed end moments from expressions (3 – 40), (3 – 43), (3 – 45) and (3 – 46). To avoid such problems, linear interpolation is suggested in the range $0 < \sim < \frac{0.2}{L}$ and $0 < k < \frac{0.2}{L}$ (for axial compressive or axial tensile force) as follows

$$M_i = \sim k + M_j = \sim k + M_i = 0 + \left[M_i = 0 + M_i\left(\frac{0.2}{L}\right)\left(\frac{\sim L}{0.2}\right)\right]$$
$$M_i = k + M_j = k + M_i = 0 + \left[M_i = 0 + M_i\left(\frac{0.2}{L}\right)\left(\frac{L}{0.2}\right)\right] \quad \text{---------- (3 – 48)}$$

CHAPTER TWO

REVIEW OF LITERATURE

In this chapter, the review covers three aspects, the first is the developments of frame analysis. It includes general elastic frame analysis approaches and inelastic frame analysis methods. The second is the developments in the optimal design of framed structures and the third is the experimental works on reinforced concrete frames.

2.1 Frame Analysis:

The frame analysis had been the subject of research by many researchers. In 1972, **Denato and Maier [2]** formulated a mathematical programming method, namely "Imposed rotation method" for inelastic analysis of reinforced concrete frames. They formulated the problem of determining the moments and rotations at critical sections of a reinforced concrete frame subject to a given load in terms of the linear complementarity problem (**LCP**).

They also formulated the limit analysis of reinforced concrete frames in terms of another mathematical programming problem that may be solved by an algorithm which is a modification of the simplex method for a linear program. Trilinear moment – rotation law was adopted. The possibility of plastic collapse failure before local failure was also studied when the slope of the third segment of the moment – rotation law was equal to zero. Shear deformations, geometric non – linearity, local unloading were all not considered.

A significant computational development in the "imposed rotation method" was made by **Kaneko [3] in 1977**.The proposed method was

essentially a reformulation of those developments by **Denato and Maier [2]**. However, the formulation results in a new mathematical programming model for which an efficient algorithm is developed. The advantage of the proposed method is mainly computational since it requires roughly one half computer time and a storage space as compared with those of **De Donato and Maier [2]** which were employed to solve the same problem.

In 1977, **MacGregor and Hage [4]** emphasized that the effective length procedure for including the second order effects in frame analysis as recommended by ACI Code (1971) has serious shortcomings in sway frames or partially braced frames. They presented five alternative approximate procedures and made a comparison among them: (1) moment magnifier solution for second order effect. (2) negative bracing member method and (3) second order finite element analysis assuming that the stiffness matrix [k] is the sum of two stiffness matrices [k_1] and [k_2], in which [k_1] is the first order stiffness matrix and [k_2] is obtained through an iteration procedure. All presented methods were approximate and in addition, they ignored the effect of shear deformations.

In 1977, **Chugh [5]** presented a simple and direct procedure for the formulation of an element stiffness matrix on element co – ordinates for a two dimensional beam and a beam – column member including shear deformations. The resulting stiffness matrices are compared with those obtained by using the alternative formulation in terms of member flexibilities. The relative effects of axial force and shear force on stiffness coefficients were presented. The critical buckling loads, considering the effects of shear force, were computed and compared with other works. Only prismatic members were considered.

Gunnin et al [6], in 1977, described a computational technique for the general non – linear analysis of large planar frames under static

loading. The material non – linearity was included considering moment – axial force interaction. The effect of joint displacements during loading was accommodated by analysis through updating the nodal coordinates after each iteration in each load increment. The members are prismatic and the loads are applied at joints within the plane of the frames and all displacements of the frame are within that plane. The analysis based on small distorsion theory by neglecting shear deformations and the curvature of the member is assumed to be proportional to the second derivative of deformation with respect to length i.e., $\frac{1}{\rho} = \frac{d^2y}{dx^2}$. Secondary geometric non –linearity (i.e. secondary moments) was not included. The bowing effect was also neglected. Accuracy of the analysis procedure was demonstrated by comparing the computed results with eight reinforced concrete frames test. The element used is as shown in Fig. (2 – 1).

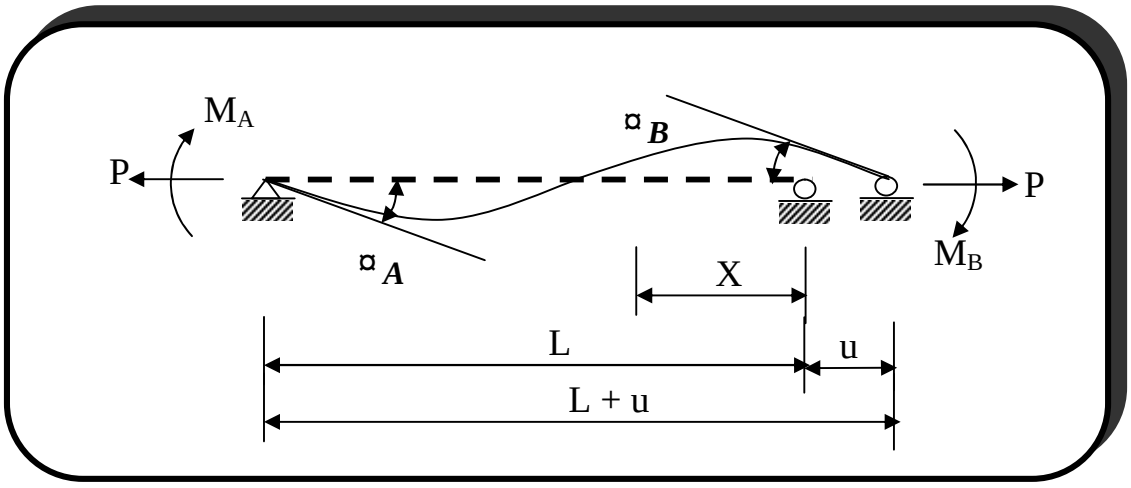

Fig. (2 – 1): Forces and Deformations of a Beam Element used by Guninn et al [6].

In 1978, **Krishnamoorthy and Panneerselvam [7]** presented a computer program (**FEPACSI**) for non –linear finite element analysis of reinforced concrete framed structures. The finite element formulation for

reinforcement in any orientation in computing the element stiffness was explained (see Fig. (2 – 2)).

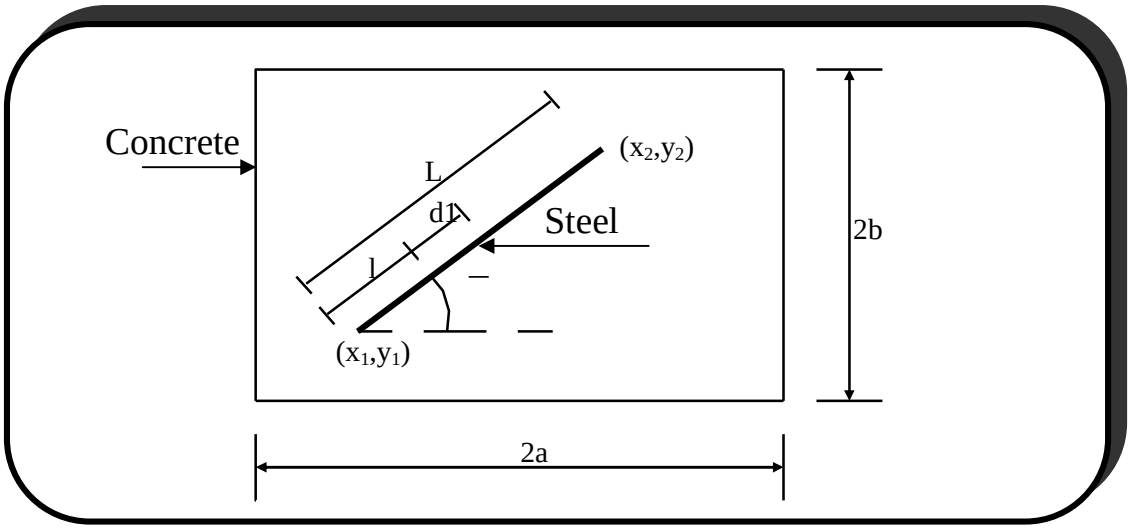

Fig. (2 – 2): Reinforced Concrete Plane Stress Element of Krishnamoorthy and Panneerselvam

A brief description of material properties used and the non –linear finite element formulation to account for the material and other non – linearities due to cracking and yielding was given. The computer program (**FEPACS1**) was explained with the aid of a flow chart and the computational steps involved in the program were described in details. Incremental iterative technique based on " Initial stress method" was adopted. Shear deformations and geometric non – linearity were not included. The application of the program was illustrated by selected examples.

Cohn and Franchi [8], in 1979, presented the main concepts, theoretical bases, means of implementation and some illustration of the potential use of a computer system for structural plasticity (**STRUPL**). The (**STRUPL**) system is conceived as a package of computer programs for structural plasticity that should be capable of automatically solving any structural plasticity problem with an ease and efficiency comparable to that of other programs. The solver bank of the package system includes

various mathematical programming (linear programming (**LP**), linear complementary problem (**LCP**), quadratic programming (**QP**), etc.) algorithms suited for the solution of engineering problem types. The computer program for **STRUPL** – analysis implements an integrated elastic – plastic procedure that essentially solves two central problem types: the historical analysis under non – proportional loading assuming either nonholonomic or holonomic behavior. The program is applicable to analyze two dimensional steel or reinforced concrete structures. The analysis neglects both geometric non – linearity and the effect of shear deformations. Several numerical examples were investigated to test the accuracy and efficiency of the computer program package.

In 1979, **Khalifa [9]** considered the problem of premature instability of optimized steel space frames. As loads increased, plastic hinges start forming in succession, resulting in the possible instability of the deteriorating frame before a plastic mechanism is reached. The problem was formulated, and a method of analysis, which provides a lower limit on the actual failure load, was presented. The analysis establishes the order in which the plastic hinges form, but avoids the repeated inversion of the frame stiffness matrix. The method developed was applied on two simple space frames.

Hsu et al [10], in 1981, described a computer program for the elastic perfectly plastic analysis of reinforced concrete planar frames. This computer program requires less computer time and memory space and it is intended as practical for analysis and design uses. The computer program is capable of a complete analysis of reinforced concrete frames from zero load until failure under any system of static gravity and lateral loads. The analysis of reinforced concrete frames uses a computer program as a subroutine to calculate the moment – curvature characteristics under a constant load applied at the section centroid. The

program efficiency was checked through comparing its results with experimental results for reinforced concrete plane frames that were tested by others. The program ignored each of; (1) geometric non – linearity (2) shear deformations and (3) local unloading. However, the program considered the possibility of each of collapse mechanism failure and local crushing failure following the plastic hinge model.

In 1986, **Al – Sarraf [11]** derived modified stability functions for two – dimensional prismatic beam – columns having any solid cross – section shapes, laced or battened built – up structural members, in terms of the shear flexibility and axial load parameters. An approximate formula for such functions were proposed which make possible the rapid prediction of the elastic critical load of structures taking into consideration the effect of shear force in the members, using a hand – computing method. The modified stability functions were related to previously existed tabulated stability functions of prismatic strut **[11]**. The approximate formula predicts accurate elastic load to within 1%.

In 1988, **Al – Rifaie and Trikha [12]** recognized the importance of the finite size of joints and shear deformations in the analysis of plane concrete structures, especially frame – shear wall type structures. They proposed rigid – ended element for idealization to carry out a step – by – step linearised limit state analysis. Simplified axial force – moment diagrams for reinforced concrete sections had been derived for detection of a plastic hinge formation. However, the analysis ignored the effect of each of geometric non –linearity, possibility of local unloading, and possibility of crushing failure at any critical section. In addition, the analysis considered that each element has only two critical sections at its ends and could not treat the case of existence of a third critical section at the zero shear point when the element is under distributed load. A computer program had been used to analyze an irregular multi – storied

frame, an industrial gable frame and a frame – shear wall structure and the results were compared to establish the validity of the procedure.

Wong and Tin – Loi [13], in 1990, developed a method for the elastic non – linear analysis of framed structures depending on the finite element method. They described the main forms of Lagrangian coordinates systems and their relative merits were also discussed. The solution strategy rested on a combination of the Newton – Raphson iterative technique and modified "arc length method" within a finite element based partially on updated Lagrangian discription. The proposed modified technique of the arc length enables a solution at the limit point to be calculated. They solved three examples and got very accurate results compared with experimental results obtained by others.

In 1993, **Dumir et al [14]** investigated the geometrically non – linear static analysis of steel space frames subjected to discrete and distributed transverse loads using the beam-column method. An exact expression of the beam – column equivalent load vector had been derived and it had been proved that the first term in its Taylor's series expansion is identical to the static consistent equivalent load vector of the finite element method. The results of a beam – column, a plane frame and a space frame obtained by the beam – column method were compared with those of the finite element method.

Alwash [15], in 1995, proposed a general non – linear method of analysis of reinforced concrete plane frames which was utilized for the analysis of reinforced concrete Virendeel trusses. It follows a step – by – step with iterations approach. Different parameters were included in the analysis, they are: combined effect of geometric non – linearity and shear deformations, material non-linearity, moment-axial force interaction, possibility of local stress unloading and the effect of the elements ends rigidity. Fixed end forces were derived for an element under uniformly

distributed load and the possibility of existence of an additional critical section at zero shear point for such element was also treated. Three possible failure criteria were predicted (collapse mechanism, local crushing failure and stability failure).The theoretical results were compared with those obtained experimentally and rather good agreement was obtained.

In 2001, **Al – Asady [16]** developed a procedure for the elastic – plastic analysis of steel space frames. It follows a step – by – step linearized elastic – plastic analysis which predicts the sequence and location of plastic hinges and the corresponding load factor at each stage of analysis. The procedure was based on the matrix displacement method. The material was assumed to be elastic – perfectly plastic, and yielding was considered to be concentrated at the member's ends in the form of plastic hinges. The members were assumed to remain elastic between the plastic hinges. Several examples had been investigated to check the accuracy of the analysis.

Kuw and Ju [17], in 2002, developed a three – dimensional (3D) non – linear beam element into a static and dynamic non –linear finite element program called (**AN** program). This 3D beam is an inelastic element for modeling beam and beam – columns to model the steel or reinforced concrete structures for the static and dynamic loading, especially for the ground motion problem. The **AN** program provides efficient solution scheme for this beam element. For example, a non – linear finite element analysis with hundred thousand nodes could be performed effectively using a personal computer. The absorbed boundary condition of the **AN** program also provides the 3D beam to perform the soil – structure interactive analysis in the time – domain. The **AN** program had the ability to perform a very complex non – linear structural analysis since it incorporated this 3D beam element.

From the preceding review, it is clear that there is no detailed study that deals with the non – linear behavior of reinforced concrete space frames. In the present study, geometric non –linearity, material non – linearity, effect of shear deformations, different failure criteria (i.e., a. plastic collapse mechanism, b. crushing failure, and c. stability failure) and possibility of existence of distributed load on any member in addition to nodal forces are all considered in the present study. All these parameters are included in detail in chapters three and four.

2.2 Optimal Design of Reinforced Concrete Frames:

In 1970, an optimal design of reinforced concrete frames was presented by **Rozvany and Cohn [18]**. The geometry of frames was given and the sizes of all members were assumed fixed and the only design variable was the amount of steel reinforcement. The analytic approach was based on the lower bound theorm to determine the limit load and forces in the sections. Yielding condition, serviceability and plastic compatibility were considered as constraints on the design optimization problem. No constraints on deflection and cracking width were considered. The design for shear, axial forces and bond was also not considered.

Munro et al [19], in 1972, formulated a more general approach of the optimal design of reinforced concrete frames using linear programming method namely “simplex method”. The constraints of the problem included equilibrium, compatibility, limited ductility and serviceability. The objective function was the amount of reinforcement for fixed cross sectional dimensions. The analysis of reinforced concrete frames was plastic under the combinations of ultimate load. The study did not consider the effect of shear in the design of beams and the effects of axial load in the design of columns.

An optimal design method for reinforced concrete structures under constraints of strength, deformability and serviceability was proposed by **Ali and Grierson [20]** in 1974. The objective function was the minimum cost of effective concrete and tension reinforcement. The section dimensions and main reinforcement were the design variables of the problem. The optimization problem was solved by the method of "Feasible Conjugate Directions". Optimal design process was based on plastic analysis which considered both the possibilities of collapse mechanism and local crushing failure state. However, the shear reinforcement and its effect on the optimal design was neglected. Also the effect of axial force on moment capacity, geometric non – linearity and shear deformations were neglected.

In 1980, a formulation of preliminary optimum design of multistory – multibay frames was presented by **Gerlein and Beaufait [21]**. The design variables were the plastic moment capacity of sections. The aim of optimization was to minimize the total volume of steel which was directly related to the plastic moment capacity of each critical section. The problem was solved using linear programming technique namely "simplex method" applied to story by story under the kinematic constraints and design constraints satisfying building code requirements and practical design considerations. The design was based on a rigid – fully plastic behavior using the upper bound approach. The plastic hinges were assumed to be formed in beams only (strong columns and weak beams) and no limitations were considered on the plastic rotations. ***P*** J a effect, shear deformations as well as axial deformations were all neglected.

Kirsch [22], in 1983, proposed a multi – level optimal design approach for reinforced concrete structures. The cost was considered as the objective function. In the third (system) level, the design moments are

found from an elastic analysis depending on the updated concrete dimensions for each cycle. In the second (element) level, the concrete dimensions of each element are optimized successively and only a single independent variable (depth) is involved by considering the width to be constant for all members. Hence the problem was reduced to a set of one dimensional explicit optimization problems subject to side constraints (deflection, shear, moment, upper bound and lower bound of depth). In the first (cross section) level, the amount of reinforcement in each critical section is found for the corresponding updated concrete dimensions and design moments from the third level. The proposed multi – level solution was found to be most suitable for micro – computer applications.

In 1984, **Majid and Tang [23]** proposed a method for the optimum design of pin – jointed steel space frames which included the undetermined shape, i.e. their geometry and topology, as a variable to be decided by the method itself. The method included stress, serviceability, buckling and stiffness requirements to be satisfied, while the cost of the material was assumed to be the objective function. In doing so the self – weight of the structure which was changed during the design process, was fully considered as a design variable. To reduce cost, members were allowed to be grouped together so that those in a group have the same cross – section. However, a member was allowed to have a variable length as the joints at its ends were allowed to move in a 3 – dimensional space. Examples were given of the design method which included a dome and a transmission tower.

Mekha [24], in 1988, presented a new algorithm, which was utilized in performing inelastic analysis for the optimal design of reinforced concrete plane frames. This new algorithm was developed to solve the problem of inelastic analysis of frames by “imposed rotation method” which was reformulated by **Kaneko [3]**. The inelastic tri – linear moment

rotation law, which was modeled to reflect the inelastic behavior at prescribed critical sections was adjusted during the incremental analysis after each load increment in order to adhere to the non – holonomic behavior of reinforced concrete when local stress unloading occurs. Optimum concrete dimensions and reinforcement were evaluated for minimum cost. Optimization, following the multi level approach, was carried out on several frames using two alternative methods, namely Rosenbrock constrained method and sequential unconstrained minimization technique.

Zielinski et al [25], in 1995, presented a procedure for the design of reinforced concrete rectangular short – tied columns using the optimization technique. The proposed procedure included two sets of iterations. The first set of iteration finds the resistance capacity of a column of given dimensions, and the second set of iteration performs the optimization process. The optimization process was formulated as finding the minimum cost design with the constraints imposed based on Canadian specification CSA CAN3 – A23.3 – M89. The internal penalty function algorithm for non – linear programming was used in the optimization procedure. For a column with uniaxial loads, the depth, and width of the cross section, and reinforcement ratio were treated as design variables and the location of the neutral axis was obtained by solving a cubic equation. For a column with biaxial loads, the dimensions of the cross section, reinforcement ratio and the number of reinforcing bars were treated as design variables, and the location of the neutral axis was determined by employing Newton – Raphson method. Numerical examples were given to show the validity of the proposed method.

Fadaee and Grierson [1], in 1996, presented minimum cost design for three dimensional reinforced concrete frames with members subjected to biaxial moments and shear forces using the optimality criteria approach

based on ACI-Code ("Building" 1995). Beams and columns were assumed to have rectangular sections. The cost function included the material costs of concrete, steel, and formwork. The focus of this work is the formulation of the appropriate constraints for combination of the axial load, biaxial bending moment, and biaxial shear. Their example is only a one – bay and one – story space frame. They conclude that the biaxial shear is an important consideration for design of columns, and its inclusion increases the cost of the optimum structure significantly.

Balling and Yao [1], in 1997, presented a comparative study of optimization of three – dimensional reinforced concrete frames with rectangular columns, and rectangular, T-, or L – shape beams according to ACI-Code ("Building" 1989) using one –, two –, and four- story frames subjected to vertical and lateral loads, and employing the sequential quadratic programming or gradient – based method. For steel reinforcement they considered two different definitions for design variables. In the first definition, the area of steel in each member is the only design variable used for steel in that member. In the second definition, they considered the number, diameter, and longitudinal distribution of the reinforcing bars and performed a two – level optimization. They attempted to include the costs of materials, fabrication, and placement in the cost function by assuming the material and fabrication cost of steel reinforcement to be proportional to its weight and its placement cost to be proportional to the number of bars, stirrups and ties. They concluded that the optimum costs based on the two definitions were very close to each other, and thus, there is no need to include the second more computationally costly definition in the optimization formulation. Based on this conclusion, the authors then discussed a simplified approach for cost optimization of space reinforced concrete frames.

In 1998, **Rafiq and Southcombe [26]** introduced a new approach to optimal design and detailing of reinforced concrete biaxial columns using genetic algorithms (**GAs**). For a biaxial column with a given set of design requirements (section size, axial load and bending about both axes of the column), it was shown how (**GAs**) conduct a global search to identify the optimal reinforcement bar sizes and bar detailing arrangements. These satisfy the maximum bending capacity about both axes of the column section and minimize the area of reinforcement which leads to an economical design. In detailing reinforcement bar arrangements within the column section, the British Standard (**BS8110**) requirements were considered to ensure that both the ultimate state (**ULS**) and the buildability (ease of construction) requirements were satisfied. A declarative approach was used to check the exact bending capacities of the section about both axes of the column for the reinforcement bar detailing suggested by the **GAs**. approved / modified and adopted by the designer. Several examples of biaxial column were examined and compared with simplified code results to show the advantages of the used declarative programming approach.

Finally, **Hashim [27]**, in 1999, presented an optimal design algorithm for reinforced concrete plane frames consisting of prismatic and / or linearly tapered elements based on a proposed inelastic analysis approach. Plastic zone model was suggested with an incremental approach to study the inelastic behavior of reinforced concrete frames. The design algorithm was based on a non – linear optimization technique namely, sequential unconstrained minimization technique (**SUMT**). In the optimization process, the member dimensions and steel reinforcement (main and lateral reinforcement) at critical sections were taken as variables and the total cost which includes the cost of steel reinforcement, concrete, and formwork, was taken to be as an objective function.

Solutions of several examples were presented to verify the validity of the proposed algorithm.

In the present work, the proposed non – linear analysis algorithm, as mentioned earlier and described in details in chapters three and four is performed for the optimal design of reinforced concrete space frames as will be given in chapter five. The objective function will be the total cost including the cost of reinforcing steel (main and lateral), cost of concrete and the cost of formwork. The independent variables are members dimensions (b, h) and the main reinforcement. The problem of optimization is solved by the "Direct search method" to obtain the optimum concrete dimensions and reinforcement.

2.3 Experimental Works on Reinforced Concrete Frames:

Several experimental studies on reinforced concrete frames are reviewed in this section.

Rad and Furlong [28], in 1980,investigated theoretically and experimentally the behavior of one story, one bay portions of multistory reinforced concrete plane frames under gravity plus lateral load. Five two – column frames, three symmetrical and two unsymmetrical, were tested up to failure. The frames were first loaded with some (75) percent of the predicted ultimate load under vertical loading followed by lateral load incremented to failure. In the analytical part, the combined effect of geometrical and material non – linearities were considered. The material was assumed to be elastic – perfectly plastic. However, the effect of shear deformation and local unloading were not considered in the analytical study. The frame capacities based on ACI Code (1977), considering a capacity reduction factor, ¯¤ Z1, were found significantly lower than the measured values.

Ford et al [29], in 1981, presented a physical and analytical modeling of a series of unbraced multi – panel concrete frames. Nine frames were tested under beam, column and lateral loads. The objectives of the test were to study the behavior and redistribution capacities of highly indeterminate concrete plane frames and, as a result, to develop correct analytical modeling technique for non – linear analysis of reinforced concrete frames. In the analytical model, a tangent stiffness iteration approach was used with general discrete element technique of (Hays) **[29]** for planar frames. All rotational and axial displacements were concentrated at rotational and piston springs respectively. Material and geometric non – linearities were considered. The effect of shear deformation was ignored.

In 1986, **Y. L. Mo [30]** carried out three types of tests involving different load paths on nine model portal reinforced concrete plane frames. The vertical load was monolithically increased until failure in the first group. In the second group, the lateral load was increased to failure while the vertical load was maintained at 53% of the ultimate load. In the third group, the vertical load was increased to failure while a lateral working load was maintained at 53% of the ultimate load according to the plastic theory. The measured results were compared with previously tested corresponding prototype frames in a previous paper by others. Also, the results were compared with those obtained theoretically. Among the conclusions obtained, the moment redistribution of reinforced concrete frames can reproduce accurately in models, made of micro-concrete and deformed steel, throughout the loading history. Also, in one-story frames with horizontal loads, the secondary effect of deformations on the moments may reach 5%, which would be taking into account according to ACI building code.

An experimental – theoretical study was conducted by **Elbehairy et al [31]** in 1989, to study the general deformational behavior, inelastic rotation and plastic hinge length at the critical sections of a reinforced concrete rectangular frames under concentrated loads. Four rectangular frames of medium scale model (1/ 5) were tested under concentrated load at the mid-point of the upper girder. The overall external dimensions of the frames were (2.4m) wide by (1.6m) height. The four frames had the same cross – sectional dimension of girders and columns sections. The girder cross – section was taken (0.15 x 0.25 m), while the column was taken (0.15 x 0.2 m). The difference between these frames was the steel content provided at the girder and column. The general deformational behavior of the tested frames were examined and reported (strains, stresses, deformations, inelastic rotation and plastic hinge length). The experimental results of the tested frames were analyzed by other available limit design methods **(Baker, Sawyer and Cohn's methods)**. A comparison was made between the experimental results and those obtained from these methods. The results of these methods were more conservatives than those obtained experimentally by about 25%. The results of this investigation were combined with other available informations to formulate some recommendations for the analysis and design of this type of structures.

As a part of **Alwash's [15]** study in 1995, an experimental investigation was carried out on three models of reinforced concrete Virendeel trusses. The main aims of the test were: (a) To assess the validity of the proposed theoretical procedure for non – linear analysis of reinforced concrete frames and (b) To investigate the size (or length) of the rigid portions of the structural members at their ends. The three models of different shapes and dimensions were cast and tested up to failure. The models were loaded at mid-span by a concentrated load

generated by a universal testing machine. The results were compared with those obtained theoretically by the proposed method of analysis. Among the conclusions obtained was, the assumption of prismatic members giving more reliable results than the rigid – ended members. Also, the adopted modeling technique using micro – concrete was suitable to a large extent in representing the behavior of the prototype Virendeel trusses.

At last, a theoretical and experimental investigation was carried out by **Terezia et al [32]**, in 2001, for the determination of the moment vs. curvature, and shear force vs. shear deformation relationships based on the stress – strain curves given in **ENV** (European pre – standard. design of concrete structures) (1991), with material characteristics obtained from the test of concrete and steel specimens were presented. A comparison of the theoretical values with the results of tests for seven reinforced concrete beams subjected to a concentrated force in the middle of the beam spans shows good agreement for both curvature and shear deformations. The values of the deformation work due to bending moments as well as those due to shear forces were also determined.

From the preceding review, it is clear that no experimental test on non – linear behavior of reinforced concrete space frames was found. Such test was carried out in the present study on a model of reinforced concrete space frame. The model was tested in the concrete laboratory of the University of Babylon and the results were used to assess the validity of the theoretical analysis approach that is proposed in the present study.

LIST OF CONTENTS

SUBJECT ***PAGE***

CHAPTER SIX: EXPERIMENTAL WORK

CHAPTER SEVEN: RESULTS, APPLICATIONS AND DISCUSSIONS

CHAPTER EIGHT: CONCLUSIONS AND RECOMMENDATIONS

TO

WHOM I AM DEEPLY

INDEBTED...

MY DEAR PARENTS

NOTATION

A	Area of cross section of a member (gross or cracked).
A_{scy}	Area of compression reinforcement (bending about y – axis).
A_{scz}	Area of compression reinforcement (bending about z – axis).
A_{sty}	Area of tension reinforcement (bending about y – axis).
A_{stz}	Area of tension reinforcement (bending about z – axis).
A_l	Area of longitudinal torsional reinforcement.
A_t	Area of one leg of a closed stirrup resisting torsion.
A_{sv}	Cross – sectional area of shear reinforcement bar.
A_s	Area of tension reinforcement (axial compression + uniaxial bending).
$A_s^{'}$	Area of compression reinforcement (axial compression + uniaxial bending).
A_{sT}	Area of total main reinforcement.
$\overline{B}$	Shear factor.
B	Width of a member.
b_1	Depth of compression reinforcement (bending about y – axis).
c	Depth of the neutral axis.
c_o	Minimum concrete cover.
C_c	Unit price of concrete involving material and labor cost.
C_f	Unit price of formwork.
C_s	Unit price of steel reinforcement involving material and labor cost.
d	Effective depth of a member.
d_1	Depth of compression reinforcement (bending about z – axis).
d_b	Diameter of main reinforcement bars.

d_{sv}	Bar diameter of shear reinforcement.
E_s	Modulus of elasticity of steel.
E_c	Modulus of elasticity of concrete.
e_y	Eccentricity of axial load in the direction of z – axis.
e_z	Eccentricity of axial load in the direction of y – axis.
$f_{\grave{c}}$	Cylinder strength of concrete.
f_{yv}	Yield strength of transverse torsional reinforcement.
f_y	Yield strength of steel.
f_{yl}	Yield strength of longitudinal torsional reinforcement.
f_{sc}	Stress in compression reinforcement.
f_{st}	Stress in tension reinforcement.
G	Shear modulus of rigidity.
h	Overall depth of a member.
I_y	Moment of inertia of a section (gross, cracked or effective)about y J axis.
I_z	Moment of inertia of a section (gross, cracked or effective)about z J axis.
J_m	Torsional constant of a section (see appendix A).
L	Total length of member.
L_P	Length of plastic hinge region.
N_{sv}	Number of ties in a member.
P_h	Perimeter of centerline of outermost closed transverse torsional reinforcement.
P_{cr}	Axial force at cracking stage.
S_b	Spacing of longitudinal main steel reinforcing bars in the direction of the width of the member.
S_h	Spacing of longitudinal main steel reinforcing bars in the direction of the depth of the member.

S_v	Spacing of ties.
T_n	Nominal torsional moment strength.
V_{cy}	Nominal shear strength provided by concrete (in y – direction).
V_{cz}	Nominal shear strength provided by concrete (in z – direction).
V_{ny}	Nominal shear strength of a section (in y – direction).
V_{nz}	Nominal shear strength of a section (in z – direction).
W_y	Uniformly distributed load in the direction of the y – axis.
W_z	Uniformly distributed load in the direction of the z – axis.
W_s	Unit weight of steel.
W_c	Unit weight of concrete.
ε_c	Strain in extreme compression fiber of concrete.
ε_u	Ultimate strain of concrete.
ε_o	Yield strain of concrete.
ϕ	Strength reduction factor for flexure.
$\bar{\phi}$	Strength reduction factor for shear and torsion.
λ	Load factor.
ν	Poisson's ratio.
ρ_t	Tensile steel ratio $Z\frac{A_{sty}}{bh}$ $Z\frac{A_{stz}}{bh}$ (for biaxial bending).
ρ_c	Compression steel ratio $Z\frac{A_{scy}}{bh}$ $Z\frac{A_{scz}}{bh}$ (for biaxial bending).
ρ	Total steel ratio $Z\frac{A_{sT}}{bh}$.
$\bar{}_{yi}$	Yield rotation of a section about y – axis.
$\bar{}_{zi}$	Yield rotation of a section about z – axis.

NOTATION

$\bar{\ }_{y\,inel}$	Inelastic rotation of a section about y – axis.
$\bar{\ }_{z\ inel}$	Inelastic rotation of a section about z – axis.
$\bar{\ }_{yto}$	Total rotation of a section about y – axis (after plastic hinge formation).
$\bar{\ }_{zto}$	Total rotation of a section about z – axis (after plastic hinge formation).
$\bar{\ }_{zy}$	Resulting rotation due to the rotations ($\bar{\ }_{zto}$ and $\bar{\ }_{yto}$) respectively.
$\bar{\ }_{u}$	Ultimate rotation of a section.

Note: *Any other notation may be explained where it appears in the thesis.*

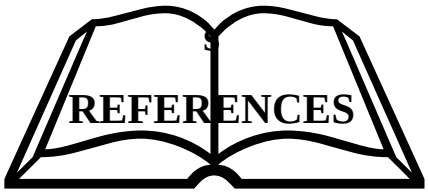

REFERENCES

1- Sarma, K.C. and Adeli, H. “Cost Optimization of Concrete Structures”, J. of Structural Engg., Vol.124, No.5, PP.570 – 577, May (1998).

2- Denato, O. and Maier, G. “A Mathematical Programming Method for Inelastic Analysis of R.C. Frames Allowing for Limited Rotation Capacity”, Int. J. Num. Meth. Engg. Vol.4, PP.307 – 329, (1973).

3- Kaneko, I. “A Mathematical Programming Method for the Inelastic Analysis of Reinforced Concrete Frames”, Int. J. Num. Meth. Engg., Vol.11, PP.1137 – 1154, (1977).

4- MacGregor, J. G. and Hage, E. “Stability Analysis and Design of Concrete Frames”, J. Structural Div., ASCE, Vol.103, No.ST10, PP.1953 – 1970, Oct. (1977).

5- Ghugh, A. K. “Stiffness Matrix for A Beam Element Including Transverse Shear and Axial Force Effects”. Int. J. Num. Meth. Engg., Vol.11, PP.1681 – 1697, (1977).

6- Gunnin, B.L, Rad, F.N. and Furlong, R.W. “A General Nonlinear Analysis of Concrete Structures and Comparison with Frame Tests”, Computers and Structures, Vol.7, PP.257 – 265, Pergamon Press, (1977).

7- Krishnamoorthy, C.S. and Panneerselvam, A. “FEPACSI – A Finite Element Program for Nonlinear Analysis of Reinforced Concrete Framed Structures”, Computers and Structures, Vol.9, No.5, PP.451 – 461, Pergamon Press, (1978).

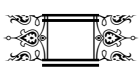

8- Cohn, M.Z and Franchi, A. " Structural Plasticity Computer System: STRUPL" J. Structural Div., ASCE, Vol.105, No.ST4, PP.789 – 804, April (1979).

9- Khalifa, M. M. K. "Plastic – Instability Analysis of Space Frames", The Structural Engineer, Vol.57B, No.3, PP.55 – 61,Sept. (1979).

10- Hsu, C–T. T., Mirza, M.S. and C. S. S. Sea "Nonlinear Analysis of Reinforced Concrete Frames", Computers and Structures, Vol.13, No.1 – 3, PP.223 – 227, Pergamon Press, June (1981).

11- Al–Sarraf, S.Z. "Shear Effect on The Elastic Stability of Frames", The Structural Engineer, Vol.64B, No.2, PP.43 – 47,June. (1986).

12- Al–Rifaie, W.N. and Trikha, D.N. "Limit State Analysis of Reinforced Concrete Structures With Finite Sized Joints", J. of Structural Engg., Vol.14, PP.129 – 138, Jan. (1988).

13- Wong, M.B. and Tin – Loi, F. "Geometrically Nonlinear Analysis of Elastic Framed Structures", Computers and Structures, Vol.34, No.4, PP.633 – 640, (1990).

14- Dumir, P.C., Saha, D.C. and Sengupta, S. "Beam – Column Method for Frames Under Distributed Loads", Computers and Structures, Vol.46, No.1, PP.141 – 148, (1993).

15- Alwash, N.A–A.H. "Nonlinear Behavior and Optimal Design of Reinforced Concrete Virendeel Trusses", Ph.D Thesis, Department of Building and Construction, University of Technology, (1995).

16- Al – Asady, N. H. S. "Elastic – Plastic Analysis of Steel Space Structures", M.Sc. Thesis, Department of Building and Construction, University of Technology, (2001).

17- Kuw, C.T. and Ju, S.H. "Developing a Three – Dimensional Nonlinear Beam Element for Static and Dynamic Analyses", National

Science Council, Republic of China, under contract No.: NSC – 90 – 2211 – E – 006 – 068, (2002).

18- Rozvany, G.I.N. and Cohn, M.Z. “Lower – Bound Optimal Design of Concrete Structures”, J. Engg. Mechanics Div., ASCE, Vol.96, No.EM6, PP.1013 – 1030, Dec. (1970).

19- Munro, J., Krishnamoorthy, K.S. and Yu, C.W. “Optimal Design of R.C. Frames”, J. of Structural. Engg., Vol.50, No.7, PP.251 – 264, (1972).

20- Ali, M. M. and Grierson, D.E. “Reinforced Concrete Design for Strength and Deformability”, J. Engg. Mechanics Div., ASCE, Vol.100, No.EM5, PP.839 – 860, Oct. (1974).

21- Gerlein, M.A., and Beaufait, F.W. “An Optimum Preliminary Strength Design of Reinforced Concrete Frames”, Computers and Structures, Vol.11, PP.515 – 524, (1980).

22- Kirsch, U. “Multilevel Optimal Design of Reinforced Concrete Structures”, Engg. Optimization, Vol.6, PP.207 – 212, (1983).

23- Majid, K.I. and Tang, X. “The Optimum Design of Pin – Jointed Space structures With Variable Shape”, The Structural Engineer, Vol.62B, No.2, PP.31 – 37, June (1984).

24- Mekha, B.B. “Optimal Design of Reinforced Concrete Frames Based on Inelastic Analysis”, M.Sc.Thesis, College of Engineering, University of Baghdad, (1988).

25- Zielinski, Z.A., Wenyi, Long and Troitsky, M. S. “Designing Reinforced Concrete Short – Tied Columns Using the Optimization Technique”, ACI Structural Journal, PP.619 – 626, Sept. – Oct. (1995).

26- Rafiq, M.Y. and South Combe, C. “Genetic Algorithms in Optimal Design and Detailing of Reinforced Concrete Biaxial Columns Supported By A Declarative Approach for Capacity

Checking", Computers and Structures, Vol.69, PP.443 – 457, Pergamon Press, (1998).

27- Hashim, R.K. "Inelastic Analysis and Optimal Design of Reinforced Concrete Frames With Non – Prismatic Members", M.Sc. Thesis, College of Engineering, University of Babylon. (1999).

28- Rad, F.N. and Furlong, R.W. "Behavior of Unbraced Reinforced Concrete Frames", ACI Journal, Vol.77, No.4, PP.269 – 278, July – Aug. (1980).

29- Ford, J.S., Chang, D.C. and Breen, J.E. "Experimental and Analytical Modeling of Unbraced Multipanel Concrete Frames", ACI Journal, Vol.78, No.1, PP.21 – 35, Jan. – Feb. (1981).

30- Mo, Y.L. "Moment Redistribution in Reinforced Concrete Frames", ACI Journal, Vol.83, No.4, PP.577 – 587, July – Aug. (1986).

31- Elbehairy, S., Mohamed, I.S. and Abdallah AbuZaeid "Non linear Analysis of Reinforced Concrete Frames". Structural Faults and Repair, P.P.65 – 74. (1989).

32- Terezia, N., Martin, K. and Jan, H. "Theoretical Model of the Determination of the Deformation Rates of R.C. Beams", Construction and Building Materials, Vol.15, PP.169 – 176, (2001).

33- Ekhande, S.G., Selvappalam, M. and Madugula, M. K. S. "Stability Functions For Three – Dimensional Beam – Columns", J. of Structural Engg., Vol.115, No.2, PP.467 – 479, Feb. (1989).

34- Pannel, F.N. "Failure Surfaces For Members in Compression and Biaxial Bending", ACI Journal, Proceedings V.60, No.1, PP. 129 – 140, Jan. (1963).

35- Nilson, A.H. and Winter, G. "Design of Concrete Structures", Tenth Edition, McGraw Hill Company, (1988).

36- Sakai, K. and Kakuta, Y. “Moment-Curvature Relationships of Reinforced concrete Members Subjected to Combined Bending and Axial Force”, ACI Journal, Vol.77, No.3, pp.189-194, May-June (1980)

37- Al – Raunduzy, A.A.K “Large Displacement Elastic Stability Analysis of Plane Steel Frames under Static and Dynamic Loads” M.Sc. Thesis, Department of Building and Construction, University of Technology, (1996).

38- ACI Committee 318“Building Code Requirements for Structural Concrete (ACI.318 – 95) and Commentary (ACI 318 RM-95)”, American Concrete Institute, 1995.

39- Bunday, B.D. “Basic Optimization Methods”, Edward Arnold Ltd., (1984).

40- Oden, J.T “Mechanics of Elastic Structures”, McGraw Hill Company, (1967).

OPTIMAL DESIGN OF REINFORCED CONCRETE SPACE STRUCTURES BASED ON NONLINEAR ANALYSIS

A THESIS

SUBMITTED TO THE COLLEGE OF ENGINEERING OF THE UNIVERSITY OF BABYLON IN PARTIAL FULFILLMENT OF THE REQUIREMENTS FOR THE DEGREE OF

MASTER OF SCIENCE IN CIVIL ENGINEERING

(STRUCTURAL ENGINEERING)

=

BY

MUS'AB AIED Q. AL-JANABI

(B.Sc.)

OCTOBER - 2003

SUPERVISION

Asst.Prof.Dr.Nameer.A.Alwash Asst.Prof.Dr.Ammar.Y.Ali


بسم الله الرحمن الرحيم
وَيَسأَلونَكَ عنِ الرُّوحِ قُلِ الرُّوحُ مِنْ أَمْرِ
رَبّي وَمَا أُوتِيتُم مِنَ العِلمِ إلا قَلِيلا
صدق الله العظيم